The Microgenesis of Object-based vis-à-vis Space-based Visual Attention:
A Temporal-Spectral-Spatial Approach and Analysis

Linda H. Moya
Department of Psychology
Carnegie Mellon University

Dissertation Committee:
Marlene Behrmann (chair)
Carl Olson
David Plaut

Submitted in partial fulfillment of the requirements for the degree of
Doctor of Philosophy

Acknowledgements

First, I would like to thank my dissertation committee, Drs. Marlene Behrmann (chair), Carl Olson, and David Plaut, for their time and energy in enabling this dissertation to be possible. I benefitted greatly from Dr. Behrmann's vision for the field. I learned from and admire her ability to structure optimal experimental paradigms and powerful presentations, and I learned from her the complex ANOVA statistical analysis evident in this dissertation. I am grateful to Dr. Olson, as it is the cognitive neuroscience course he co-taught with Dr. Jay McClelland in 2005, which enabled me to enter the neurosciences with the perspective of "hey, I can be GOOD at this!". Thank you to other faculty for valuable feedback and expressed support for my research and research ideas: in particular Drs. Michael Tarr, Dean Pomerleau and Mark Wheeler. Many thanks to my CNBC cohorts for technical discussions on neuronal oscillations' role in cognition, and to the VISCOG team for feedback. The Pittsburgh MEG community has provided indispensible support. Thank you to Dr. Anto Bagic who allowed me to conduct pilot MEG scans without the means to pay for them, without these pilot scans the present dissertation would have not happened. Thank you to Anna Haridis for indispensible help in running my experiments, and overall integrity in day-to-day dealings. Thank you to Gus Sudre and Bronwyn Woods (also Eli Kanal and Erika Laing) with whom discussions enabled me to cross any given technical hurdle I came across. Thank you to Anna Hegedus, who always made sure I had the necessary computing resources available to conduct my analysis. The CNBC staff is a joy to work with, as is Erin Donahoe in the psychology department: all helped me resolve administrative issues. Thank you to the MNTP training grant committee, especially Dr. Seong-Gi Kim and Dr. Carl Olson, who chose me to receive a stipend and research fund support for two years; support which

set me on the path to MEG research in the first place, and paid for all MEG scans comprising the analyses in this document. Thank you to my advisor Dr. Marlene Behrmann for funding the MRI scans. Finally thank you, so much, to my family: my husband Phil whose mathematical and logical acumen transcends all computational scientific fields, and whose steadfast support was essential to my completing this dissertation, and to Mira and Daniel whom we love unconditionally: God's children who have been entrusted to our care, so that we can help them grow up to be of benefit to other living beings, and true citizens of the world.

Abstract

Visual cognition involves processes such as selective attention and object perception that exist at the intersection of perception and cognition. This research focuses on visual selective attention and the set of processes that determine how some subset of the visual input is selected for further cognitive processing. It also investigates perceptual objects as candidate units on which attentional selection operates. Using a well-established behavioral paradigm together with EEG, MEG and MRI structural neuroimaging, this research investigates the microgenesis of object-based vis-à-vis space-based attention: how attentional cognition evolves across time and space, elucidating the spectral characteristics along the way. The results suggest that selective attention is in part comprised of a set of oscillatory processes including the alpha gating/inhibition process and the theta communication control process. Widespread posterior alpha-band oscillatory activity is interpreted as activity that inhibits task irrelevant areas in order to enable only attended stimuli to be further processed. Widespread theta-band activity, which interacts with hemifield presentation side, is interpreted as a long-range communication process in the attentional network, enabling communication between frontal and more posterior areas, and between hemispheres. The results also suggest a time-course of faster processing for targets presented in the left versus right hemifields, lending support to and providing a specific manifestation of previous findings of right hemisphere dominance in selective attention. In summary, the results reveal the microgenesis of object-based vis-à-vis space-based attention in terms of these oscillatory processes, and how they evolve in time and across space.

Contents

1. Visual Attention

Visual cognition involves processes such as selective attention and object perception that exist at the intersection of perception and cognition. This research focuses on visual selective attention and the set of processes that allow and determine how some subset of the visual input is selected for further cognitive processing, and investigates perceptual objects as candidate units on which attentional selection operates. Attention serves the function of focusing on and enhancing those stimuli that are highly salient in the input and/or behaviorally relevant for the observer. One way of perceptually organizing a complex visual scene is to attend selectively to a particular spatial location unbiased by the different features or elements that comprise the input at that location. This is known as visuospatial or space-based attention (SBA). Another way is to attend selectively to an entire perceptual object in the scene and to process its features and elements preferentially relative to points outside that perceptual object. This form of attention is known as object-based attention (OBA). In the extensive literature on visual attention, perhaps the topics most investigated are those which concern the underlying representations upon which this attentional selection operates and how the attentional selection processes are manifested: is attention space-based, and/or object-based, and/or are there other representations that can selectively be enhanced? What are the set of processes that allow and determine how some subset of the visual input is selected for further cognitive processing? How are these attentional processes manifest in the time-space course of cognitive processing? How do these attentional processes differ when the underlying representations of attentional selection differ? How are they the same? These topics remain active areas of research in

psychology and neuroscience, and there is still much to be done in order to fully characterize the cognitive process of attention in order to find answers to these key research questions.

In my dissertation, I focus on two forms of attentional selection as identified in extant literature: object-based attention and space-based attention (c.f. Kastner and Ungerleider, 2000; Olson, 2001; Scholl, 2001; Yantis and Serences, 2003; Hopf et al., 2005; Roelfsema et al., 2006). A large body of literature exists on both forms of attention in cognitive psychology using a multitude of behavioral paradigms, as well as in research with primates. Space-based attention in particular has been studied extensively using neuroimaging methods such as electroencephalography (EEG) and functional magnetic resonance imaging (fMRI) and, more recently magnetoencephalography (MEG). These neuroimaging studies afford better insight into the neural underpinnings of space-based attention. Object-based attention, in contrast, has been the subject of relatively fewer neuroimaging studies, and there is still much opportunity to investigate the neural underpinnings of OBA. Given the presumption of the underlying representations of attentional selection as spatial location (via SBA) and perceptual objects (via OBA), my dissertation research contributes to the growing body of research into OBA vis-à-vis SBA, and to answering the research questions as to how the attentional processes differ when the units of attentional selection differ, and how they are manifest in the time-space course of cognitive processing. My dissertation does this by investigating the microgenesis of the OBA vis-à-vis SBA, where the goal is to map out with millisecond resolution how attention evolves in time and across the brain, elucidating its characteristics along the way.

1.1 Literature review – object-based vis-à-vis space-based attention

OBA and SBA have been contrasted and compared in several reported investigations and these are reviewed here. That the presence of perceptual objects in the visual scene have been observed to influence behavioral reaction time (RT) to stimuli in the environment (which in the cognitive psychology literature - e.g. Egly et al., 1994 - has been taken as behavioral evidence of attention selection of perceptual objects), additionally makes OBA an interesting phenomenon in and of itself, independently of its role in other cognitive processes. Furthermore, the phenomenon of OBA provides insight into how the visual system groups perceptual information for subsequent cognitive processing.

1.1.1 Behavioral studies

Object-based models of attention, although eluded to earlier, clearly emerged with the work of Duncan (1984) among others. The models suggest attention is directed to perceptual objects or groups that result from a preattentive segmentation of the visual scene in accordance with Gestalt grouping principles. In 1994, Egly and colleagues used a paradigm that was destined to become a classic in subsequent studies of object-based attention. In their paradigm (Figure 1), two rectangles appear on either side of a central fixation cross. The rectangles are oriented either vertically on either side of fixation, or horizontally above and below fixation. Attention is cued to one end of one rectangle and then a target appears in the cued location (valid trial), at the opposite end of the same, cued rectangle (same object trial), or horizontally/vertically across/down (vertical and horizontal displays respectively) to the adjacent un-cued rectangle (different object trial). The finding is that RT to detect or discriminate the target is faster for valid trials than invalid trials, reflecting the advantage of space-based attention (SBA). More relevant,

however, is that performance is faster for “same object” than “different object” invalid trials. The behavioral performance difference between these last two conditions is taken as evidence of OBA. The presumption is that between cue onset and target onset, attention is spread within the perceptual object within which the cue appears, and that this spread subsequently contributes to a significantly faster reaction for a target that appears in the same perceptual object as the cue, than for a target that appears outside that object. In response to Egly and colleagues’ findings, Vecera (1994) established that any spatial component to OBA must be held constant in order to attain the effect: if the different-object target is much closer to the cue position than is the same-object target, then the OBA effect disappears and space-based attention dominates.

The Egly et al. (1994) stimulus paradigm

Stimulus Fields

Fixation 1000 ms | Cue 100 ms | ISI 200 ms | Target (valid) or Target (invalid)

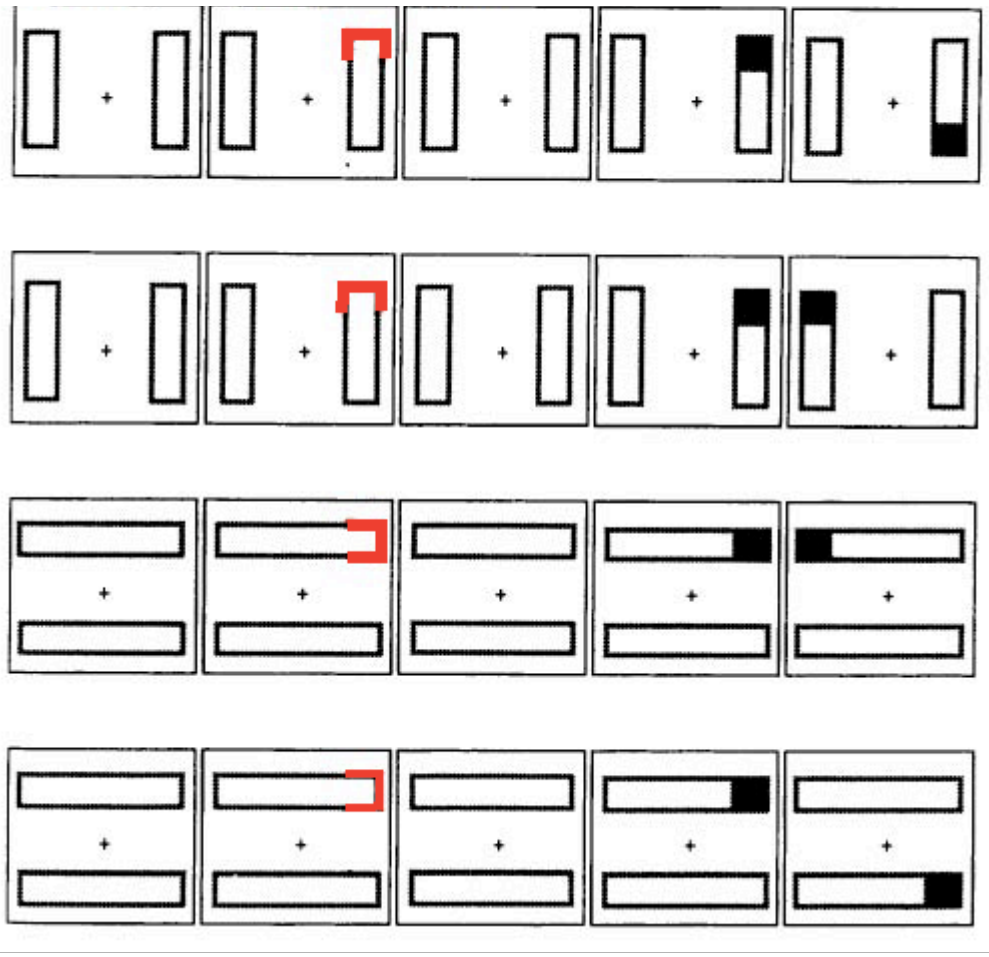

Vertical Display

valid vs. same object invalid

valid vs. different object invalid

Horizontal Display

valid vs. same object invalid

valid vs. different object invalid

Typical sequence of events (running left to right). Fixation is present for 1000 ms, then the cue is present for 100 ms. The ISI (inter-stimulus interval) follows for 200 ms. The target is then present for a maximum of 2000 ms or the response time of the participant, whichever comes first. The heavy red lines in the panels of the second column represent cues. The small filled squares in the panels of the last two columns represent subsequent targets. The invalidly cued target illustrated at the right of the top row requires a within-object shift of attention from the preceding cue and likewise for the invalidly cued target in the third row. In contrast, the invalidly cued targets illustrated in the second and fourth rows require a between-objects shift of attention from the cue. (Image and description adapted from Egly et al., 1994)

Figure 1

OBA has been demonstrated extensively under a host of varying conditions. For example, it has been demonstrated to exist with occluded objects (Behrmann et al., 1998, 2000) and previously occluded objects (Moore & Fulton, 2005). Behrmann and colleagues (1998, 2000) demonstrated that the grouping heuristic of common fate leads to OBA in

occluded objects. They further theorized and demonstrated using computational modeling that perceptual learning and experience play an important role in determining what features are grouped together in forming perceptual objects. OBA exists in multiple-region objects when there is clear perceptual edge continuation between the regions, but disappears when the edge continuation is not well demarcated (Matsukura & Vecera, 2006). The OBA effect can be obtained with parallel lines and illusory contours (Avrahami, 1999, Moore et al., 1998), but the effect is substantially greater when the perceptual object's boundaries are closed (Marino & Scholl, 2005). Furthermore, corners of perceptual objects enhance onsetting stimuli near them more so than do straight edges (Cole et al., 2001). OBA exists when cued or primed endogenously via top-down goal-directed attention and exogenously via bottom-up stimulus driven attention (Watson & Kramer, 1999; Abrams & Law, 2000). OBA can even be directed across perceptual objects that cross the visual and auditory modalities (Turatto et al., 2005).

Studies have also tested and established the limits beyond which OBA disappears. For example, OBA has been demonstrated to evolve into inhibition of return (IOR) with longer stimulus onset asynchronies (SOAs) (List & Robertson, 2007). The advantage for the same object over the different object condition has been found to disappear when attention remained broadly or tightly focused due to task demands, as opposed to following an unconstrained spread along a perceptual object as might naturally occur in same-object perceptual processing (Lamy & Egeth, 2002, Goldsmith & Yeari, 2003). But in a flanker task, Chen & Cave (2006) were able to attain the OBA effect in the case where attention remained tightly focused given that the target's position was known with certainty. In their experiment, perceptual objects surrounding the target influenced how

quickly the target was accurately processed. When distractors in the same perceptual object flanked the target, accurate processing was slower than when distractors in different adjacent perceptual objects flanked the target. The same object advantage also disappears with lower cue validity than was utilized in the Egly and similar, subsequent experiments (He, 2004), and when the subject makes a pointing action to the cued part (Linell et al., 2005). OBA falls off with perceptual load as the distance from the cue increases (Ho & Atchley, 2009). Ho & Yeh (2009) attempted to determine whether it was the existence of the cued object that causes OBA, or the act of changing from the cue to the target that causes the effect. OBA was found to exist even when the object perceptually changed between the cue and target, but not if the object disappeared altogether in the target time frame, suggesting that the OBA effect is due to both the existence of the object and the change from the cue to the target.

Brian Scholl in 2001 published a comprehensive review of the state of the art of objects and attention. Particularly relevant to the present research was his conclusion that the "units" of attention could vary depending on the experimental paradigm, the nature of the stimuli, or the intentions of the observer. Likewise, in a more recent review, Hopf et al. (2005) concluded that depending on task demands, location-based, feature-based or object-based selection might be given temporal priority on a time scale of tens of milliseconds. In summary, the evidence suggests that OBA is a robust phenomenon as evidenced in behavior, but at the same time it is but one of several mechanisms that operate in the attentional selection of visual stimuli for subsequent cognitive processing. The challenge in the present dissertation is to replicate OBA behavioral results while at the

same time exploring its neural underpinnings in time and space. Relevant neural correlate studies are reviewed in the next section.

1.1.2 Neural correlate studies

A fronto-parietal-occipital network has been established in extant literature as subserving the cognitive process of visual attention, including OBA. For example, Roelfsema et al. (1998) found that V1 neurons with receptive fields that fall along a line segment of a curve simultaneously exhibit enhanced firing rates, suggesting a neural correlate of processing according to Gestalt principle of continuity in primary visual cortex, and Gestalt principles have been shown to be instrumental in OBA (e.g. Behrmann et al., 1998). In functional magnetic resonance imaging (fMRI) studies of OBA, the superior parietal lobule (SPL) has been observed to exhibit a transient increase in blood-oxygen-level-dependent (BOLD) response during shifts of OBA similar to that observed in spatial attention (Yantis & Serences, 2003). The left posterior parietal cortex (PPC) was found to mediate attention in that BOLD was more active for shifts within than between objects (Shomstein & Behrmann, 2006). A combined ERP (event-related potential)/fMRI study identified the lateral occipital complex (LOC) as the source of N1 component (160-190 ms) enhancement during OBA and space-based attention (Martinez et al., 2006, 2007). Frontal and parietal areas modulate occipital areas as indexed by theta θ frequency (4-7Hz) neuronal activity (Green & McDonald, 2008).

In summary, a fronto-parietal-occipital network has been established to subserve OBA. Modulation of the N1 attentional component because of OBA relative to SBA has been observed and localized to the LOC. Finally, theta activity has been established to be a communication mechanism in the network for SBA. It remains to be determined whether

theta activity is associated with OBA communication as well. One goal of the present dissertation research is to replicate the findings that a distributed neural network subserves OBA, and furthermore, to establish the role of theta activity in communication within this network.

1.1.3 Time domain studies

OBA has been investigated in the time domain. Martinez and colleagues (2006) found that the N1 attentional component (160-190ms) is modulated by both SBA and OBA, while P1 (80-120ms) is modulated only by SBA. Hopfinger & Mangun (2008) determined that reflexive (bottom-up) attention modulates the P1 attentional component in extrastriate cortex.

Roelfsema et al., (2007) established a time course for selective attention: at 48 ms latency from stimulus onset, V1 neurons register features, at 57 ms latency they segregate figures from the background, and at 147ms latency, the neurons select relevant features over irrelevant ones for further cognitive processing. Saalmann et al. (2007) suggested that attentional signals flow from LIP to MT based on their observation that LIP exhibits a slight phase lead (5-7 ms at ~35 Hz) in the spike train coherence between LIP and MT during sustained attention. Herrington and Assad (2010) in single unit recordings in monkeys demonstrated that attentional modulation begins ~60 ms earlier in LIP than in MT, consistent with a top-down flow of attentional information. The time course and characteristics collectively established by these studies is for SBA. A goal of the present research is to set the groundwork for establishing the timecourse and its characteristics for OBA, vis-à-vis SBA.

1.1.4 Spectral content studies

There has been a rapid increase of studies particularly in MEG neuroimaging research characterizing the spectral content of the electro-magnetic brain signals modulated by attention. Three frequency ranges have emerged as being differentially important in attentional processing. The theta (θ) range (4-7 Hz), the alpha (α) range (8-12 Hz respectively), and the gamma (γ) range (30-80 Hz). Jensen and Mazaheri (2010) propose that alpha-band synchrony is instrumental in gating information to task relevant areas (see also Mathewson et al., 2009). Specifically, they suggest that increased alpha-activity in a given region is associated with inhibition of function in that region, so that only task-relevant areas are involved in the functional architecture underlying a given cognitive process. Green & McDonald (2008) demonstrated that θ (4-7Hz) activity in EEG is an indicator of attentional control: they show that parietal cortex provides the initial signals to shift attention by modulating activity in this frequency range. Chen (2003) also found that attention modulates magnetic brain signals in the θ-α range. Yamagishi et al., (2003) localized this activity to the calcarine & parieto-occipital cortex. In the gamma range, the attention-gamma hypothesis proposes that synchronized gamma band (40-70Hz) activity mediates attentional processing (Jensen et al., 2007; Bauer et al., 2009). Fries (2001) demonstrated that neurons activated by the attended stimulus have increased gamma activity (35-90Hz) in V4 compared to unattended distractors. In contrast, Tallon-Baudry et al. (2005) recorded local field potentials (LFPs) intracortically in human epileptic subject during pre-surgical screening. LFPs were in response to an attended or unattended shape stimulus. Two regions consistently showed gamma-frequency synchronization (the fusiform gyrus and the lateral occipital sulcus) in response to attended versus unattended

stimuli. Muller et al. (1996) found stronger induced gamma oscillations in human EEG recordings in response to a attended single moving bar than in two bars moving incoherently in the opposite direction (such that attention is not on one or the other). Chalk et al. (2010) found that attention reduces stimulus-driven gamma frequency (30-50Hz) oscillations and spike field coherence in V1. Whether increased or decreased oscillatory activity, what is clear is that attention modulates oscillatory activity in the gamma range. Although primarily established for SBA, these studies collectively suggest candidate mechanisms for network communication during OBA. The primary goal of the present research is to establish the role these mechanisms have in OBA relative to SBA.

1.1.5 Novel theories of attention and object representation

The increasingly interdisciplinary study of attention using behavioral, temporal- and spectral-analysis approaches has given rise to novel theories of attention and object representation within the past ten years. Fries (2001, 2005) suggested that selective attention is the mechanism underlying dynamic control of effective interaction of long-range neuronal communication. The work of Womelsdorf et al., (2006); Womelsdorf & Fries, (2007); and Womelsdorf et al., (2007) theorized that attention regulates neuronal synchronization and is the basic computational mechanism that underlies dynamic cognitive control. Gross et al., (2004) theorized that the visual attention network communicates by neural phase synchronization. This work as well as that of Varela et al., 2001) contended that while local processing can be assessed by amplitude modulation (as is done in many ERP studies on attention), distributed processing of a network can only be assessed by phase synchronization. This theory is consistent with the work of von Stein and Sarnthein (von Stein & Sarnthein, 2000b) who suggested that different frequencies are

essential for different scales of cortical communication-integration, specifically that gamma synchrony is important for local processing while alpha/theta synchronization plays a role in longer range communication. Palva et al., (2005) proposed that gamma-band synchrony is essential for feedforward/bottom-up communication while α-band synchrony is essential for feedback/top-down synchrony. Engel et al., (2001) asserted that neural synchrony with millisecond range precision is crucial for object representation and attention. We know that a fronto-parietal-occipital network has been established in extant literature as subserving the cognitive process of visual attention, including OBA. What remains to be investigated is how communication through this network is accomplished, how OBA differs from SBA, and what are the characteristics of OBA in particular. These studies suggest that short and long-range communication via frequency synchronization and cross-frequency phase-locking might be the mechanism for communication in the attentional fronto-parietal-occipital network.

1.1.6 Theta-band frequency and information processing / communication

As in extant literature, in the present research there are three frequency bands of particular interest: the theta θ-band (center frequency 5 Hz), alpha α-band (center frequency 10 Hz), and the gamma γ-band (30-80Hz). While consistent roles have been ascribed to alpha and gamma frequencies in extant literature (the alpha gating/inhibition theory, and the gamma attention theory), theta band has been implicated in a myriad of cognitive functions. To start, theta waves have been implicated in information processing between the amygdala and the hippocampus in memory retrieval and consolidation in rats (Karashima et al., 2010). Neurons within rats' orbitofrontal cortex are phase-locked in the theta range in anticipation of a reward (van Wingerden et al., 2010), and theta activity has

been found within the hippocampus (CA1 to CA3 and vice-versa) in rats running for a reward (Diba & Buzsaki, 2008). In a study of the role of cortico-amygdala projections in emotional learning, long term potentiation (LTP) was produced by theta bursts in the rat ventral perirhinal cortex (vPRC) (Yaniv & Richter Levine, 2000). Theta activity has been implicated in associative learning during fear conditioning in mice (Seidenbecher et al., 2003); and in gerbils subjected to tone-conditioned avoidance training, theta activity in medial pre-frontal cortex was negatively correlated with increased learning, suggesting that theta decrease (increase) reflects decreasing (increasing) demands on information processing (Stark et al., 2007).

In humans, theta activity has been implicated in synchronization within the amygdala, and in communications between the amygdala and neocortex in the processing of negative affect words in humans (Garolera et al., 2007); within prefrontal cortex (medial to lateral and vice-versa) as part of an action-monitoring network where error signals are needed for increased cognitive control (Cavanagh et al., 2009); between the hippocampus and neocortex during goal conflict resolution (as reported in Moore et al., 2008); and widespread across the neocortex in continuous monitoring of a target detection task where period goal conflicts were introduced (Moore et al., 2006). Increased theta power and coherence has been implicated in episodic memory recall (Sato & Yamaguchi, 2007), and has been found to be phase-locked between the prefrontal cortex and the hippocampus in support of working and episodic memory tasks (Jensen, 2005). Prefrontal to medial temporal cortex communication in the theta range has also been found in epilepsy patients during recall (Anderson et al., 2010).

In summary, it is clear that theta θ activity is implicated in a myriad of cognitive functions across both subcortical and cortical areas. Cognitive functions include working and episodic memory, memory retrieval and consolidation, long term potentiation (LTP), associative learning, fear conditioning and negative affect, reward processing, cognitive control, goal conflict resolution and target detection. Subcortical brain areas include the amygdala, hippocampus, and perirhinal cortex. Specific cortical areas include medial and lateral pre-frontal cortex, orbitofrontal cortex and temporal cortex. In a few studies theta activity is found to be widespread across the neocortex. In a review, Kahana et al., (2001) proposed that θ-band oscillations have a primary role in information processing and communications for the cognitive function for which the given specific distributed network is specialized. What the cognitive functions discussed above have in common, is information processing and synchronized communication between neuronal groups within and between subcortical and cortical areas. It indeed may be that theta θ activity is a key architectural mechanism underlying information processing and synchronized communication in a given cognitive function for which the given network is specialized. This theta θ-band "communication" theory is discussed below in section Dual Theoretical Frameworks.

1.2 Summary and Motivation

These studies collectively suggest that the next generation of attention research will include considering attention as a basic mechanism underlying cognitive control, that involves the formation of dynamic networks in which there is critical and differential involvement of oscillation frequency. Furthermore, it remains to be determined how OBA vis-a-vis SBA is manifest in this basic mechanism.

My dissertation research "The Microgenesis of Object-based vis-à-vis Space-based Visual Attention", is intended to address in part how these two forms of attention are manifest as such a basic cognitive mechanism. I presume the overarching theoretical framework that dynamic neuronal networks communicating via oscillating frequencies is the mechanism underlying attention. I present dual detailed theoretical frameworks based upon extant literature, the specific paradigm and a contrast used here. Then, I characterize the electromagnetic fields present in scalp surface recordings during visual attention cognitive processing with respect to this framework. I describe the nature of how these attention processes unfold over time, differentially across the brain, and how their composition change over time and space.

1.3 Dual Theoretical Frameworks

Two theoretical frameworks provide the basis for analysis and interpretation in the present research. The first is based on EEG/ERP research traditions and employs analysis predominantly in the time domain. The second is developed from research traditions using MEG and employs analysis primarily in the frequency domain.

The first is built on the theoretical framework of the classic ERP method (e.g. Luck, 2005). Here the EEG/ERP activity is meaningful in terms of "components". A component is assumed to be a manifestation of neurophysiologic activity that corresponds to some psychological process. (See appendix A.4 ERP "Components" for additional definitions of what constitutes a "component"). Scientific inquiry is about identifying components and establishing how they are modulated given different conditions. Much less often is scientific inquiry in the ERP approach is about understanding the neural underpinnings of

these components[1] (i.e. localizing the activity to a neural location) beyond observing which electrodes at which a given component is the strongest. In this first framework for the present dissertation research, the goal is to be faithful to this perspective, hence the focus will be on the components, and at which electrodes they are significant. Specifically, the focus is on the classic attention components: P1 (80 – 120 ms) and N1 (160 – 190ms) post target onset respectively, and the goal is to identify posterior electrodes at which they are significant. Analyses presented here test the hypothesis that different conditions will differentially modulate the P1 and N1 attentional components. Martinez at al. (2006) had demonstrated that SBA modulates the P1 and N1 components (i.e. they are significantly different in positive and negative amplitude respectively), while OBA modulates only the N1 component[2]. Consider the impact the Egly et al., (1994) paradigm (Figure 1) has on ERP generation over the course of a trial (Figure 2). First two rectangles appear on either side of a center fixation (Figure 2 (a)). This appearance causes the typical visual ERP waveform to be evoked. This waveform resolves within 1000 ms. A red cue then appears for 100 ms (Figure 2(b)). The cue appearance evokes the visual ERP waveform again. Three-hundred ms after cue onset, the target appears, and evokes a new ERP (Figure 2(c)). The P1 and N1 components of the target evoked ERP are the components of interest (circled in red). Different target placement relative to the previous cue placement corresponds to different conditions (e.g. valid, same object invalid, different object invalid), which are hypothesized to modulate the target P1 and N1 components differently. In contrasting two conditions, the hypothesis (based on the findings of Martinez et al., 2006) that different conditions

[1] At the 2009 ERP Bootcamp, camp director Steve Luck stated that ERP is not a neuroimaging technique, but rather a tool for psychological scientific inquiry. He was also skeptical about efforts to localize the neural sources of the ERP.

[2] Their paradigm was similar to Egly-style paradigms, in that it is presumed that ERP modulations of the P1 and N1 component post target onset reflect space-based or object-based attentional spread that presumably occurred just prior, between cue onset and target onset.

differentially modulate the P1 and N1 attentional components is tested: specifically that SBA (tested by contrasting valid with invalid, or valid with DO) modulates both P1 and N1; and that OBA (tested by contrasting SO with DO) modulates the N1 component. This hypothesis is tested in both EEG and MEG in section 4. Temporal Analysis. For reference, this first theoretical framework will be referred to as the "Egly-inspired ERP microgenesis" or "EiEM" framework.

Microgenesis of a Trial in an Egly-inspired Paradigm, In Terms of the Idealized ERP

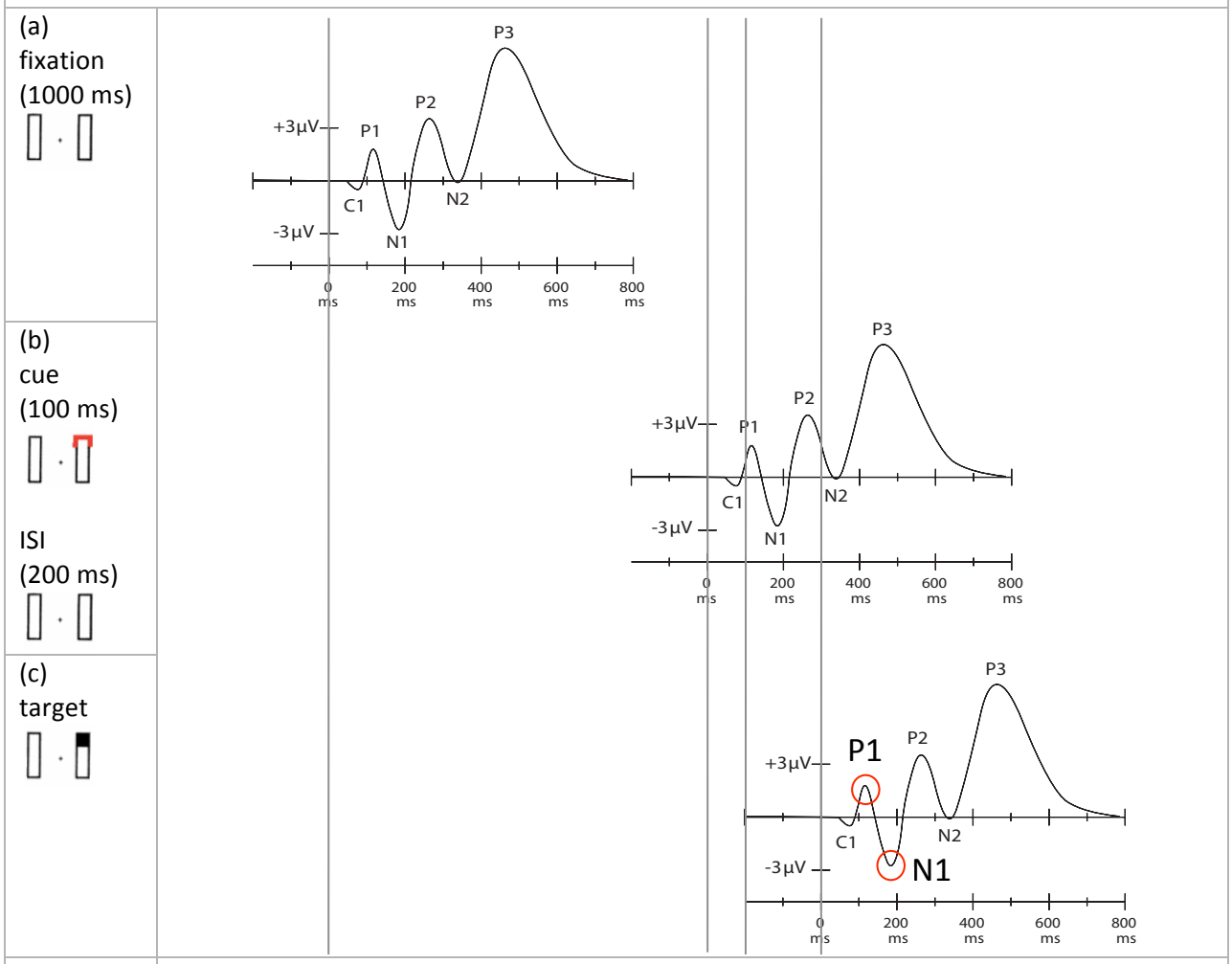

(a) the appearance of fixation will cause the typical visual ERP waveform to be evoked. (b) 1000 ms later the cue will appear for 100 ms causing a second typical visual ERP waveform to be evoked. (c) 300 ms after cue onset the target will appear, again causing the typical visual ERP waveform to be evoked. The P1 and N1 components (circled in red) of the target ERP waveform are of interest, as they are expected to be modulated differently by different conditions. Note that the P1 and N1 components of the target ERP are convolved with the cue ERP P3 component. The practical implication is that the target P1 and N1 components will not have the typical shape (e.g. positive and negative latencies). But since this convolution occurs across all conditions effectively equally, it is controlled for in analysis that contrasts conditions as in the ANOVA analysis done here.

Figure 2

The second theoretical framework is suited to elucidating how attentional processing is manifest in time, space and spectral content; and in distinguishing aspects of attentional processing along these dimensions. As discussed in 1.1.4 Spectral content studies, three frequency ranges have emerged as being differentially important in attention. The theta (θ) range (4-7 Hz), the alpha (α) range (8-12 Hz), and the gamma (γ)

range (30-90 Hz). Theta has been associated with attentional control (Green & McDonald, 2008); and it is proposed to be a carrier frequency enabling long range phase synchronization and communication at higher frequencies between distant brain areas (Canolty et al., 2006): for example, between hemispheres, or from anterior to more posterior areas. Alpha is hypothesized to have a role in inhibition of task irrelevant areas (Mathewson et al;, 2009; Jensen & Mazaheri, 2010); Gamma is associated with feature binding (Bertrand, 2000; Palva et al., 2005; Fries, 2007), and attention (Muller et al., 1996; Fries et al. 2001; Tallon-Baudry et al., 2005). It is possible to build a theory of time-space-frequency processing from this literature and to hypothesize how it will manifest along these dimensions. Here, I focus on a condition contrast that tests for OBA when shifts of attention from cue to target are controlled to be within a hemifield. In this contrast, shifts between different objects (DO condition) in horizontal rectangles are contrast with shifts within a single object (SO condition) in vertical rectangles as schematized in Figure 3. The motivation for this contrast will be discussed fully in subsequent section 3.2.5 Condition Contrasts used in the analysis. Here, the contrast is used to theorize how OBA may manifest in spectral power in the gamma, theta and alpha frequency ranges.

First, consider the gamma attention theory. Induced gamma activity is associated with attended versus unattended stimuli[3]. Given that in our contrast, conditions are attended (SO and DO although different, are both attended conditions), induced gamma activity should exist, but is hypothesized to not be significantly different between the two

[3] In Muller et al. (1996), the unattended condition consisted of two bars moving incoherently in opposite directions so that attention would not be focused on one or the other; In Fries et al. (2001), monkeys attended to relevant stimulus, while ignoring an irrelevant one (attention is never focused on the irrelevant stimulus over the course of a trial); In Tallon-Baudry et al., (2005), in the unattended condition the shape on the screen is never attended to over the course of the trial because it is irrelevant to the task of specifying the color change in the fixation cross.

attended in either left or right targets (Figure 5 γ). Furthermore, since induced gamma is not phase-locked to the stimulus, significance would not be apparent in conventional averaging techniques (such as that used in the ANOVA analysis here)[4]. To test for gamma significance a paradigm that contrasts attended with non-attended stimuli, and/or alternative statistical testing would have to be conducted.

Next consider the alpha inhibition/gating theory. Since the role of attention is to select a subset of the visual stimuli for further cognitive processing, it is hypothesized that alpha activity will inhibit non-attended visual stimuli from further processing. If we further theorize that attention is more easily spread within a perceptual object than between two perceptual objects, then inhibition for within object processing must be stronger when such processing is task irrelevant. Therefore the hypothesis is that alpha activity is significantly greater in SO than DO everywhere except in the specific areas associated with processing the attended stimuli (Figure 5 α).

[4] When electromagnetic signals are phase-locked to stimulus onset (i.e. they are "evoked"), the first peak occurs, from trial to trial, at very nearly the same time after stimulus onset. When electromagnetic signal oscillations are induced, they emerge, each trial in possibly a different phase relative to target onset. The peaks and troughs may not correspond across trials; hence averaging across trials is ineffective.

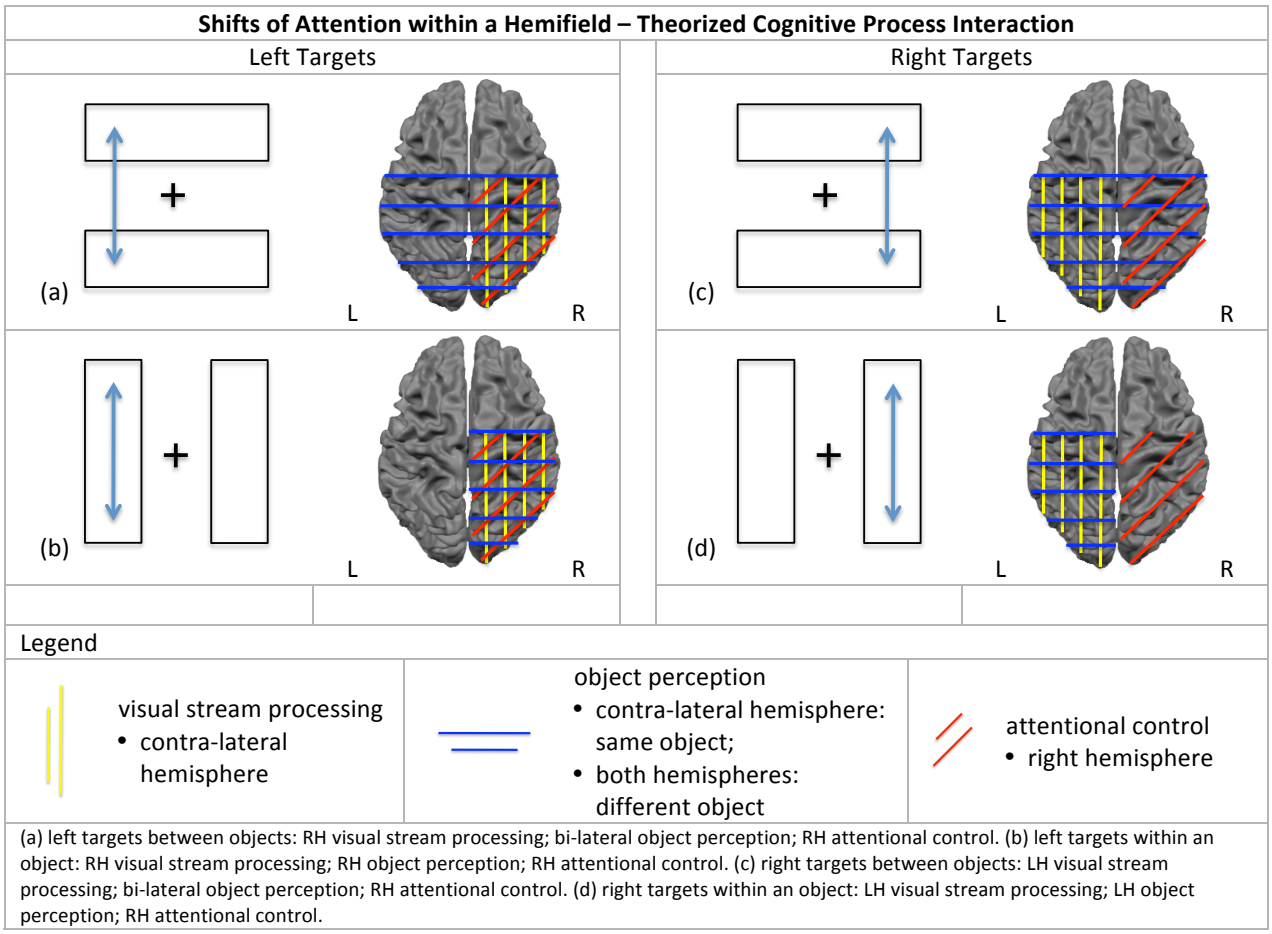

Figure 3

Finally consider the theta long-range communication theory. Theta activity should he higher when communication is necessary between hemispheres and/or between anterior and posterior areas than within a hemisphere. To theorize the strength of theta activity necessary to process a given stimulus, I hypothesize that cognitive processes may be additive and combined differentially to meet the visual processing task at hand. Specifically, I hypothesize three additive cognitive processes: visual perception/visual stream processing; object perception; and attentional control. I consider the hypothetical additive nature of object perception over and above early visual stream processing in primary cortex, and the hypothetical additive nature of attention to either or both of these cognitive processes. In this way, it is possible to allocate to each the "amount" of

communication resources needed for these processes to work together depending where the locus of their control resides.

Consider the four visual processing tasks represented in Figure 3. When shifts of attention between the cue and target are controlled to be within the left hemifield, these visual stream stimuli are processed in the contralateral right hemisphere (yellow vertical bars in Figure 3(a) and (b)). When shifts of attention are controlled to be within the right hemifield, the visual stream stimuli are processed in the contralateral left hemisphere (yellow vertical bars in Figure 3(c) and (d)). If we consider object perception as an additive process to visual perception/visual stream-processing, then in the case a perceptual object lies within a hemifield, we can theorize that object perception resides in the contra-lateral hemifield (blue horizontal bars in Figure 3(b) and (d)). In the case that the perceptual object crosses hemifields, then we can consider object perception to employed in both hemispheres (Figure 3(a) and (c)). The right hemisphere however, is believed to be dominant for attentional processing (Corbetta & Shulman, 2002) for stimuli in both hemifields (red up diagonal bars in (a) through (d)).

Shifts of Attention within a Hemifield - Theorized Communication Cost in the Theta Band				
(a) Left targets, horizontal display DO	attentional communication cost		(c) Right targets, horizontal display DO	attentional communication cost
visual stream processing: RH	0		visual stream processing: LH	1
object perception: both, RH to LH	½		object perception: both, LH to RH	1/2
attentional control: RH	na		attentional control: RH	na
Total	½		Total	1 ½
(b) Left targets, vertical display SO			(d) Right targets, vertical display SO	
visual stream processing: RH	0		visual stream processing: LH	1
object perception: RH	0		object perception: LH	1
attentional control: RH	na		attentional control: RH	na
Total	0		Total	2
SO < DO			**SO > DO**	

(a) left targets between objects: RH attentional control cost of communication with RH visual stream processing is 0, since both are within the same hemisphere and no long distance communication is needed. RH attentional control cost of communication with object perception is ½ since ½ of the perception is within the same hemisphere and the other half is other hemisphere. Total communication cost is ½. (b) left targets within an object: no long distance communication necessary between these processes, hence cost is 0. Therefore, for left targets SO costs less than DO, hence less theta communication power is needed: SO < DO. (c) right targets between objects: RH attentional control cost of communication with LH visual stream processing is 1, since communication occurs between hemispheres. RH attentional cost of communication with object perception is ½ since ½ of the perception is within the same hemisphere and the other half in the other hemisphere. Total communication cost is 1 ½. (d) right targets within an object: RH attentional communication cost with LH visual stream processing and with object perception is 1 for each, since communication crosses hemispheres. Total communication cost is 2. Therefore, for right targets SO cotst more than DO, hence more theta communication power is needed: SO > DO.

Figure 4

Shifts of Attention within a Hemifield – Theorized Frequency-Band Power Relationships				
Left Targets			Right Targets	
γ	not sig		γ	not sig
α	SO > DO except in task relevant areas: SO < DO		α	SO > DO except in task relevant areas: SO < DO
θ	SO < DO		θ	SO > DO

Left targets: no significant difference between SO and DO gamma-band power; SO significantly greater than DO in alpha-band power in posterior regions except those engaged in task processing; SO less than DO in theta-hand power. Right targets: no significant difference between SO and DO gamma-band power; SO significantly greater than DO in alpha-band power in posterior regions except those engaged in task processing; SO significantly greater than DO power in theta-band power.

Figure 5

To develop an index of relative communication necessary in the four tasks outlined above, consider the "communication cost" algorithm depicted in Figure 4. The idea is that the higher the cost of communication, the more theta power necessary to accomplish communication in the dynamic network. In the case of left targets in the horizontal display (Figure 4(a)): shifts of attention occur between the two rectangles (DO condition) in the

left hemifield (Figure 3 (a)). The cost of RH attentional control communication with RH visual stream processing is 0 (since both processes are within the same hemisphere), and the cost of RH attentional control of communication with object perception that starts in the RH and shifts to the LH is ½, since ½ of the object processing is in the same hemisphere and the other ½ is done contra-laterally. The total communication cost is thus ½. In the case of left targets in the vertical display (Figure 4(b)): shifts of attention occur within the rectangle object (SO condition) in the left hemifield (Figure 3(b)). The total cost is 0 since the locus of control of all three processes is in the RH: no long-distance communication is needed. In comparing the relative costs of shifting attention between different objects (a) versus within an object (b), the latter has less cost: therefore less theta power is necessary for SO vs. DO processing in left targets (Figure 5 θ, left targets). In the case of right targets in the horizontal display (Figure 4(c)): shifts of attention occur between two rectangles (DO condition) in the right hemifield (Figure 3(c)). The cost of RH attentional control communication with LH visual stream processing is 1 (since cross-hemisphere communication is needed), and the cost of RH attentional control of communication with object perception that starts in the LH and shifts to the RH is ½, since ½ of the object processing is in the same hemisphere and the other ½ is done contra-laterally. The total communication cost is thus 1 ½. In the case of right targets in the vertical display (Figure 4(d)): shifts of attention occur within the rectangle perceptual object (SO condition) in the right hemifield (Figure 3(d)). The cost of RH attentional control communication with LH visual stream processing is 1, and the cost of RH attentional control of communication with object perception is also 1 (since both require cross-hemisphere communication). The total communication cost is thus 2. Therefore, in comparing the relative costs of shifting

attention between different objects (c) versus within an object (d), the latter has greater cost:therefore more theta power is necessary for SO vs. DO processing in right targets (Figure 5 θ, right targets).

All three hypotheses schematized in Figure 5 will all be tested for MEG in section 5.2 MEG/ERMF: the hypothesis that induced gamma activity will be found to be not significantly different between conditions given the paradigm conditions and choice of ANOVA analysis; the alpha inhibition/gating hypothesis; and the theta communication hypothesis. For reference, this second theoretical framework will be referred to as the "Within-hemifield SO vis-à-vis DO spectral power", or "WhOBAP" framework.

2. Neurophysiology Methods

EEG/ERP (electroencephalography/event related potential) and MEG/ERMF (magnetoencephalography/event related magnetic field) are complementary cognitive neuroimaging techniques. While the subject is engaged in a sensory task (a visual attention task in the present research), EEG/ERP measures the electrical component of electromagnetic brain activity while MEG/ERMF measures the magnetic component. In this chapter I give a brief overview of the methods and analysis traditions of the two approaches as both motivate the analysis procedures adopted in the present research. I compare and contrast the characteristics of the signals as this overview provides the backdrop for interpreting EEG/ERP vis-à-vis MEG/ERMF results. Finally, I summarize how EEG/ERP and MEG/ERMF are analyzed in the present research with respect to this discussion. Throughout the remainder of the document, a simple reference to EEG will represent a reference to EEG/ERP in the appropriate context. Similarly a simple reference to MEG will represent a reference to MEG/ERMF.

2.1 EEG and MEG: complementary techniques

2.1.1 Characteristics of the signals

While the electric and magnetic brain signals are clearly related (the magnetic fields result from the existence of electrical dipoles due to brain activity), they have fundamentally different characteristics when measured as local field potentials (LFPs) from the surface of the skull. EEG signals are smeared when passing through the scalp and

skull, whereas magnetic signals are not. The result is that magnetic signals are much more focal in space and time. The measurement of a magnetic signal from one channel to a neighboring channel, or one time bin to the next, can yield different information, whereas in EEG, the same information can be available at a number of neighboring electrodes, and possibly multiple subsequent time bins[5].

The resulting EEG signal at any given electrode is fully dependent on the choice of reference electrode because electrical potentials are measured as the difference between two points, across a resistive medium: this creates the circuit from which the EEG is measured (Nunez & Srinivasan, 2005). In the component analysis ERP method born of the psychological tradition (Luck, 2005), the reference typically used is the average of the left and right mastoid. This average reference leads to the "typical" visual ERP waveform as shown in Figure 7(a). Note that this waveform is highly idealized in that the different components marked in the figure are actually best measured and most clearly visible at different electrodes. Furthermore, it is the case that when an EEG signal is re-referenced from one to a different electrode, the signal will change in amplitude, polarity and even in shape, as visualized in Figure 7(b).

In contrast, MEG signal measurements are made using SQUIDS (superconducting quantum interference devices), which are manufactured containing closed-loop circuits in each device. In an electrical sense, each SQUID has its own reference, so there is no equivalent concept in MEG of a separate reference node from the SQUID sensor. The SQUID measures the magnetic flux resulting from the electrical current that flows within the device's circuit (Fagaly, 2006). One can imagine then, that MEG may or may not show

[5] Discussion with Steve Luck at the ERP Bootcamp 2009, U.C. Davis re: focal nature of MEG versus EEG, and my empirical observation having conducted extensive exploratory analysis on both electrical and magnetic data.

similar “components” to the EEG signal as in Figure 7(a), since in an electrical sense, each SQUID has a different reference point in its closed-loop circuit from which the magnetic flux is measured.

Furthermore, electrical signals on the surface of the skull emanate from neuronal currents occurring both perpendicularly and tangential to the scalp surface (i.e. those occurring in the gyri and sulci respectively), whereas MEG signals emanate from magnetic fields associated with neuronal currents occurring only tangential to the scalp surface as pictured in Figure 6(a). Tangential currents occur in the sulci (Figure 6(b)). This is because magnetic fields surrounding tangential currents appear outside the scalp whereas fields surrounding perpendicular currents do not; rather the latter only exist inside the skull, where MEG sensors cannot measure them.

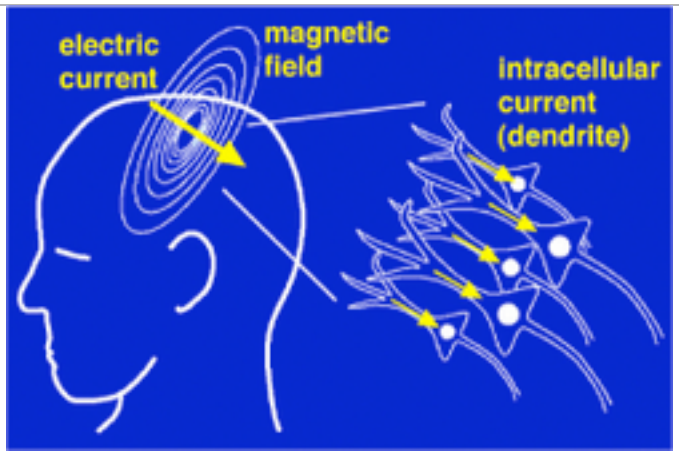

(a)

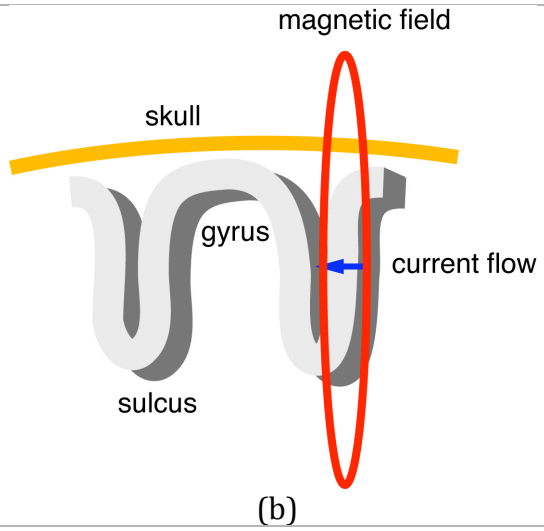

(b)

(a) MEG sensors measure magnetic fields associated with neuronal currents occurring tangential to the scalp surface. (image from www.websters-online-dictionary.org) (b) Tangential currents occur in the sulci. (image from www.neuroactivity.org)

Figure 6

In one early study that directly compares and contrasts the information available from EEG versus MEG recordings obtained concurrently, Cohen (1972) found that in an epileptic subject, theta θ waves that were visible in the EEG, were not in the MEG recording.

Two possible reasons are offered for this apparent discrepancy. First, the theta waves may have been due to EEG voltage when there are no currents (so there would be corresponding magnetic field). Second, there may have been nonzero theta currents that were symmetrically distributed such that they cancel, resulting in a zero external magnetic field. The point here is that it is possible that EEG and MEG will not reveal the same results even when they are clearly measuring the same activity.

Clearly the electrical signal measured by EEG, and the magnetic flux measured by MEG are borne of the same neurophysiologic process and are intimately related (c.f. Cohen, 1972; Hamalainen et al., 1993; Hansen et al., 2010). What is important to note here and to consider when evaluating the results, is because of the differences in the nature of the signals themselves and how they are impacted by the skull and scalp, and because of the different mechanisms for their measurement, the signal information available to EEG vis-à-vis MEG may differ in amplitude, polarity, shape, and frequency content, which in turn effect the timing and latency of positive and negative peaks in the waveforms.

Idealized and actual ERP waveforms

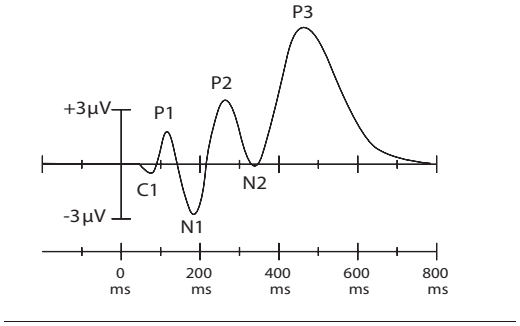

(a)

Image from ERP Bootcamp 2009, U.C. Davis

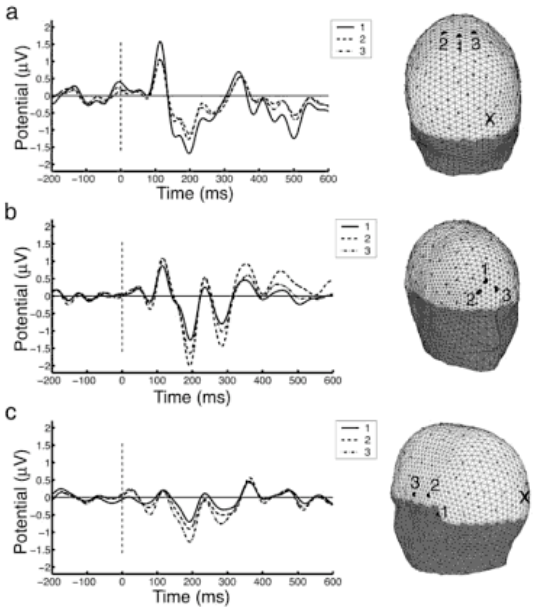

Image from Nunez & Srinivasan, 2005 (b)

(a) The idealized "typical" visual ERP waveform is observed when the electrodes are referenced to the average of the left and right mastoids (alternative reference schemes may also result in this waveform), and a given component is viewed at an electrode which best shows that component. (b) When a given electrode is referenced to different points, the ERP waveform measured at that electrode will change in amplitude, polarity and shape. The image depicts electrode O1 (marked with an X) referenced to each of three points on the top of the head (panel a), the front of the head (panel b) and the left side of the head (panel c).

Figure 7

2.1.2 Methods and Analysis Traditions

EEG has been prevalent in clinical endeavors since the 1970s and the modern era of ERP research began in 1964 when the first cognitive ERP component – the contingent negative variation (CNV) was reported (Swartz & Goldensohn, 1998; Luck, 2005). In contrast, MEG is a relatively new research neuroimaging technique that started gaining momentum about the turn of the century. Perhaps for this reason, at least in part, they have different analyses traditions. One dominant ERP technique is primarily concerned with analyzing the electrical brain signals in the time domain, by identifying signal "components" that are viewed as markers of cognitive processes (for example the N1 and

P1 components are presumed to be markers of the cognitive process of attention)[6], where N1 and P1 refer to the modulation of the signal within a particular time window post stimulus onset and the sign of the signal (N=negative, P= positive). A robust set of literature has been established using component analysis in the time domain, and a respected methods handbook has been written (Luck, 2005). The statistical tool of choice is often ANOVA with the dependent measure being the mean amplitude of the signal in a given latency window. Oftentimes, the signal from a single electrode or perhaps pair of electrodes is chosen for the analysis if the desired component is present (e.g. there is a large peak or mean amplitude increase/decrease in known component time-frames compared to baseline). Some investigators perform an ANOVA for each electrode site, while others will include electrode site as a factor in a single ANOVA. In contrast with the components-based approach, alternative analytic procedures can be utilized. In another methods handbook edited by Handy et al. (2005), Otten and Rugg compare and contrast "component" analysis with "non-component" approaches to ERP analysis. The authors discuss that to do component analysis is to make inferences based on prior knowledge and the presumption that components represent underlying cognitive processes. In contrast, a non-component analysis concentrates on whether there are differences between conditions at **any** time point independently of the shape of the waveform of when these differences start and end across time, and regardless of the exact neural source of the signal (Otten and Rugg, 2005). Non-component analysis can be done using a myriad of statistical analytical procedures borrowed from the fields of statistics and engineering: particularly the engineering sub-field of signal processing.

[6] A more detailed discussion of what constitutes an ERP component is given in Appendix A.4 ERP "Components".

Investigations over the past ten years often take advantage of the newer engineering and statistical advances in analysis methods. Analyses are predominantly conducted in the frequency domain, and there is neither one method nor one statistical tool of choice. As one example, consider the research of Gross et al. (2004), whose approach the present research roughly parallels up to a point. Given subject data from a RSVP paradigm with two conditions, the time frequency representations (using Morlet wavelets) of the correct, baseline-normalized trials (lock to target onset) over all the sensors were computed. The frequency of strongest target activity was identified (Beta 13-18). Subsequent analysis focused on this frequency band. The cross-spectral density of all combinations of channels was then computed: this information was used in DICS (dynamic imaging of coherent sources) source localization. Synchronization analysis was performed on the wavelet transforms with the goal of identifying signal phase coupling between regions. Finally significance was ascertained using the Kruskal-Wallis non-parametric form of ANOVA statistical analysis. As a second example, consider the work of Pavlova et al. (2006) that studied attention effects on biological motion using MEG. The two conditions of interest were attended and unattended point-light walkers. First a broad-band spectral power analysis was conducted and the frequency band with significant changes in MEG activity was identified (~25 Hz). Then a narrow-band acausal Gaussian shaped Gabor filter with center frequency 25 +/- 5 Hz was applied. To assess the time course of this narrow-band activity, an amplitude demodulation using a Hilbert transformation was then used. Finally, significance between conditions was assessed using a statistical probability

mapping approach based on permutation tests that corrected for both multiple comparisons and possible correlations in the data.

In these newer investigations, there is no singular approach that is adopted across individual researchers or research teams. Rather, researchers pull from a toolbox of analytical techniques to apply given the unique characteristics of the research problem at hand. A possible reason for this is the increasing interdisciplinary involvement of different fields: from engineering to statistics and computer science, to physics to psychology.

2.1.3 Source Localization

Localizing the neural source of electrical or magnetic signals involves using sophisticated mathematical techniques to identify the primary current source distributions (the unknown) given the distribution of electromagnetic activity on the scalp (which is visible and measurable). Solving this problem is considered to be "ill-defined" in mathematical terms, meaning that there are an infinite number of solutions. It is not possible to positively identify the neural source of electrical or magnetic activity given what can be measured at the scalp.

It is the case however, that using electrical and magnetic information together during source localization constrains the solution space, which means that while it may still be large, there is a finite (as opposed to infinite) number of solutions. Furthermore, the more sources of converging information, the more constrained the solution space. Sources of converging information range from the consideration of related EEG and/or fMRI/MRI results to the use of a priori knowledge in choosing the likely solutions. One method that can use EEG and MEG data together with structural MRI is minimum norm estimation

(MNE), which is an application of estimation theory[7] to the specific problem of determining primary current distributions from measured electromagnetic fields (Hamalainen & Iimonieme, 1994). In this procedure, essentially nothing is assumed about the source currents, except that they are spatially restricted to a given region. Another method is dynamical statistical parametric map (dSPM) modeling. While standard MNE modeling represent results in terms of baseline-subtracted current distribution, dSPM respresents results in terms of signal-to-noise ratios. The noise used in dSPM is estimated from the measured data (Jensen & Hesse, 2010). In dSPM the source estimation is performed for each trial after filtering with a complex Morlet wavelet. A third method is low-resolution brain electromagnetic tomography (sLORETA), which is another variation of the noise-normalized MNE. There are other source localization methods available, discussion of which is beyond the scope of the present dissertation research. Furthermore, the endeavor to identify ever-better source localization methods for MEG and EEG data is an active area of research in statistics and related fields.

The present dissertation research employs MNE, dSPM and sLORETA modeling techniques, as implemented in MNE Suite (Martinos Center for Biomedical Imaging, Harvard University) on the MEG and EEG data together with high resolution T1-weighted MRI structural scans.

2.2 EEG and MEG in the present research

The methods and analysis approach adopted in the present research combines the contrasting EEG and MEG traditions discussed above. In the ERP analysis, the focus is on

[7] Estimation theory is a branch of statistics concerned with extracting parameters from noise-corrupted observations. (definition source: www.math.harvard.edu/~knill/sofia/data/statistics.pdf).

results that occur in the P1 and N1 attentional component time frames: these results are compared with OBA research that uses component analysis. However, the analyses here extend beyond traditional component analysis in using sliding latency windows for a non-component approach in which the entire time course is examined and explored. The primary statistical tool of choice to statistically compare experimental conditions is ANOVA: this is done in order to be comparable to the cognitive science research borne out of the tradition of cognitive psychology[8]. Furthermore, research results in the cognitive psychology tradition are typically conducted only in the time domain (e.g. reaction time in behavioral results, latency windows in ERP analysis). Borrowing from the MEG research stream however, spectral analysis is considered of import in addition to temporal analysis in the present research. To that end, mathematical wavelet analysis is used to elucidate spectral information. Finally, as discussed above, to localize the primary current distribution source(s) of the measured electromagnetic fields, three estimation methods are employed: MNE, dSPM and sLORETA, as implemented in MNE Suite (Martinos Center for Biomedical Imaging, Harvard University). These methods are used given the EEG and MEG data together with high resolution T1-weighted structural MRI.

[8] Comparing conditions is testing the hypothesis that one condition is significantly different from another. There exist numerous statistical methods for hypothesis testing. Specific examples include linear regression, the bootstrap, the Welch test, Brown and Forsythe test, and the Kruskal-Wallis test, and the inverse normal scores tests (c.f. Efron & Tibshirani, 1994; Tomarken, & Serlin, 1986). ANOVA analysis is most popular in the field of psychology.

3. Experiment: Classic Egly Paradigm

3.1 Methods

3.1.1 The paradigm

The Egly paradigm is adopted in the present research because of its robust ability to elicit OBA (recall from the discussion in section 1.1.1 Behavioral studies that the presumption is that object-based effects resulting after cue onset can be observed after subsequent presentation of the target in the form of faster RTs for targets in the same perceptual object as the cue, than for targets in a different perceptual object). Observers performed target discrimination (rather than detection as in the original study). This means that a response is offered on every trial. The target was either a "T" or "L" which was presented in one of four orientations: 0, 90, 180 or 270 degrees at one end of one rectangle, along with distractors at the remaining three ends. The subject was instructed to press the button on the left response pad[9] for a "T" and the button on the right response pad for a "L". All stimuli were white on a black background, and the cue was red, as shown in the schematic of the three conditions in Figure 8. Vertical and horizontal displays were used and rectangle orientation served as a between-subject variable. There were three conditions: the valid condition in which the trial appeared in the same location as the previous cue, the same object (SO) invalid condition in which the target appeared across or down/up (horizontal or vertical displays respectively) in the same rectangle object as the

[9] The response recording system for the Elekta Neuromag includes two independent, one-finger optical response pads (lift/press).

cue, and the different object (DO) invalid condition in which the target appeared across or down/up (vertical or horizontal displays respectively) in the non-cued rectangle object. In a trial, fixation was present for 1000 ms, then the cue was present for 100 ms. The ISI (inter-stimulus interval) followed for 200 ms. The target was then present for a maximum of 2000 ms or the response time of the participant, whichever came first. The distance between the center of mass of each of the cue and the target in invalid condition trials, and between the target and the two distractors' across and down/up (vertical and horizontal displays respectively) was 5.5 cm. The distance from the subject's eyes to the projector screen was 119.38 cm. The stimuli thus subtended a visual angle of 2.64°.

Experimental Paradigm Conditions

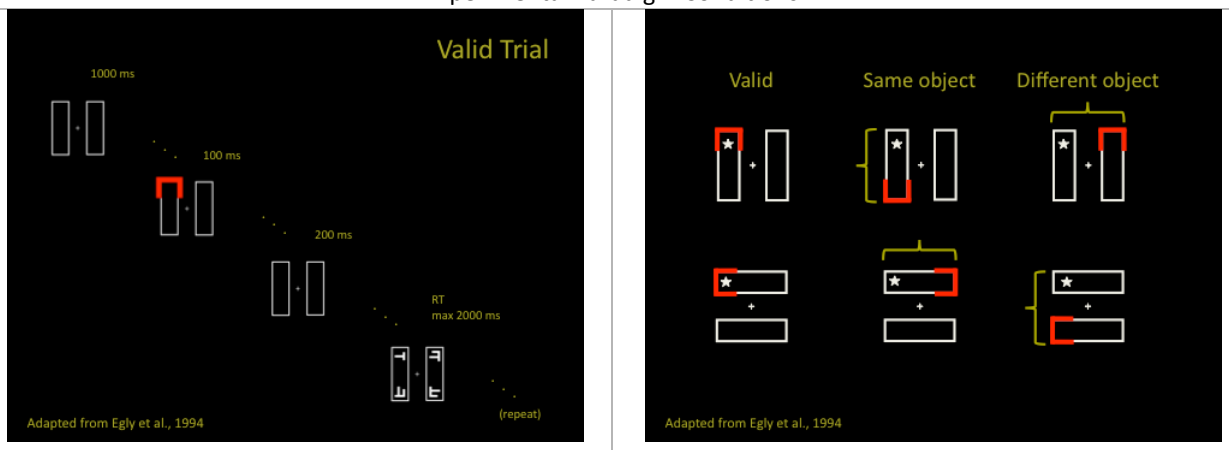

The experimental paradigm was adapted from Egly et al., (1994) and had three conditions: in the valid condition (a), the target (T or L oriented 0, 90, 180, 270 degrees) appeared at the same location as the previous cue (red flash at one end of one rectangle). Distractors filled the other three ends. (b) In the same object condition (b) the target appeared in the same perceptual object, but at the opposite end as the previous cue. In the difference object condition, the target appeared in the other perceptual object straight across from the previous cue (vertical displays) or up/down from the previous cue (horizontal displays – not shown). In all condition, fixation was present for 1000 ms, followed by the cue which was present for 100 ms. The ISI (inter-stimulus interval) followed for 200 ms. The target was then present for a maximum of 2000 ms or the response time of the participant, whichever came first. In all conditions, the distance between the four possible target/distractor locations (upper left, upper right, lower right, lower left) was the same.

Figure 8

3.1.2 Participants

Eighteen subjects performed the experiment while undergoing a MEG/EEG scan. Half the subjects performed the experiment with vertical displays, while the other half

performed the experiment with horizontal displays. Each subject performed two runs in one scanning session, and the location of the head relative to the sensors in the MEG scanner was measured prior to each run (these measurements are used in the pre-processing software discussed below, and in the co-registration process for source localization discussed in 6. Source Localization). Each run consisted of four blocks of 112 trials: 64 (57.14%) Valid trials, 24 (21.43%) SO trials, and 24 (21.43%) DO trials. Between each block there was a break, the length of time of which was controlled by the subject. Thus each subject completed 896 trials over 8 blocks across 2 runs in one of the horizontal or vertical display conditions.

3.1.3 MEG and EEG acquisition protocol

All 18 participants were scanned on the Elekta Neuromag® Vectorview (Helsinki, Finland) system at the University of Pittsburgh Medical School (UPMC) Brain Mapping Center. The participant sat in an upright position and the sensor helmet was lowered over their head (Figure 9a). Encased in the helmet are 306 magnetoencephalography (MEG) channels (102 magnetometers, 204 planar gradiometers) as schematized in Figure 9b. Applied to the participant's head and chest prior to entering the scanner were 19 Electroencephalography **(**EEG) channels using a modified 10-20-system montage and a left mastoid reference, two electrooculography (EOG) channels and 1 electrocardiography (ECG) channel. The MEG and EEG channels together measured the electromagnetic signatures of the subject's intracranial ionic currents associated with brain function. The EEG was recorded using reusable silver electrode disks with silicone-coated lead wires. A small amount of electrode cream was used under each disk placed on the head and situated with gauze pads together with Collodion adhesive. The two EOG channels measured the

electrical signals due to eye movements: horizontal eye movements were monitored via electrodes at the left and right outer canthi; blinks were recorded with electrodes above and below the left eye. The ECG channel measured cardiac artifacts. The EOG and ECG electrodes were affixed in place with tape. Data was acquired at a sampling rate of 1000 Hz and band-pass filtered between 0.01 and 330Hz by the acquisition system. The detailed sensor and electrode layouts for MEG and EEG are given in Appendix A (Figure 34 and Figure 33 respectively). Visual stimuli were delivered on a Microsoft Windows® system using E-Prime® software (Psychology Software Tools, Inc., Pittsburgh, PA, USA). A Panasonic® PT-D7700 premium projector (Panasonic Corporation of North America, Secaucus, NJ, USA) was used for the visual presentation.

The Elekta Neuromag ® Magnetoencephalography (MEG) system

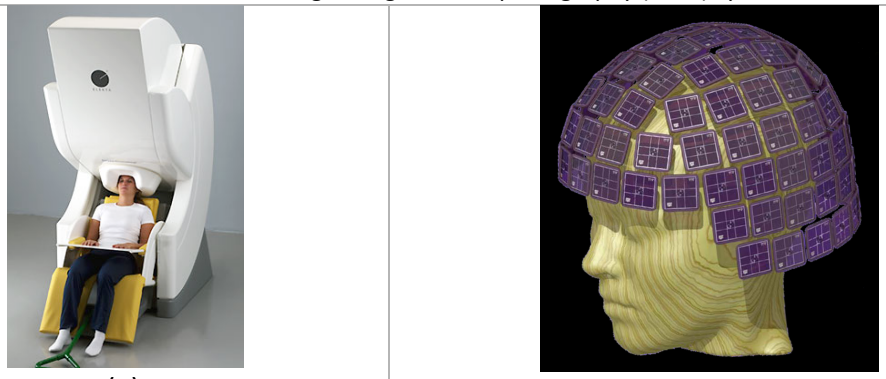

(a) (b)

(a) Picture of the Elekta Neuromag® MEG system. (b) The helmet array has 102 triple-sensors evenly distributed over the surface of the head. Each sensor has two planar gradiometers and one magnetometer. The two gradiometers measure change in magnetic strength with respect to latitude and longitude respectively. The magnetometer measures the strength of the magnetic signal at that location.

Figure 9

3.2 Data Analysis

3.2.1 Behavioral Data

Accuracy between valid and invalid trials was significant at $F(1,17) = 7.90$, $p = 0.01$: average accuracy for valid trials was 91% while average accuracy for invalid trials was

90%. Accuracy between valid and DO trials was not significantly different. Accuracy between SO and DO trials was also not significantly different. There was no significant interaction with display orientation in any of the three ANOVAs (each ANOVA was condition X display orientation (vertical, horizontal); where condition was valid-invalid, valid-DO, or SO-DO respectively). Only correct trials are included in the RT analysis. Outlier trials (whose RT was greater than two standard deviations from the mean per subject, per condition) were excluded from this analysis. Percentage of outliers per condition was 4% for valid trials, 5% for SO trials and 4% for DO trials. Finally, trials that had eye movement artifacts, as measured in the EOG to be greater than 100 microvolts peak-peak, were also discarded. Space-based attention is assessed by contrasting valid with invalid trials (Egly et al, 1994), or valid with DO trials (Martinez et al, 2006). Contrasting SO with DO trials assesses object-based attention. Results exhibited the classic pattern: RT to discriminate targets was significantly faster for valid trials (mean 708 ms), than for invalid trials (mean 771 ms), $F(1,17) = 43.81$, $p < 0.001$. This 63 ms difference is somewhat greater than that observed in the initial Egly et al. (1994) study in which the mean valid RT was 324 ms, and mean invalid RT 364 ms, yielding a 40 ms validity effect. The absolute RTs are longer here too than in the original study, and while this may be a difference in the base RTs of the different participants or the response pad and testing conditions used here, the validity effect expressed as a percentage of the base RT (%(valid-invalid)/(valid+invalid)) is roughly the same magnitude here and in the Egly et al. study (5.18% in Egly et al., 4.26% here). RT to discriminate targets was significantly faster for valid trials, than for DO trials (mean 780 ms), $F(1,17) = 45.27$, $p < 0.001$. Considering only invalid trials, SO was

significantly faster (mean 762 ms) than DO trials (mean 780 ms), F (1,17) = 7.69, p = 0.01 (Figure 10).

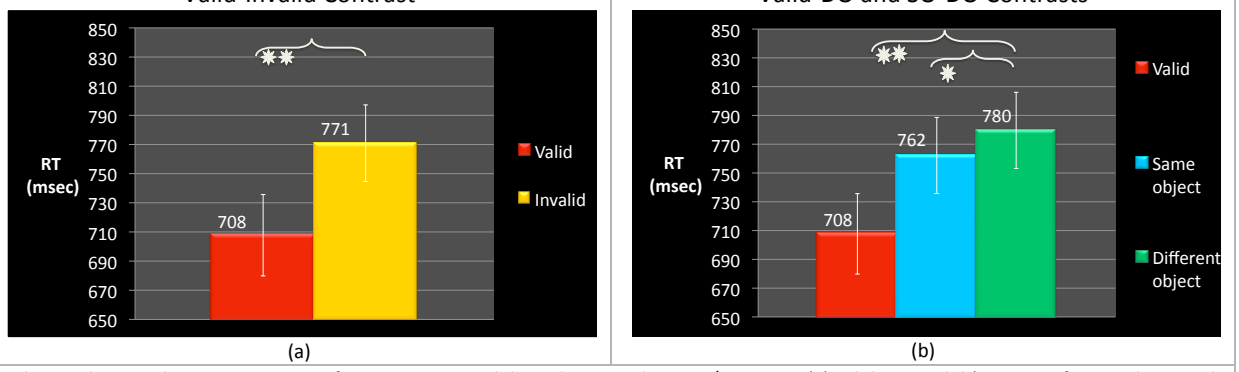

Behavioral RT results to target onset of 18 participants while undergoing the MEG/EEG scan. (a) valid vs. invalid (average of same object and different object) condition. (b) valid, same object, and different object conditions. $p < 0.05$ denoted by *, $p < 0.001$ denoted by **. . The presumption is that between cue onset and target onset, attention is spread within the perceptual object within which the cue appears, and that this spread subsequently contributes to a significantly faster reaction for a target that appears in the same perceptual object as the cue, than for a target that appears outside that object. This faster reaction time for the SO vs DO condition is taken as evidence of object-based attention (OBA).

Figure 10

3.2.2 Preprocessing

EEG and MEG data were acquired simultaneously during acquisition and stored in real time in binary format with an extension of "fif" on an HP-UX system. Following acquisition, the subject's two fif files (one file per run) were pre-processed using the Elekta Neuromag Maxfilter® software. This pre-processing affects the MEG data only. First the data were filtered using the spatio-temporal signal space separation method (Taulu & Simola, 2006) implemented in the Maxfilter software. In the application of the temporal signal space separation, the defaults of the MaxFilter® program were used (e.g. a 4 second buffer was used which corresponds to a highpass filter of 0.25 Hz). Second, the subject's

data were transformed into the default head position, so that in subsequent group analysis, all subjects' data had the same head position relative to the MEG sensors.

The EEG data, which were collected referenced to the left mastoid, were mathematically re-referenced to the CZ electrode (see Figure 33 in Appendix A), before creating and averaging the trial epochs, and subsequent statistical analysis.

3.2.3 Epoching and Averaging

Averaging epochs in the time domain

For EEG analysis, the subject's fif files in their raw form before the application of Maxfilter were used[10], while in the MEG analysis the filtered fif files were used. Otherwise all processing steps were the same. The fif files were transferred to a Linux computing cluster at the Center for the Neural Basis of Cognition (CNBC) at Carnegie Mellon University. The MNE Suite software (Martinos Center for Biomedical Imaging, Harvard University) was used in batch mode to epoch the trials starting at target trigger onset[11], remove all trials with EOG artifacts (rejection limit of 100 microvolts peak-to-peak), baseline (to the per trial average signal 200 ms pre-target until target trigger onset), lowpass filter at 80 Hz (no highpass filter specified), average the trials in the time domain, and convert them into MATLAB structures. All subsequent analysis was done in MATLAB. As input into the batch mode processing, only correct trials that were also not outliers, for that subject as identified in the behavioral analysis were included. Therefore the trial

[10] I have since verified with Eleckta Neuromag representatives that the Maxfilter software only processes MEG data, leaving all EEG data untouched. Therefore the analysis could have been done on the filtered files with the same results.

[11] In the present experiment implementation, "target trigger onset" is the point in time at which the E-prime software puts a trigger into the data file during MEG/EEG recording. "Target onset", in contrast, is the point in time at which the visual stimulus appears to the participant. In the present paradigm there is a fixed delay of 36ms between target trigger onset and target onset. The analyses reported here are done on epochs that are locked to target trigger onset.

averages contained only correct, inlier trials that had no eye artifacts greater than 100 microvolts peak-to-peak. The output text file log of the batch processing identified the trials that ultimately contributed to each average. This log information was used in the analysis in which the trials were epoched and averaged for that subject directly in MATLAB (instead of using the batch epoching mechanism in MNE Suite), which was done for the mathematically re-referenced EEG data, and the frequency analysis discussed below.

Averaging epochs in the frequency domain

Because the MNE Suite batch averaging process epochs and averages trials in the time domain only on the data as originally collected, I implemented the mechanism to epoch and average the trials in MATLAB. The same process was used for EEG and MEG data. The list of trials obtained from the log information in the time-domain epoching together with lower level MNE Suite routines were used to identify and extract the trials of interest from the binary fif files. Using the log information from the time domain epoching guaranteed that the same set of trials contributed to both analyses. Each trial was baselined to the average signal 200 ms pre-target trigger until the target trigger for that trial, and then its frequency transform was computed using wavelet transforms. The wavelet transforms were then averaged together per target side, per condition, per channel (electrode, or magnetometer and gradiometer for EEG and MEG respectively), per subject and stored in MATLAB files for the subsequent analysis. I used Gaussian order 8 wavelet frequency transforms, discussed below.

3.2.4 Wavelets

Wavelet theory

Wavelets, like the Fourier transform, analyze time-domain signals for their frequency content. Unlike the Fourier transform however, wavelet theory uses scale-varying basis functions, which means that the window in which to conduct the Fourier analysis is matched to the particular frequency component (longer for lower frequencies, shorter for higher frequencies). Schematics of Fourier versus wavelet analysis are given in Figure 11.

There are several wavelet families, each resulting in a different tradeoff in time-frequency resolution of the result, with respect to the time series under consideration. Perhaps the most important consideration in choosing the wavelet family is to reflect the types of features present in the time series. For time series with sharp jumps or steps, one should choose a box-car function such as the Harr, while for smoothly varying time series one would choose a smooth function such as a damped cosine (Torrence and Compo, 1997). In the present research, Gaussian wavelets of order 8 were used. Gaussian transforms in general are regarded as providing a balance between time-frequency localization[12]. Precedence has been set for using Morlet wavelets in MEG and EEG analysis in the study of recognition memory in analysis methods similar to those proposed here (Duzel et al., 2003). An example signal from data of the present research, as compared with Gaussian order 8 filter and the Morlet filter are given in Figure 12. The Gaussian order 8 filter and the Morlet filter are similar and both appear to match the signal characteristics.

[12] Discussion with Steve Luck at the ERP Bootcamp 2009, U.C. Davis

Schematics of Fourier vs. Wavelet Analysis

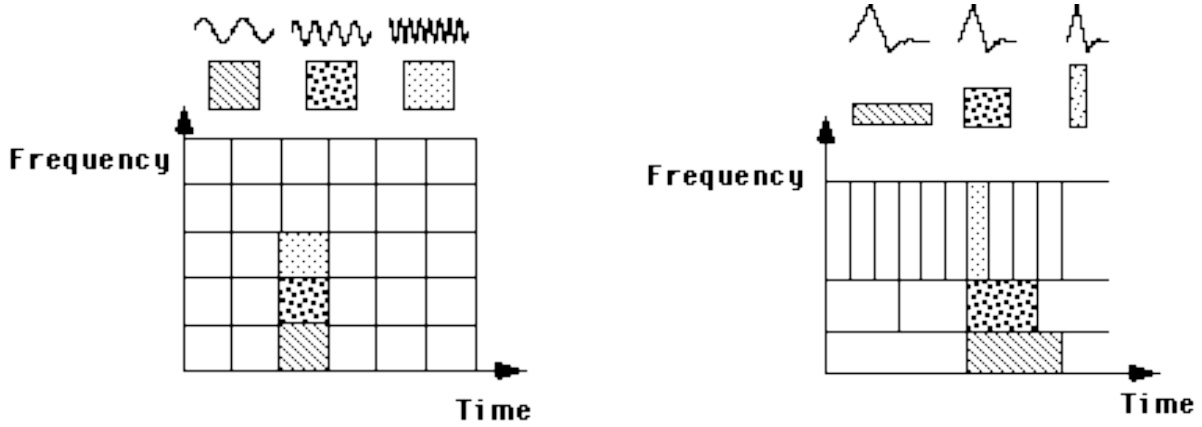

(a) Fourier basis functions (utilizes sines and cosines), time-frequency tiles, and coverage of the time-frequency plane.

(b) Wavelet basis functions, time-frequency tiles, and coverage of the time-frequency domain (Daubechies wavelets shown)

Images source: http://www.amara.IEEEwave/IEEEwavelet.html

Figure 11

Wavelet characteristics vis-à-vis signal characteristics

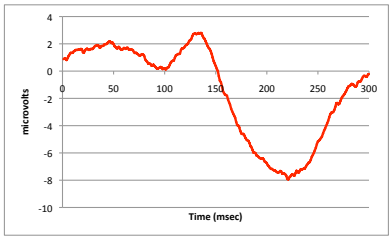

(a) Example ERP signal

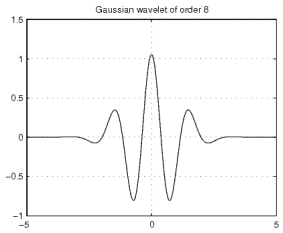

(b) Gaussian wavelet of order 8

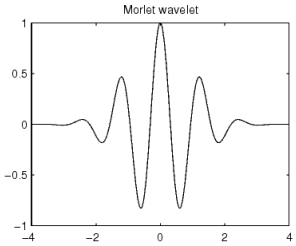

(c) Morlet wavelet

Figure 12

Wavelet application in the present research

The specification of frequency bands of interest in the wavelet transform is done via scales, where the number of scales specified determines the number of wavelets generated for the given signal, and the value of a scale determines the center frequency of its associated wavelet. Each wavelet can be seen as a bandpass filter of the signal (Vetterli, 1992). In the present research the number and value of the scales were chosen in the context of the Gaussian order-8 wavelet family to correspond to nine frequency bands with

center frequencies 5, 10, 20, 30, 40, 50, 60, 70 and 80. These values were chosen to provide coverage of the frequency oscillations of interest, and to correspond to the approximate center frequencies of the θ band (4-7 Hz), α band (8-12 Hz), beta band (12-30 Hz), and gamma band (30-80 Hz), as discussed in extant literature. The resulting nine wavelets can be viewed as a time-scale or time-"pseudo-frequency" representation of the original signal. Scalograms are the standard visual mechanism for communicating the time-"pseudo-frequency" of the signal. In this image-plot, the wavelet scale (corresponding to pseudo-frequency) is plotted on the y-axis, and time is plotted on the x-axis. The color of the image at each x-y position corresponds to the percent energy of that point relative to the whole.

As an example, consider the scalograms shown in Figure 13, which are displayed with scales on the y-axis in (a) and then with the corresponding pseudo-frequency on the y-axis in (b). These scalograms are of the ERP signal for valid left targets in left occipital electrode O1. The electrode signal is plotted in the lower left. In this case it is clear that the highest power is in the theta (θ – center frequency 5 pseudoHz) and alpha (α – center frequency 10 pseudoHz) frequency bands.

The input into the wavelet transform is the original signal as measured by a given channel (electrode for EEG, magnetometer or gradiometer for MEG). Mechanistically, it is a time series of amplitude values for each millisecond from 1 to 1000 post target trigger onset: it is thus a time series of 1000 amplitude values. This time series is input into the wavelet transform together with the scale specification. Given the scale specification used in the present research with nine scales, the resulting output was two sets of nine time series of 1000 points each. The first set contains the wavelet coefficients. Each of the nine wavelet coefficients or simply "wavelet" represents a band-pass filtered signal of the

original at the frequency band specified by the scale. Its units are the same as the original signal. Given the scales specified here, there was a wavelet (time series of 1000 time points) for each of the pseudo frequencies 5, 10, 20, 30, 40, 50, 60, 70, 80 pseudo-Hz. The nine wavelets for the ERP signal shown in Figure 13 are plotted in Figure 14(a): the x-axis is time in milliseconds, while the y-axis is amplitude in volts. The second set of nine time series contains the scalogram. Each of the nine time series contains percent total power for the corresponding wavelet. Therefore each scalogram time series is a series of 1000, percent power values for its corresponding wavelet. These nine scalogram time series are plotted in Figure 14(b) the x-axis is time in milliseconds, while the y-axis is % total power. Traditionally, the scalograms time series are only visualized as the images shown in Figure 13; not plotted as done in Figure 14(b). However, the latter is useful in visualizing how the wavelets were stored for purposes of subsequent statistical analysis in the present research. Each of the scalogram time series were averaged together per target side, per condition, per channel (electrode or magnetometer and gradiometer for EEG and MEG respectively), per subject and stored in MATLAB files.

Scalogram and EEG Signal at Electrode O1

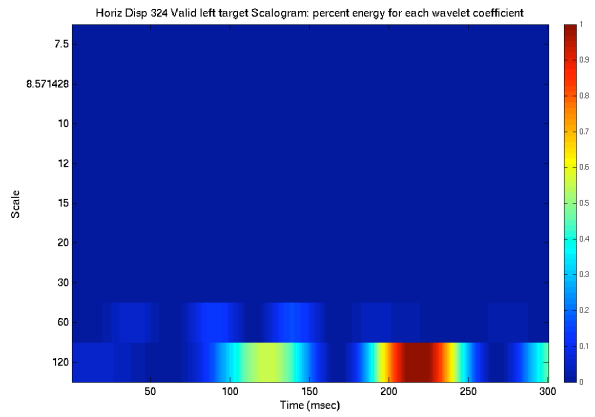

(a) Scalogram: Valid left targets in Electrode O1
Scale on y-axis

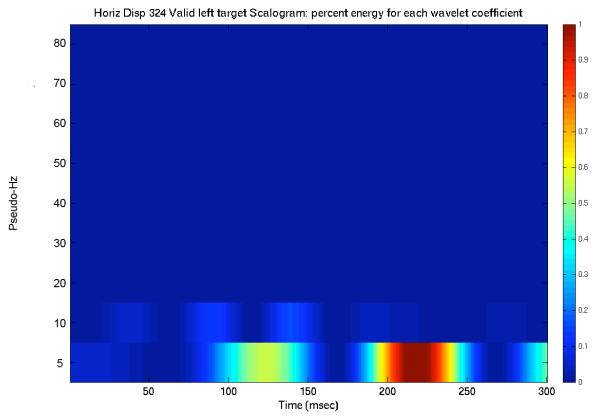

(b) Scalogram: Valid left targets in Electrode O1
Pseudo-Hz on y-axis

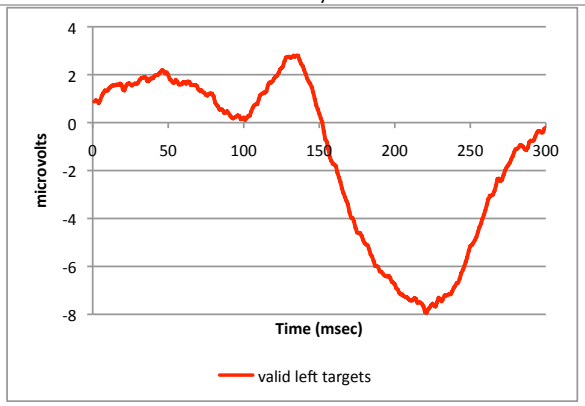

(c) ERP signal: Valid left targets in Electrode O1

(a) the scalogram of the Gaussian order 8 wavelet transform of the ERP signal given in (c). The scale value (y-axis) associated with each wavelet is related to the window size used for the Fourier transform of the signal in a particular frequency. (b) the same scalogram labeled (y-axis) with the associated frequency (pseudo-Hz).

Figure 13

Wavelet Coefficients and Scalogram Plot, Electrode O1

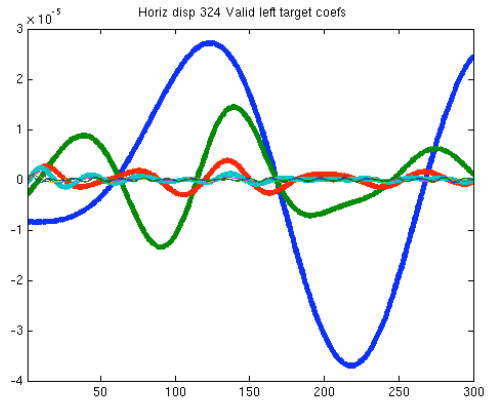

(a) Wavelet coefficients for the ERP signal shown in Figure 13(c). The nine wavelets collectively represent the original signal in the frequency band with center frequencies: 5, 10, 20, 30, 40, 50, 60, 70, 80 pseudo-Hz. One wavelet per frequency band.

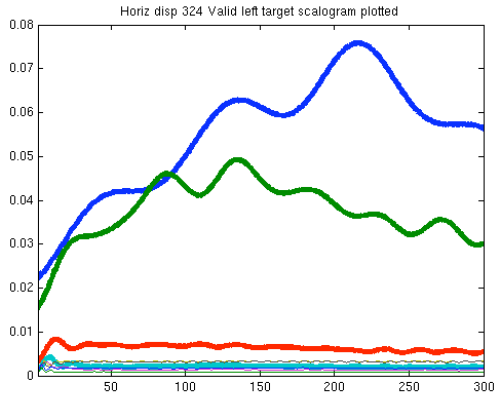

(b) Wavelet scalogram time series for the ERP signal shown in Figure 13(c). Each time series shows the percent total power of the corresponding wavelet. Typically these time series are shown as scalogram image-plots as in Figure 13.

Figure 14

3.2.5 Condition Contrasts used in the analysis

Object-based attention studies using Egly-style paradigms typically assess space-based attention by comparing valid vs. invalid trials (e.g., Egly et al., 1994), or by comparing valid vs. DO trials (e.g. Martinez et al., 2006), while object-based attention is assessed in comparing SO vs. DO trials (c.f. Egly et al., 1994; Martinez et al., 2006). In the EEG temporal results in the current research, the first analysis of these contrasts is that which is typically done: Valid vs. Invalid, Valid vs. DO and SO vs. DO. These contrasts are used in the behavioral data, the EEG component analysis (4.1.1 Analysis Methods - Components) and the EEG sliding window analysis (4.1.3 Analysis Methods – Sliding windows).

Then, to control for shifts of attention within versus between hemifields when contrasting SO and DO, difference scores are calculated between the Valid and DO conditions in each of the four target locations in the horizontal (vertical) display, and similarly calculated between the Valid and SO conditions in the vertical (horizontal) display. DO-Valid (horizontal display) is then contrasted with SO-Valid (vertical display),

and DO-Valid (vertical display) with SO-Valid (horizontal display)[13]. The former is referred to as the "HV" condition-display contrast and assesses object-based attention when shifts of attention are within hemifield (Figure 15), while the latter is the "VH" condition-display contrast and assesses object-based attention when shifts of attention are between hemifields (Figure 16). The difference scores between DO and Valid, and SO and Valid, were used instead of simply DO and SO: subtracting Valid from the concomitant DO and SO, controls for possible baseline differences which may exists between the two groups of individuals, as display orientation was a between-subjects factor.

The difference-score contrasts are done for the EEG temporal analysis (4.1.5 Analysis Methods – Sliding windows with condition-display contrast and 4.1.6 Results – Sliding windows with condition-display) and MEG temporal analysis (4.2 MEG/ERMF) and temporal-spectral analyses for both EEG and MEG/ERMF (5. Temporal-Spectral Analysis).

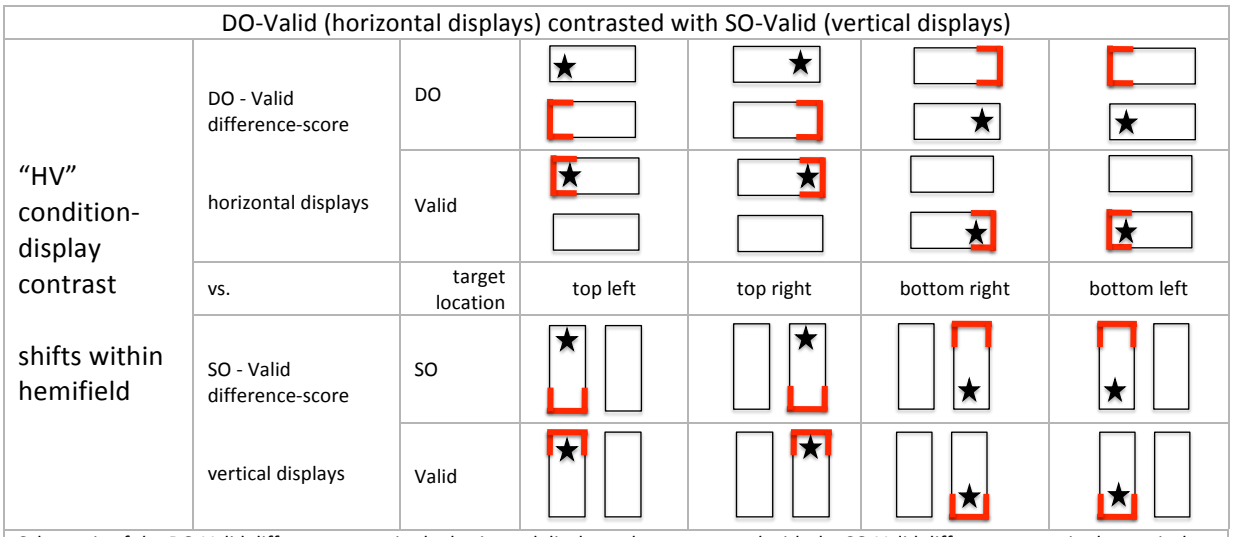

Schematic of the DO-Valid difference score in the horizontal displays when contrasted with the SO-Valid difference score in the vertical displays. This contrast controls for shifts of attention within hemifield. Note that display orientation is a between-subjects variable.

Figure 15

[13] Display orientation is a between subjects variable.

<table>
<tr><td colspan="6">DO-Valid (vertical displays) contrasted with SO-Valid (horizontal displays)</td></tr>
<tr><td rowspan="4">“VH” condition-display contrast

shifts between hemifields</td><td rowspan="2">DO - Valid difference-score

vertical displays</td><td>DO</td><td> 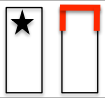 </td><td> 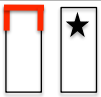 </td><td> 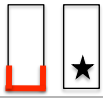 </td><td> 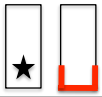 </td></tr>
<tr><td>Valid</td><td>  </td><td> 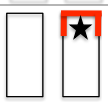 </td><td> 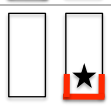 </td><td> 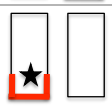 </td></tr>
<tr><td>vs.</td><td>target location</td><td>top left</td><td>top right</td><td>bottom right</td><td>bottom left</td></tr>
<tr><td rowspan="2">SO - Valid difference-score

horizontal displays</td><td>SO</td><td> 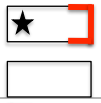 </td><td> 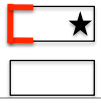 </td><td> 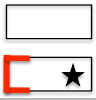 </td><td>  </td></tr>
<tr><td>Valid</td><td> 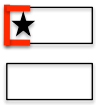 </td><td> 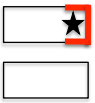 </td><td> 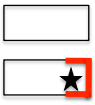 </td><td> 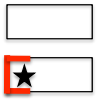 </td></tr>
<tr><td colspan="6">Schematic of the DO-Valid difference score in the vertical displays when contrasted with the SO-Valid in the horizontal displays. This contrast controls for shifts of attention to between hemifields. Note that display orientation is a between-subjects variable.</td></tr>
</table>

Figure 16

4. Temporal Analysis

4.1 EEG/ERP

4.1.1 Analysis Methods - Components

Attention components: Previous ERP studies have identified two components influenced by attention: the positive P1 which typically occurs 60-80 ms after stimulus onset and peaks at 100-130 ms, and the negative N1 which typically peaks between 150-200 ms after stimulus onset (Luck, 2005; Martinez et al., 2006). The ERP component method considers the data to select the exact latency windows to analyze, and then runs the appropriate ANOVA to test for differences between conditions in the defined windows encompassing the component of interest. In the present research the P1 and N1 latency windows are defined as 75-125 ms and 150-200 ms respectively. These windows are chosen to encompass the P1 and N1 component windows defined in Martinez et al. (2006), and to fit in with the sliding window scheme described in the next section (4.1.3 Analysis Methods – Sliding windows).

Dependent variable: The dependent variable in a given ANOVA is the mean amplitude of the condition signal within the given P1 or N1 latency window from a specific electrode.

Electrode pairs: In the analysis, electrodes are paired across the left and right hemispheres, and one pair is entered into each ANOVA. The anterior pairs are F3, F4; F7, F8; and FP1, FP2. The posterior pairs are O1, O2; P3, P4; and P7, P8. A schematic of the

electrode layout is given in Figure 17 below, and Figure 33 in the Appendix. The electrode pairs used in the analysis are circled in red. For the analysis here, only the posterior electrode pairs are considered, as these electrodes are standard choices for analysis in the study of the attentional P1 and N1 components. For the sliding window analysis (next section 4.1.3 Analysis Methods – Sliding windows) all six pairs are considered.

EEG Electrode Layout

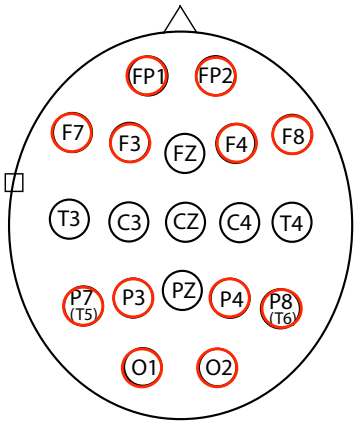

EEG Electrode Layout (10-20 electrode layout system) with 19 electrodes and left mastoid reference (square). Electrodes circled in red are used in the analyses

Figure 17

ANOVA: Each ANOVA has the following within-subject factors: condition (exact conditions depend on the ANOVA) X target-side (left, right) X electrode-side (left, right). ANOVAs are done separately for the vertical and horizontal display conditions with nine subjects in each. Condition is either a Valid–DO, Valid-Invalid or SO–DO contrast. The Valid-Invalid and Valid-DO contrasts are used to assess SBA, while the SO-DO contrast is used to assess OBA. One electrode pair is entered into each ANOVA. Thus, ANOVA analyses are done per display type, for each sliding window (including the P1 and N1 components), per condition contrast, per electrode pair.

4.1.2 Results - Components

The first important result is the presence of a space-based main effect of valid vs. invalid in the P1 time frame in the O1, O2 electrode-pair, and in the N1 time frame in the P7 electrode (condition x electrode-side interaction). See Figure 18(a). The presence of SBA is also seen in the N1 time frame in O1 and P7, P8 (both due to condition X electrode-side interactions) when contrasting valid vs. DO (Figure 18 (b)). The second important result is that object-based effects (SO vs. DO) are found in the N1 time frame in the O1, O2 electrode-pair in the left targets (condition X target-side interaction) and in the P8 electrode (condition x electrode-side interaction) See Figure 18(c). There results are in the vertical display. No significant results were found in the horizontal display.

The hypothesis of the EiEM framework (section 1.3), that SBA modulates both the P1 and N1 component, and that OBA modulates the N1 component is thus supported for vertical displays. The fact that the hypothesis is not supported for horizontal displays is intriguing. It could be that SBA and OBA as theoretically conceived in Martinez et al. (2006) does not exist when shifts of attention cross hemifields, and that their results are slightly misleading in that their approach to analysis is to collapse across vertical and horizontal display conditions. It could be that the significance found is such analysis is really driven by the vertical display component of the data. Alternatively, it could be that our results are compromised by the fact that the target P1 and N1 components are convolved with the previous cue P3 component as exemplified in Figure 2, and that this negatively effects our results when shifts of attention cross hemifields. Martinez et al., (2006) used an endogenous cue, rather than a bright red flash as is done here. It is possible that the endogenous cue does not evoke a typical ERP waveform. In this case there would be no cue

associated P3 component, and the subsequent target P1 and N1 components would not be impacted. As a third alternative, even if the endogenous cue evoked a typical visual ERP waveform, Martinez and colleagues' target onset was jittered at random intervals of 400 to 600 ms after the endogenous cue. Presumably in their subsequent analysis, trials would be locked to target onset before averaging. The impact of the previous cue P3 component would thus be averaged out.

Space-based attention (SBA) and object-based attention (OBA) - (vertical display)

(a) **Valid – Invalid (SBA)**

Main effect of condition in O1, O2
P1 time frame
F(1,8) = 5.21, p = 0.026

Condition X electrode-side interaction,
P7 significant
N1 time frame
F(1,8) = 4.34, p = 0.042

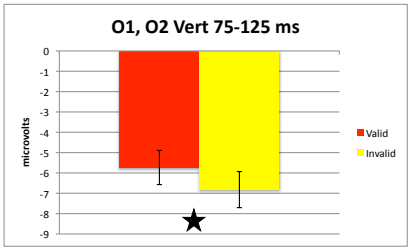

P1

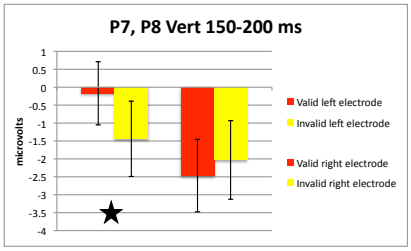

N1

(b) **Valid – DO (SBA)**

Condition X electrode-side interaction,
O1 significant
N1 time frame
F(1,8) = 7.86, p = 0.007

Condition X electrode-side interaction,
P7 & P8 significant
N1 time frame
F(1,8) = 14.72, p < 0.001

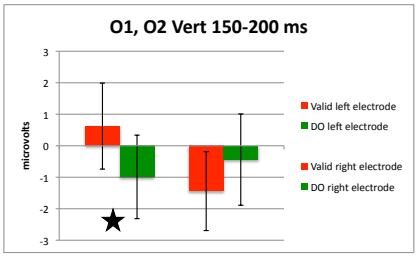

N1

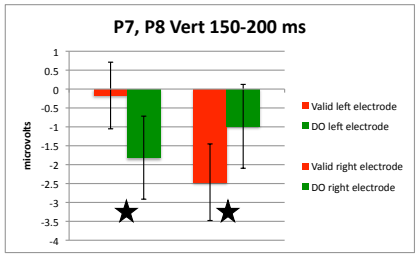

N1

(c) **SO – DO (OBA)**

Condition X target-side interaction, left
targets significant in O1, O2 pair
N1 time frame
F(1,8) = 4.05, p = 0.049

Condition X electrode-side interaction,
P8 electrode significant
N1 time frame
F(1,8) = 6.68, p = 0.012

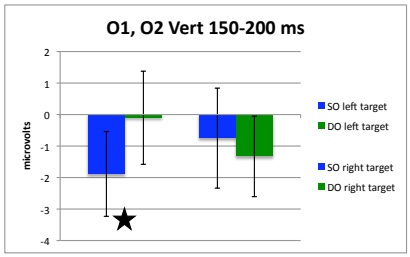

N1

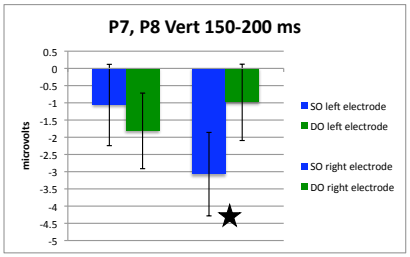

N1

Significant differences are denoted with a ★. Valid is red, Invalid is yellow, SO is blue and DO is green. a) There is a space-based effect in the P1 time frame in the O1, O2 electrode pair, and in the N1 time frame in P7. b) There is a space-based effect in the N1 time-frame in O1, and the P7,P8 electrode-pair. c) There is an object based effect in the N1 time frame in left targets in the O1,O2 electrode pair and in P8.

Figure 18

Martinez et al. (2006) established that SBA modulated both the P1 and N1 components, and that OBA modulated the N1 component. As evident in Figure 18(a) and

(b), this holds here too. The Martinez et al. (2006) SBA results demonstrated that valid was more positive than DO in the P1 component, and more negative than DO in the N1 component. Their OBA results demonstrated that SO was more negative than DO in the N1 component. Critical to the positive/negative directionality of the P1/N1 components in their results is the fact that the electrodes were referenced to the average of the left and right mastoids. In contrast, our choice of the CZ electrode as reference does not guarantee these directionalities. Rather what is important is that significant differences between conditions are evident in the P1 and N1 time frames in the results presented here, as is the case with the results from Martinez and colleagues. Furthermore, Martinez et al. (2006) established their SBA and OBA results via main effects of condition and main effects of hemisphere. Either there were no significant interactions of the two factors, or they were simply not reported. In their results, all electrodes were referenced to the average of the left and right mastoids. With one exception, the results reported here are via interaction with target-side or hemisphere (electrode-side). It is possible that the hemisphere interactions are an artifact of the reference to the CZ electrode. It is possible to explore this conjecture further given a data set with both the left and right mastoid as well as CZ information available. The current data set does not have right mastoid information. Reported in Figure 18 are all significant main effects and interactions in our results.

Even if the interactions in Figure 18 are an artifact of the reference to the CZ electrode, consider that they might be meaningful. It is possible that the choice of reference node is critical to elucidating or masking the existence of these hemispheric interactions. First note that the interactions only occur in the N1 time frame (P1 significance is due to a main effect of condition as was the case with Martinez and colleagues). For SBA, the left

hemisphere P7 electrode significance in Figure 18(a) (via the Valid-Invalid contrast) suggests that right targets are significant; while the lack of right hemisphere P8 electrode significance suggests that left targets are not. Similarly the left hemisphere O1 electrode in Figure 18(b) (via the Valid-DO contrast) suggests right targets are significant while the lack of right hemisphere O2 electrode significance suggests that left targets are not. However both the P7 and P8 electrodes in Figure 18(b) (also via the Valid-DO contrast) are found to be significant, albeit differentially, suggesting that both right and left targets are significant in SBA. In comparison, the interactions for OBA suggest that left targets (independently of electrode side) and the right hemisphere P8 electrode (which processes left targets) alone demonstrate significant differences. This possibly suggests a right hemisphere/left targets dominance in OBA. These results possibly suggest that significance between conditions in SBA and OBA occurs differentially in left and right hemisphere (right and left targets), a distinction that would not be apparent in an analysis that elicited only main effects. However, these implications should be explored further in subsequent research.

4.1.3 Analysis Methods – Sliding windows

Sliding windows: In addition to component analysis, a sliding latency window analysis was done starting at 50 and ending at 300 ms post-target trigger onset. Each window is 50 ms in width with a 25 ms overlap from one window to the next (e.g. 50-100 ms, 75-125 ms, 100-150 ms etc.). The analysis thus encompasses the P1 (75 – 125 ms) and N1 (150 – 200 ms) components, and additionally includes the surrounding time frames. There are nine 50 ms windows between 50 and 300 ms post-target trigger onset.

Dependent variable: The dependent variable in a given ANOVA is the mean amplitude of the condition signal within a given latency window per electrode.

Electrode pairs: In the analysis, electrodes are paired across the left and right hemispheres, and one pair is entered into each ANOVA. The anterior pairs are F3, F4; F7, F8; and FP1, FP2. The posterior pairs are O1, O2; P3, P4; and P7, P8. A schematic of the electrode layout is given in Figure 17 and Figure 33 in the Appendix. The three posterior electrode pairs are standard choices for analysis in the study of the attentional P1 and N1 components. The three anterior electrode pairs are chosen to establish a pair wise match to the three posterior electrode pairs and to explore potential effects in more anterior regions of the fronto-parietal network.

ANOVA: As is done in the component analysis (4.1.1 Analysis Methods - Components), each ANOVA has the following within-subject factors: condition (exact conditions depend on the ANOVA) X target-side (left, right) X electrode-side (left, right). ANOVAs are done separately for the vertical and horizontal display conditions with nine subjects in each. Condition is either a Valid–Invalid, Valid-DO or SO–DO contrast.

Multiple comparisons: In order to use multiple sliding latency windows in the ANOVA analysis and to allow for time-space results comparison across time between electrode pairs, multiple comparisons are accounted for using the Holm adjustment to the Bonferroni correction method. [14]

4.1.4 Results – Sliding windows

No significant results were found in the sliding latency window analysis using the traditional condition contrasts (Valid-Invalid, Valid-DO, SO-DO) when correcting for

[14] The p-values included in the correction are those associated with the effects and interactions of interest (all those that contain condition as a factor) from all ANOVAs across six electrode pairs, per condition-display contrast. The Holm adjustment for a given p-value in an increasing sorted sequence is 0.05/(N-n+1), where N is the number of tests and n is the position in the sequence. N in this case is calculated as 4 (1 main effect and 3 interactions of interest) X 9 latency windows X 6 electrode pairs = 216. The main effect and 3 interactions of interest are (condition, condition X target-side, condition X electrode-side, condition X target-side X electrode-side).

multiple comparisons using the Holm adjustment to the Bonferroni correction method, because multiple comparison correction necessitates a more conservative p-value. If the p value is relaxed to p = 0.05, the component results discussed in 4.1.2 Results - Components are replicated.

4.1.5 Analysis Methods – Sliding windows with condition-display contrast

Sliding windows, Dependent variable, Electrode pairs: these are the same as those discussed in 4.1.3 Analysis Methods – Sliding windows.

To assess OBA while controlling for shifts of attention within versus between hemifields, the difference signals between the Valid and DO conditions, and the Valid and SO conditions are contrasted as follows. DO-Valid difference signals (horizontal displays) are contrasted with SO-Valid difference signals (vertical displays) in order to assess OBA when shifts of attention are within a hemifield, while DO-Valid difference signals (vertical displays) are contrasted with SO-Valid difference signals (horizontal displays) in order to assess OBA when shifts of attention are between hemifields. The former is referred to as the "HV" condition-display contrast, while the latter is the "VH" condition-display contrast. (The rationale is explained in detail in section 3.2.5 Condition Contrasts used in the analysis).

ANOVA: The ANOVA is a mixed design with the following factors: difference-score (DO-Valid, SO-Valid) X target-side (left, right) X electrode-side (left, right). ANOVAs are done separately for each of the HV and VH condition contrasts, for each sliding window (including the P1 and N1 components), per electrode pair. Difference-score is used in place of condition.

Multiple comparisons: the multiple comparisons correction described in 4.1.3 Analysis Methods – Sliding windows, is used here.

4.1.6 Results – Sliding windows with condition-display

In the difference-score contrasts in Figure 19 (DO-Valid vs. SO-Valid), there were main effects of difference score in the P1 and N1 time frames in the O1, O2 and P7, P8 electrode pairs in the HV condition contrast. This indicates that there is an object-based effect in both the P1 and N1 attentional components. No statistically significant difference was found in any posterior electrodes in these time frames in the VH display contrast. This may be because the VH condition-display contrast involves shifts of attention across hemifields for which associated electromagnetic signal activity may be so large so as to swamp out signal modulations associated with the condition effects of interest.

In no case do the results in Figure 19 pass multiple comparison correction via the Holm adjustment to the Bonferroni, such that sliding latency windows, the inclusion of the anterior electrode pairs, and time-space comparison across electrode pairs, can be done. However, the results in Figure 19 are significant at $p <= 0.05$ when assessed only in the P1 and N1 component windows chosen a priori in the 3 posterior electrode pairs.

Object-based attention (OBA) for shifts within hemifield (HV condition contrast)

HV

(a) Main effect of difference score P7, P8 P1 time frame
F(1,1) = 10.19, p = 0.002

(b) Main effect of difference score P7, P8 N1 time frame
F(1,1) = 6.04, p = 0.017

(c) Main effect of difference score O1, O2 P1 time frame
F(1,1) = 7.88, p = 0.007

(d) Main effect of difference score O1, O2 N1 time frame
F(1,1) = 4.56, p = 0.037

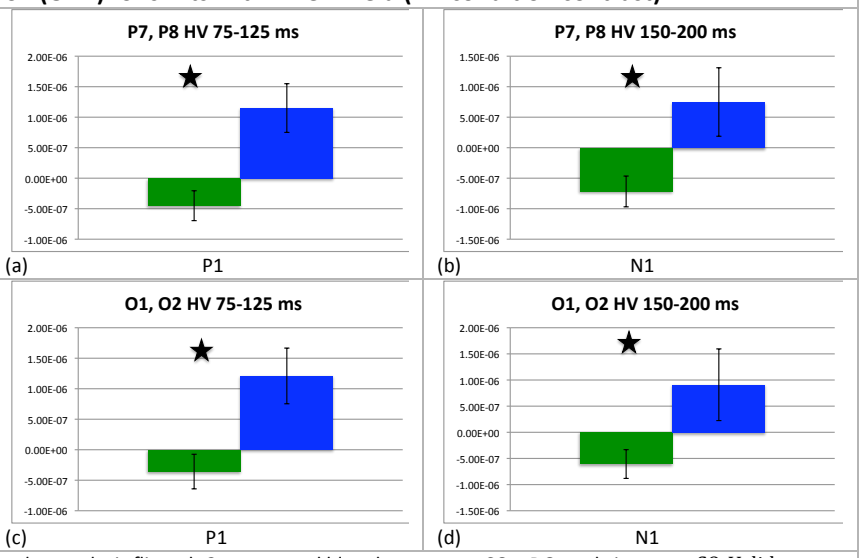

DO-Valid is green, SO-Valid is blue. The y-axis on the graphs is flipped. Green up and blue down means SO > DO, and vice-versa.SO-Valid power is less than DO-Valid power in (a), (b), (c), and (d). Object-based attention effects are found in the P1 (a) and the N1 (b) time frames in the P7, P8 electrode-pair. OBA effects are also found in the P1 (c) and N1 (d) time frames in the O1, O2 electrode-pair.

Figure 19

4.1.7 Comparison with behavioral results

To evaluate whether there is any association between the observed reaction times of the participants and the magnitude of the significant differences in the above analyses, each significant EEG ANOVA result (main effect or interaction) in the posterior electrode pairs was correlated with the concomitant behavioral reaction times using Pearson correlation. No significant relationship was found in any case.

4.1.8 Discussion of EEG/ERP temporal analyses

Previous research using an Egly-style paradigm found a space-based effect in the P1 and N1 component time frames, and an object-based effect in the N1 time frame (Martinez et al., 2006). The classic approach to ascertain space-based effects (SBA) is to contrast valid trials with invalid trials (both same and different object trials are invalid trials) or valid trials with different object trials (Valid-Invalid and Valid-DO contrasts respectively). Object-based effects (OBA) are assessed by contrasting same object with different object

trials (SO-DO contrast). Typically the paradigm utilizes both vertically- and horizontally-oriented displays, and the standard analysis collapses across display orientation. Critical in this approach is that shifts of attention within versus between objects are confounded with shifts within versus between hemifields. A goal of the present research was to remove this confound.

The present research first uses the standard approach of contrasting valid with invalid trials and valid with different object (DO) trials to assess SBA, and same object (SO) with different object (DO) trials to assess OBA. Since the experiment is a between subjects design on display orientation, separate analyses were conducted for vertically- and horizontally-oriented displays. The results replicate the classic component findings in the vertical-display only. Specifically, the results (considering significance at $p = 0.05$) agree with the findings of Martinez and colleagues that found a space-based effect in both the P1 and N1 attentional component time frames (75-125 ms and 150-200 ms respectively), and an object-based effect in the N1 time frame. The present results however, do not find significant effects in the horizontal displays using the classic contrasts: it is possible that nine subjects are not enough to elicit classic SBA and OBA effects. It is also possible that Martinez' et al. results are driven primarily by the vertically oriented displays in the analyses, even though the analysis, which was collapsed across display orientation, had both vertical and horizontal displays.

Furthermore, Martinez and colleagues' results reported only main effects of condition and hemisphere (electrode-side)[15]. The present component analysis elicits and

[15] Condition and hemisphere were two factors in the same ANOVA, hence interaction information would have been available if queried for in the statistical package that was used. However no interactions were reported, and it is not clear from the paper write-up whether or not they were evaluated.

reports target-side and electrode-side interactions as well as main effects of condition. In the conventional contrasts (Valid-Invalid, Valid-DO, SO-DO), while the significant result in the P1 time frame was due to main effect of condition, all the results in the N1 time frame were due to interactions with electrode-side or target-side (Figure 18).

After capturing EEG data with a single reference node, Martinez algebraically re-referenced the electrode signals to the average of the left and right mastoid, which has the pragmatic effect that subjects' grand average data demonstrated the typical visual ERP waveform shown in Figure 7a. In the present research, right mastoid data was not collected, so the re-reference to the average could not be computed. In this case, the data was captured referenced to the left mastoid, then algebraically re-referenced to the CZ electrode because it is the sole electrode in the montage (Figure 17) that eliminates lateralization or anterior/posterior biases into the waveforms. Referenced to CZ the waveform shape changes (consider Figure 7b), This fact, together with the fact the P1 and N1 components response to target trigger onset in our data are convolved with the P3 component of the previous cue trigger onset (cue trigger onset was 300 ms prior to target trigger onset), means that the data do not show the typical waveform shape evident in Figure 7a. What is significant in the current results however is that significant differences between contrasts are apparent in the P1 and N1 component time frames, just as was the case with Martinez and colleagues. That we can replicate these findings attests to the robustness of our results and our ability to replicate known effects, notwithstanding the small differences in procedure.

Furthermore, the present research assesses OBA by contrasting same object shifts of attention with between objects shifts of attention when both sets of shifts are within a

hemifield (HV condition-display contrast), or when both sets of shifts are between hemifields (VH condition-display contrast). In this approach, a finding of OBA is not confounded with shifts of attention within versus between hemifields. Notably, using the HV condition-display contrast in the present results show object-based effects in both the P1 and N1 time frames (significance is p = 0.05), meaning that OBA has been demonstrated when shifts of attention are controlled to be within hemifield in both the P1 and N1 component time frames. These results provide evidence for the hypothesis put forward in section 1.3, that OBA modulates the N1 component. Furthermore, our results additionally found that OBA additionally modulates the P1 component

In summary, the significant unique contribution of the EEG temporal condition-display contrast analysis over and above that which has been demonstrated in extant literature is that OBA exists when shifts of attention are controlled to be within hemifield. Furthermore these results demonstrate that OBA exists in the P1 as well as the N1 component time frames. The results are found in the posterior O1, O2 and P7, P8 electrode pairs.

4.2 MEG/ERMF

4.2.1 Analysis Methods – Components

Attention components: The P1 and N1 component windows used in the EEG component analysis (4.1.1 Analysis Methods - Components) are used here. The P1 and N1 latency windows are defined as 75-125 ms and 150-200 ms respectively.

Dependent variable: As with the EEG component analysis (4.1.1 Analysis Methods - Components) the dependent variable in a given ANOVA is the mean amplitude of the

difference-score signal (justified in the discussion in the ANOVA below) within the P1 and N1 components.

Magnetometer pairs: A key challenge is how to identify, in a principled manner, the channel pairs to be included in the analysis. There are 306 MEG channels (102 magnetometers, 204 gradiometers): to include them all in the channel-pair analysis would result in a large number of multiple comparisons that would make significance hard to achieve. The present research analyses focus on magnetometers, as they measure the strength of the magnetic field (in units of Tesla) over time in the same way that EEG channels measure the strength of the associated electrical signal (in units of Volts) over time. Gradiometers in contrast, measure the strength of the change in the magnetic field over space, over time. Its units are Tesla/meter[16]. As with the EEG electrodes, the magnetometers are paired across hemisphere. Of the 102 magnetometers, 6 are midline, leaving 96 individual, or 48 pairs. Of the 48 pairs, 12 are identified for analysis. There are 2 frontal lobe pairs of magnetometers, 4 temporal lobe pairs, 2 parietal lobe pairs, and 4 occipital lobe pairs. The magnetometers chosen are delineated with a red square outline, and their placement is shown in Figure 20 below, and Figure 35 in the Appendix.

[16] It is worth conducting similar analyses on the gradiometers as part of post-dissertation research.

MEG Magnetometer Sensor Layout – paired across hemisphere

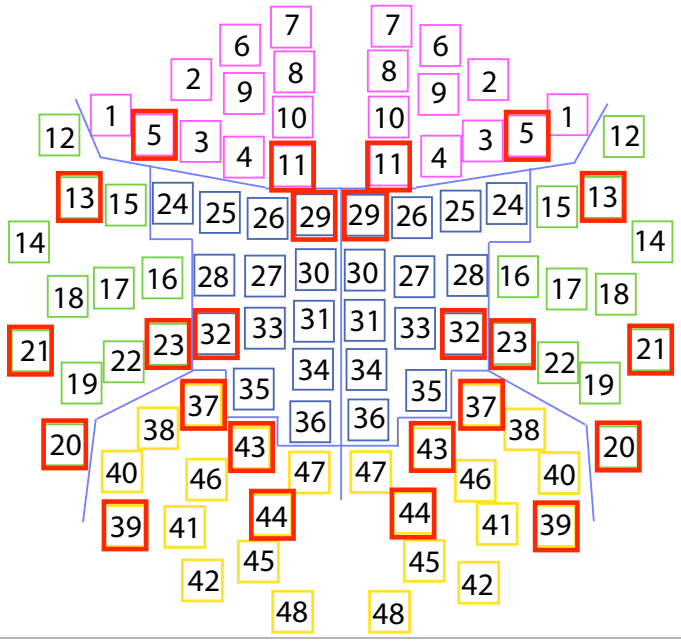

Magnetometers

Frontal pairs (mag left, right)
5 (mag 0341, 1221)
11 (mag 0641, 1032)

Temporal pairs
13 (mag 0131, 1441)
23 (mag 1621, 2411)
21 (mag 1541, 2621)
20 (mag 1531, 2631)

Parietal pairs
29 (mag 0631, 1041)
32 (mag 1811, 2221)

Occipital pairs
37 (mag 1631, 2441)
43 (mag 1911, 2311)
44 (mag 1921, 2341)
39 (mag 1711, 2531)

Pairs delineated with a red square are those used in the magnetometer analysis in all MEG analyses in this dissertation research.

Figure 20

The method for identifying the 12 of the 48 pairs was done with the temporal-spectral analysis in mind, and then applied here[17,18]. Specifically, a spectral wavelet analysis was done on all magnetometers in the 48 pairs for each of the two condition-display contrasts: "HV" where DO-Valid in the horizontal displays is contrast with SO-Valid in the vertical displays, and "VH" where DO-Valid in the vertical displays is contrast with SO-Valid in the horizontal displays. The spectral wavelet analysis resulted in eight wavelets for the signal in each magnetometer, one for each band with center frequency: 5, 10, 20, 30,

[17] Spectral analysis is common in MEG research, more so than temporal analysis.

[18] The method used in the present research was that suggested during the dissertation proposal meeting: scan all sensors across time, and chose the time points and sensors of interest with the highest amplitude or power. The implementation of this statement has many solutions, as it is not an algorithmically precise statement, rather a suggested direction. Any given implementation of this statement could lead to different sensors chosen. For example, the present research applied this stated method separately to the HV and VH contrasts (sets of time series) and then combined the two resulting sensor lists in order to insure that both were equally represented in the final combination. Another implementation would have been to combine the HV and VH contrasts (order the combined sets of time series according to highest power), and then apply the stated method. If one contrast had more power in several sensors relative to the other, then the resulting sensor list would be biased toward the former. The resulting sensor list would likely be different from the sensor list ultimately chosen in the present research.

40, 50, 70, and 80[19]. In each contrast (HV, VH), for each magnetometer, each of the eight wavelets were scanned across time starting in the N1 time frame (150 ms post target trigger onset), and the time point containing the largest power was noted, along with the time point and the sensor[20]. Then for each contrast, across all magnetometers, and all wavelets, the power values were ordered in descending value. In each contrast, the magnetometer with the highest power value was selected as well as its hemisphere counterpart. Then the magnetometer with the next highest power value was selected as well as its hemisphere counterpart (if the hemisphere counterpart was not already selected in the previous step). Magnetometers were selected using this algorithm in each contrast until 12 pairs (24 magnetometers) were selected for each contrast (HV, VH). Figure 36 in appendix A.2 MEG Sensor Layout graphs the 12 magnetometer pairs that resulted from this algorithm for each of the HV and VH condition-display contrasts. A single merged list of 12 pairs was selected as follows: the five magnetometer pairs in common between the two contrasts were selected (Temporal lobe 21, Parietal lobe 29 & 32, Occipital Lobe 37 & 43). Since no magnetometers were common in the frontal lobe and one pair was identified in each contrast, they were both added to the list (5 from the HV contrast, and 11 from the VH contrast). Since the occipital lobe is key in visual perception, one pair from each contrast was added to the list (39 from the HV contrast, and 44 from the HV contrast). To insure broad coverage of the head, the next most anterior magnetometer was added to the list: Temporal pair 13 from the VH contrast. To counter, the most posterior temporal pair 20 in

[19] Often a notch filter is used to remove 60 Hz power line noise in electromagnetic signals. In the present research the 60 Hz wavelet is not included in the analysis as the way to eliminate the 60 Hz power line noise.

[20] Scanning started in the N1 time frame 1) because this is the time-frame in which OBA modulations occur as demonstrated in the results here and in extant literature, and 2) to minimize the power from the P3 component of the previous cue, since that component is non-interesting yet is convolved with the signal of interest post target onset. The purpose in delaying search by 150 ms was to let that component resolve to baseline as much as possible.

the HV contrast was added. Finally, from visual inspection of the two graphs in Figure 36, it is clear that the parietal-temporal-occipital junction was key. Also, visual inspection of the source signals revealed that the largest signal modulations were in the temporal lobe. Therefore the temporal lobe pair 23 that abuts this junction, from the VH contrast list was added. The resulting 12 magnetometers are graphed in Figure 20.

ANOVA: Because the difference-score ANOVA done in the EEG condition-display temporal analysis (4.1.5 Analysis Methods – Sliding windows with condition-display contrast) yielded significant OBA results (4.1.8 Discussion of EEG/ERP temporal analyses), whereas the traditional contrasts (Valid-Invalid, Valid-DO, SO-DO) did not, the difference-score contrast is used as the starting point for the MEG temporal analysis. The ANOVA is a mixed design with the following factors: difference-score (DO-Valid, SO-Valid) X target-side (left, right) X magnetometer-side (left, right). ANOVAs are done separately for each of the HV and VH condition contrasts, for each of the P1 and N1 latency windows, per magnetometer-pair.

4.2.2 Results – Components

The posterior magnetometer pairs were analyzed for significance in the P1 and N1 component time frames (75 – 125 ms and 150 – 200 ms respectively) at $p = 0.05$. The results in Figure 21 and Figure 22 show the significant interactions in the ANOVA for the given condition contrast (HV or VH respectively), given magnetometer pair, and P1 or N1 time window. In the HV contrast (Figure 21), while significant interactions are found in the ANOVA, none subsequently pass Tukey post-doc analysis designed to determine the source of significance. However, subsequent paired t-tests reveal that right targets are significantly different in the N1 time frame, in the ventral-lateral occipital magnetometer

pair 39. In the VH contrast, paired t-tests reveal that right targets are found to be significantly different in the N1 time frame, in the relatively more dorsal-medial occipital magnetometer pair 37.

These results are meager compared to the concomitant EEG component results. The reasons for this are explored in subsequent section 4.2.6 Discussion of MEG/ERMF temporal results, together with the sliding window results of the next section.

Object-based attention (OBA) for shifts within hemifield (HV condition contrast)

(a) occipital lobe mag pair 37
difference-score X mag-side
F(1,1) = 4.3, p = 0.042

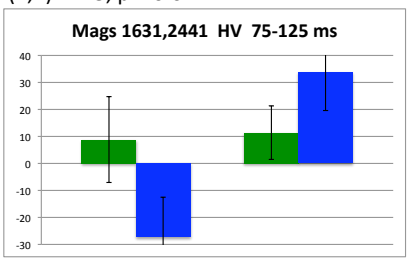

P1 time frame

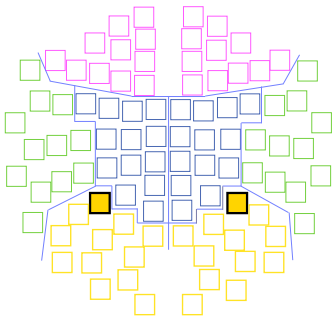

mag pair 37 (1631 left, 2441 right)

(b) temporal lobe mag pair 20
difference-score X mag-side
F(1,1) = 5.07, p = 0.028

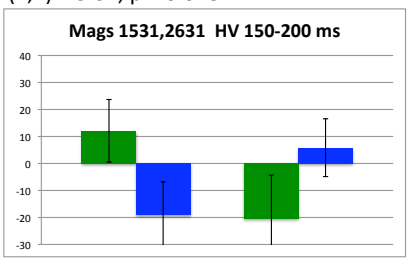

N1 time frame

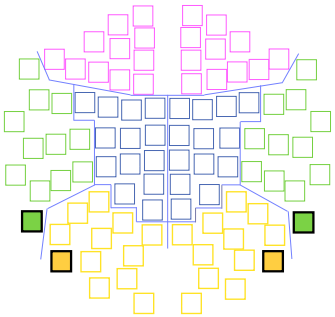

temporal
mag pair 20 (1531 left, 2631 right)

occipital
mag pair 39 (1711 left, 2531 right)

(c) occipital lobe mag pair 39
difference-score X mag-side
F(1,1) = 4.45, p = 0.039

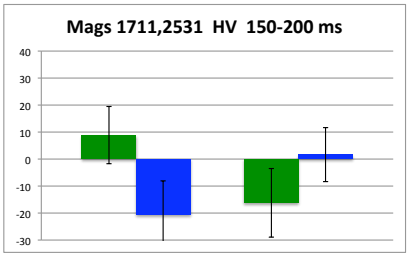

occipital lobe mag pair 39
difference-score X target-side
F(1,1) = 4.44, p = 0.039
right targets significant, p = 0.002

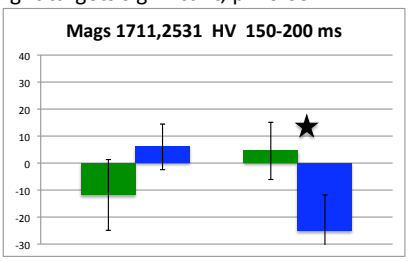

Shown are sources of significance. DO-Valid is green, SO-Valid is blue. The y-axis on the graphs is flipped. Green up and blue down means SO > DO, and vice-versa.(a) in the HV condition-display contrast, occipital magnetometer pair 37 has a significant difference-score X magnetometer-side interaction in the P1 time frame, (b) temporal lobe magnetometer pair 20 has a significant difference-score X magnetometer-side interaction in the N1 time frame; while occipital lobe magnetometer pair 39 has both a significant difference-score X magnetometer-side interaction, and difference-score X target-side interaction, also in the N1 time frame. None of the interactions pass Tukey post-hoc analysis designed to elucidate the source of the interaction. However, subsequent paired ttests reveal that right targets were significantly different in the occipital magnetometer pair 39, p = 0.002.

Figure 21

Object-based attention (OBA) for shifts between hemifields (VH condition contrast)

N1 time frame

occipital lobe mag pair 37
difference-score X mag-side
F (1,1) = 4.04, p = 0.049

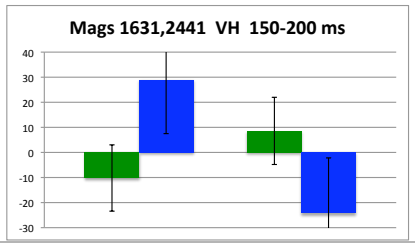

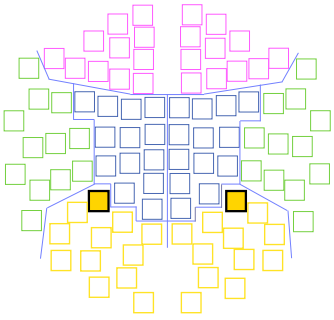

mag pair 37 (1631 left, 2441 right)

occipital lobe mag pair 37
difference-score X target-side
F(1,1) = 4.05, p = 0.048
right targets significant, p = 0.013

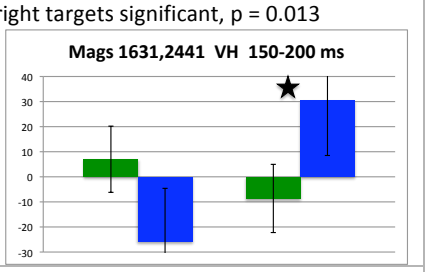

Shown are sources of significance. DO-Valid is green, SO-Valid is blue. The y-axis on the graphs is flipped. Green up and blue down means SO > DO, and vice-versa.(a) the occipital lobe magnetometer pair 37 has both a significant difference-score X magnetometer-side interaction, and significant difference-score X magnetometer-side interaction, in the N1 time frame. None of the interactions pass Tukey post-hoc analysis designed to elucidate the source of the interaction. However, subsequent paired ttests reveal that right targets are significantly different in the occipital magnetometer pair 37.

Figure 22

4.2.3 Analysis Methods – Sliding windows

Sliding windows: The temporal MEG analysis uses the same sliding window approach discussed in the temporal EEG analysis (4.1.3 Analysis Methods – Sliding windows). Windows start at 50 and end at 300 ms post-target trigger onset. Each window is 50 ms in width with a 25 ms overlap from one window to the next. The windows encompass the P1 (75 – 125 ms) and N1 (150 – 200 ms) components.

Dependent variable: As in EEG sliding window analysis (4.1.5 Analysis Methods – Sliding windows with condition-display contrast), the dependent variable in a given ANOVA is the mean amplitude of the difference-score signal within a given latency window. There are nine 50 ms windows between 50 and 300 ms post-target trigger onset.

Magnetometer pairs: The 12 magnetometer-pairs identified in the MEG temporal components analysis (4.2.1 Analysis Methods – Components) are used here. There are 2 frontal lobe pairs of magnetometers, 4 temporal lobe pairs, 2 parietal lobe pairs, and 4

occipital lobe pairs. The magnetometers chosen are shown in red and their placement is shown in Figure 20 above, and Figure 35 in the Appendix.

ANOVA: As in the MEG component analysis (4.2.1 Analysis Methods – Components) the ANOVA is a mixed design with the following factors: difference-score (DO-Valid, SO-Valid) X target-side (left, right) X magnetometer-side (left, right). ANOVAs are done separately for each of the HV and VH condition contrasts, for each latency window across the sliding window scheme, per magnetometer-pair.

Multiple Comparisons: In using sliding windows in the ANOVA analysis, multiple comparisons are addressed using the Holm adjustment to the Bonferroni correction method.[21]

4.2.4 Results – Sliding windows

No significant differences are found in either the HV or VH contrasts when using multiple comparison correction to account for multiple latency windows and the 12 pairs of magnetometers across the anterior and posterior brain. When only two latency windows are considered, those that correspond to the P1 and N1 components, and $p = 0.05$, then the component results discussed in 4.2.2 Results – Components are replicated.

[21] The p-values included in the correction are those associated with the effects and interactions of interest (all those that contain difference-score as a factor) from all ANOVAs across twelve magnetometer pairs, per condition-display contrast. The Holm adjustment for a given p-value in an increasing sorted sequence is $0.05/(N-n+1)$, where N is the number of tests and n is the position in the sequence. N is this case was calculated as 4 (1 main effect and 3 interactions of interest) X 9 latency windows X 12 magnetometer pairs = 432. The main effect and 3 interactions of interest are (difference-score, difference-score X target-side, difference-score X magnetometer-side, difference-score X target-side X magnetometer-side).

4.2.5 Comparison with behavioral results

A Pearson correlation was conducted between the two significant MEG ANOVA difference-score x target side interactions, with the concomitant behavioral reaction times. No significant relationship was found in either case.

4.2.6 Discussion of MEG/ERMF temporal results

Temporal component analysis of the MEG magnetometers using the posterior pairs from the 12 selected as discussed in the methods section (4.2.1 Analysis Methods – Components), led to meager results, certainly as compared with the concomitant EEG component analysis. The component analysis reveals possible differences in same versus different object processing in the N1 time frame, but only in right targets. The subsequent sliding window analysis, which requires a more stringent p value to correct for multiples comparisons, reveals no significant differences at all.

One possible reason for the meager component results is that the P1 and N1 attentional components are defined for EEG, and may not exist in the same form, or at all, in MEG signals as recorded on the scalp surface. The summation characteristics of the electric and magnetic component of the brain signals are different: the neuronal activity that electrically sums to give the P1 and N1 components, may not sum the same way across magnetic fields (see the discussion on the characteristics of EEG versus MEG signals in 2.1.1 Characteristics of the signals for a full explanation).

It is also possible that the choice of magnetometer pair may not be optimal for elucidating such information, as MEG signals at a given magnetometer can differ dramatically from the next spatially adjacent magnetometer, more so than do the signals from one EEG electrode to the next spatially adjacent electrode. Given more focal sensor

readings in MEG, compounded with the fact that there are a large number of sensors, it is more difficult to know a priori which sensors are the best choice given the goal of assessing significant differences between conditions.

Another consideration is that time-only domain analysis is not common for MEG analysis. Such a tradition exists only for EEG. Rather time-frequency domain analysis is the norm for research conducted using MEG. Although a rich literature has been culled for EEG/ERP using time-domain component analysis, there is no reason to presume that it is the best approach for MEG analysis, given the very complex nature of the electrical versus magnetic components of the signals, the differential characteristics of how they summate, and how they differentially emanate through the scalp and skull.

4.3 Temporal Analysis Discussion

To assess object-based attention (OBA) vis-à-vis space-based attention (SBA), the conventional contrasts of Valid vs. Invalid, Valid vs. different-object (DO), and same-object (SO) vs. DO were employed in the present analysis. To assess OBA while controlling for shifts of attention *within hemifield*, DO-Valid difference signals in the horizontal displays were contrasted with SO-Valid difference signals in the vertical displays (HV condition-display contrast); and to assess OBA while controlling for shifts of attention *between hemifields*, DO-Valid difference signals in the vertical displays were contrasted with SO-Valid difference signals in the horizontal displays (VH condition-display contrast). The conventional contrasts were evaluated in the time-domain for EEG (4.1.2 Results - Components and 4.1.4 Results – Sliding windows): this to replicate previous results with the goal of extending them by identifying the full time-course of cognitive processing. The two condition-display contrasts were evaluated in the time-domain for EEG (4.1.6 Results –

Sliding windows with condition-display) and MEG (4.2.2 Results – Components and 4.2.4 Results – Sliding windows): this to establish OBA effects while controlling for shifts of attention within versus between hemifields, and to identify the full course of cognitive processing given this control, in both EEG and MEG.

The EEG conventional contrasts analyses replicated important space and object-based attention effects. SBA was found to exist in the P1 and N1 time frames, and OBA was found to exist in the N1 time frame in select posterior electrodes. The contrasts were also evaluated using multiple sliding latency windows across time, which were conducted with the goal of uncovering a full time course of cognitive processing after target trigger onset. Unlike the component analysis however, no significant results were found to exist when correcting for multiple comparisons. These analyses thus succeed in duplicating classic results, but not in extending them by uncovering a full time-course of OBA vis-à-vis SBA cognitive processing.

Next, the difference-score contrast of DO-Valid vs. SO-Valid was thus introduced with the objective of assessing OBA while controlling for shifts of attention within versus between hemifields. In the EEG analysis, a main effect of DO-Valid vs. SO-Valid was found in both the P1 and N1 component time frames in the P7, P8 and O1, O2 electrode pairs (significance at $p = 0.05$), when shifts of attention were controlled to be within hemifield (HV contrast). This result is a significant contribution to the literature: first, the existence of OBA is demonstrated to exist when shifts of attention are controlled to be within a hemifield, a control which has not been incorporated in past OBA research; and second, OBA is found to exist in the P1 as well as the N1 component time frames: previous research found OBA effects solely in the N1 time frame. In the VH contrast (controlling for shifts of

attention between hemifields) however, no significant effects were found. Nevertheless, the HV contrast is arguably the cleaner test for object effects, as the cognitive processing associated with communication between hemispheres is not a factor that can differentially impact the timing or signal characteristics of observed object effects, thus creating a confound with actual OBA effects in interpretation.

Component analysis in the time domain is well established for examining EEG/ERP signals. In this approach, specific time frames are chosen a priori and evaluated at the electrode(s) at which results are strongest. Significance is evaluated at $p = 0.05$. In particular, using this approach, Martinez et al. (2006) demonstrated that OBA exists in the N1 component time frame in select posterior electrodes. The fact that the present research duplicates and extends these results attests to the strength of this approach for examining EEG signals. Note however, the fact that ERP/EEG signals are smeared in space and time due to the scalp and skull (see 2.1.1 Characteristics of the signals), increases the likelihood that the signal of interest will be the same or sufficiently similar across adjacent electrodes and across a larger window of time, so the choices of one electrode to the next, and exact start and end points of the latency window, are not as critical in achieving the desired results.

In contrast to EEG, component analysis in the time domain for examining MEG signals produced non-impressive results. Only right targets were found to be significant, left targets were not. Furthermore, this significance was found via paired ttests as opposed to the more rigorous Tukey post-hoc analysis. One possible reason for the meager component results is that the P1 and N1 attentional components are defined for EEG, and may not exist in the same form, or at all, in MEG signals as recorded on the scalp surface.

Moreover, MEG signals are more focal than EEG signals in space and time as read from one magnetometer to the next, so the choice of magnetometer and time frame for analysis is a more critical factor in the probability that the signal of interest will be observed. It is possible that more impressive MEG results would be found with different choices of magnetometers or latency window.

Due to the focal nature of the MEG signals, the sliding window approach becomes particularly attractive, to insure all possible time points of interest are evaluated. The relative cost of this approach is a more stringent p-value necessary for multiple comparisons correction. A sliding window of 50 ms from 50 to 300 ms post target trigger onset was used in the present chapter to analyze OBA in MEG using the condition-display contrasts DO-Valid vs. SO-Valid. However, no significant differences were found in either the HV or VH display-contrasts when using multiple comparison correction to account for multiple windows and multiple pairs of magnetometers across the anterior and posterior brain.

In summary, only the EEG component and condition-display analyses produced significant results, while the counterpart MEG analyses produced meager results in the temporal analysis. Neither the EEG nor MEG sliding window analyses produced significant results; this may be due to the fact that differences could not survive the stringent p-value necessary to account for multiple comparisons. In MEG, it is possible that the P1 and N1 components (which were defined for EEG) may not exist in the same form or at all in MEG signals are recorded on the scalp surface. Also, it is possible that a different choice of magnetometer pairs or different latency windows in the analyses would lead to significant findings. While temporal analysis is commonplace in EEG, it is more common to find

temporal-spectral analyses in the MEG research. The next step is to conduct temporal-spectral analyses on both the EEG and MEG data. This is done in the next chapter: 5. Temporal-Spectral Analysis.

5. Temporal-Spectral Analysis

While it is more common to analyze EEG in the time than in the frequency domain, the opposite is the case with MEG: it is more common to analyze MEG in the frequency than in the time domain (See discussion in 2.1.2 Methods and Analysis Traditions). A key aspect of this dissertation research is that the theoretical basis is designed broadly across MEG and EEG to include the research traditions behind each. Analyses are conduced in both the time and frequency domains so as to best compare, contrast and build a bridge between the unique contribution each has to make to our understanding of OBA vis-à-vis SBA.

Since the condition-display contrast yielded the most interesting and significant results in the temporal analysis, it is used in the temporal-spectral analysis to assess OBA. To reiterate the contrast: DO-Valid in the horizontal display is contrasted with SO-Valid in the vertical display to assess OBA when shifts of attention are controlled to be within hemifield ("HV" contrast); and DO-Valid in the vertical display is contrasted with SO-Valid in the horizontal display to assess OBA when shifts of attention are controlled to be across hemifields ("VH" contrast).

5.1 EEG/ERP

5.1.1 Analysis Methods – Sliding windows

Attention components: Analysis on the P1 and N1 components discussed in the EEG temporal section (4.1.1 Analysis Methods - Components) is performed for the temporal-

spectral analysis in the context of the sliding latency windows. The components are highlighted in the results discussion for comparison.

Sliding windows: The sliding windows discussed in EEG and MEG temporal analyses (4.1.3 Analysis Methods – Sliding windows, and 4.2.3 Analysis Methods – Sliding windows) are used in the temporal-spectral analysis here. There are nine 50 ms windows from 50 to 300 ms post-target trigger onset with a 25 ms overlap from one window to the next.

Dependent variable: The sliding windows are applied to the wavelet spectrogram transformations of the EEG signal, the values of which represent percent total power in each specified frequency-band (discussed in section 3.2.4 Wavelets). For the signal there are eight wavelets, one wavelet for each Pseudo-Hz[22] band: 5, 10, 20, 30, 40, 50, 70, and 80[23]. The dependent variable in a given ANOVA is the mean power of each wavelet of the difference-score within a given latency window.

Electrode pairs: The six electrode pairs (three anterior, three posterior) discussed in 4.1.1 Analysis Methods and 4.1.3 Analysis Methods – Sliding windows, are used in the temporal-spectral analysis. They are posterior electrodes O1, O2; P3, P4; and P7, P8; and anterior electrodes F3, F4; F7, F8; and FP1, FP2.

ANOVA: The difference-score ANOVA done in the EEG and MEG temporal analyses (4.1.5 Analysis Methods – Sliding windows with condition-display contrast) is adopted with the additional factor of wavelet for the EEG temporal-spectral analysis. The ANOVA is thus a mixed design with the following factors: difference-score (DO-Valid, SO-Valid) X

---

[22] The term "Pseudo-Hz" is explained in 3.2.4 Wavelets. For our purposes it is conceptually the same as "Hz".

[23] Often a notch filter is used to remove 60 Hz power line noise in electromagnetic signals. In the present research the 60 Hz wavelet is not included in the analysis as the way to eliminate the 60 Hz power line noise.

target-side (left, right) X wavelet (5, 10, 20, 30, 40, 50, 70, 80) X electrode-side (left, right). ANOVAs are done separately for the HV and VH contrasts, for each latency window, for each electrode-pair.

Multiple Comparisons: As in the temporal analysis, multiple comparisons are addressed using the Holm adjustment to the Bonferroni correction method.[24]

5.1.2 Results – Sliding windows

Shifts of attention within hemifield: HV contrast

To assess OBA effects when shifts of attention are **within hemifield**, DO-Valid in the horizontal displays were contrasted with SO-Valid in the vertical displays (HV contrast).

In agreement with the findings in the EEG temporal component analysis, significant differences between the DO-Valid and SO-Valid difference-scores are seen in the P1 time frame, and broadly in the N1 time frame in Figure 23[25] (P1 and N1 time frames are shaded). Recall that in the temporal analysis, component analysis was done (analyzing components at select electrodes with significance at the 5 % level), because the results did not pass more restrictive significance levels necessary for sliding windows and multiple electrodes. In contrast, the results presented in Figure 23 have all passed multiple comparison correction. The results give further insight into the nature of the OBA significance in these attentional components. Apparently, the inclusion of the wavelet

[24] The p-values included in the correction are those associated with the effects and interactions of interest (all those that contain difference score as a factor) from all ANOVAs across six electrode pairs, per condition-display contrast. The Holm adjustment for a given p-value in an increasing sorted sequence is 0.05/(N-n+1), where N is the number of tests and n is the position in the sequence. N in this case was calculated as 8 (1 main effect and 7 interactions of interest) X 9 latency windows X 6 electrode pairs = 432. The main effect and 7 interactions of interest were (difference-score, difference-score X target-side, difference-score X wavelet, difference-score X target-side X wavelet, difference-score X electrode-side, difference-score X target-side X electrode-side, difference-score X wavelet X electrode-side, difference-score X target-side X wavelet X electrode-side).

[25] In all temporal-spectral graphs, only bar graphs associated with the θ and α wavelets are graphed, as when significant differences occurred it is consistently in these frequency bands.

power representation of the EEG signal instead of the signal itself elucidates information across anterior and posterior electrodes not otherwise apparent. A possible explanation for this is that different signal frequencies are significantly different in their contribution to the object based effects of interest, and considering them as levels of a factor in the ANOVA enables this contribution to be apparent. In a time domain analysis, the frequencies are not separated, and thus cannot be differentially accounted for in statistical analysis.

The power relationships between the DO-Valid and SO-Valid difference-scores follow a consistent pattern. In the theta band in both the P1 and N1 components, SO power is significantly greater than DO power in the anterior electrodes when target side is not a factor, and in right targets; while SO is significantly less than DO in left targets in posterior electrodes. These findings are consistent with the predictions of the WhOBAP framework discussed in section 1.3, Figure 9. SO power is significantly greater than DO power when communication between hemispheres is necessary (e.g . right hemifield attentional control communicates with the left hemifield visual processing of right targets), or when communication occurs between anterior and posterior areas. SO power is less than DO when long distance communication is unnecessary (because for example, attentional control and visual processing of left targets both occur in the posterior right hemisphere). Alpha band significance occurs once, in left targets in the N1 component in the posterior O1, O2 electrode pair: SO power significantly less that DO power. The WhOBAP framework predicts then that these two electrodes are task relevant in the N1 time frame for OBA since alpha inhibition for SO is relatively reduced. The O1, O2 electrodes in the N1 time frame may best represent the signal associated with OBA modulation.

In summary, the key result is that when shifts of attention are within hemifield, OBA is a result of modulated power in the theta θ range of the EEG signals in the P1 and N1 time frames. The stronger SO power for anterior and left hemisphere communications is theorized to represent the long-range communication between these areas and posterior right hemisphere attentional control, whereas the relatively weaker SO power is theorized to be representative of the fact that right hemisphere visual processing and right hemisphere attentional control do not require long-range communication. Furthermore, the finding that anterior electrodes exhibit significant differences as well as posterior electrodes is new. Typically the P1 and N1 components are traditionally measured only in posterior electrodes.

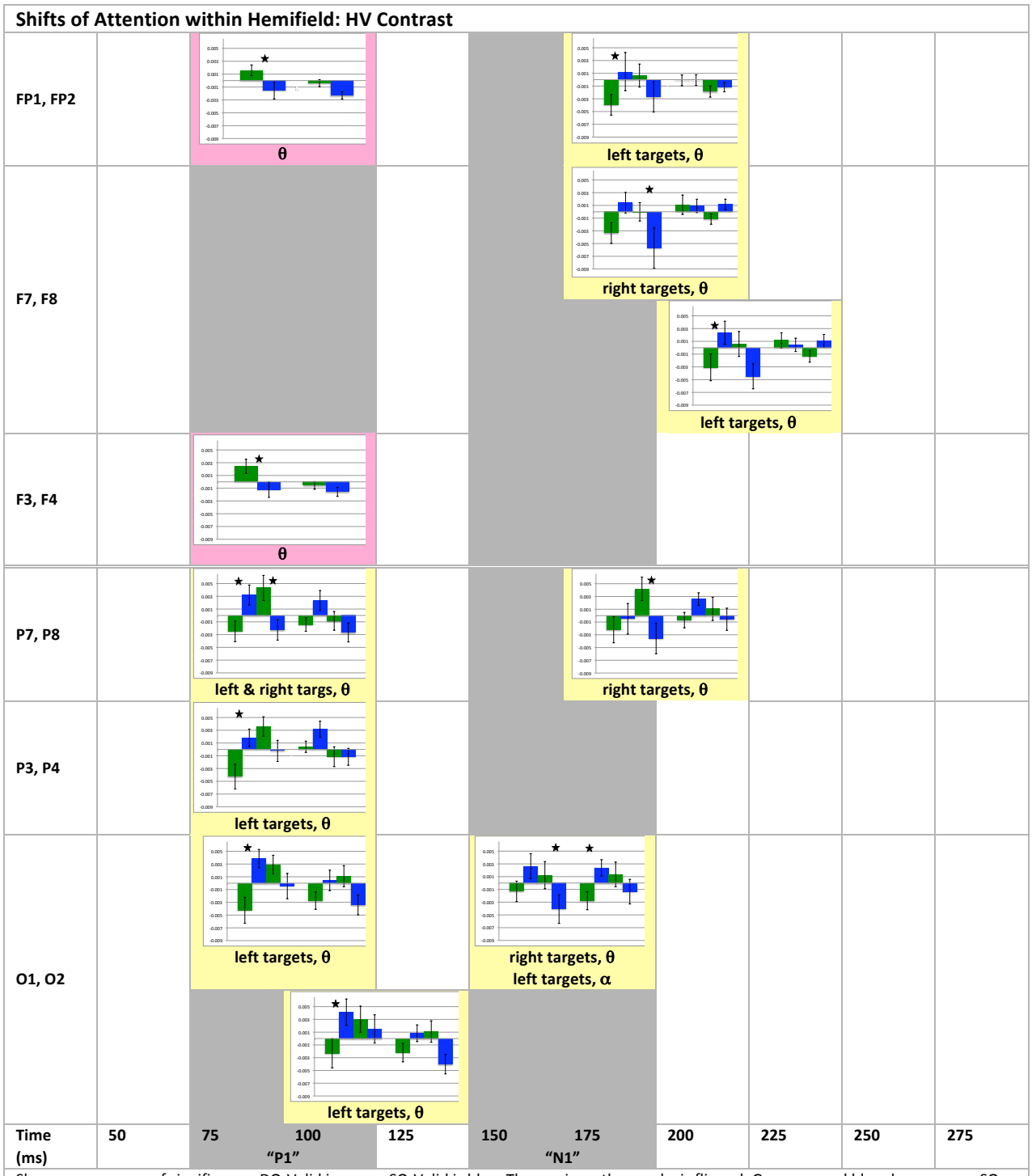

Shown are sources of significance. DO-Valid is green, SO-Valid is blue. The y-axis on the graphs is flipped. Green up and blue down means SO > DO, and vice-versa. Significant differences between difference scores are denoted with a *. A pink background in the cell indicates a difference-score X wavelet interaction, θ on the left, α on the right; a yellow background indicates a difference-score X target-side X wavelet interaction, θ on the left, α on the right, and within each frequency, left targets on the left, right targets on the right. The source of the interaction is listed below each bar graph. F-statistics for these results are given in appendix B.1 Temporal-Spectral EEG/ERP Results.

Figure 23

Shifts of attention between hemifields: VH contrast

To assess OBA effects when shifts of attention are between hemifields, DO-Valid in the vertical displays were contrasted with SO-Valid in the horizontal displays (Figure 24).

As in the HV contrast, the power relationships between the DO-Valid and SO-Valid difference-scores follow a consistent, albeit different pattern. All significant differences are in the theta band, and SO power is significantly greater than DO power in these cases. Since in this contrast all shifts of attention are between hemifields (across the hemispheres), this finding is consistent with the theta long-range communication theory discussed above. Interestingly, significant processing does not fall clearly in the P1 and N1 component time frames, as it does when shifts of attention are controlled to be within hemifield. A possible explanation for this is that OBA effects in the P1 and N1 components are truly only attained when shifts of attention are within hemifield, and that OBA effects when shifts of attention are between hemifields do not occur in these component time frames. This theory should be tested in subsequent post-dissertation research.

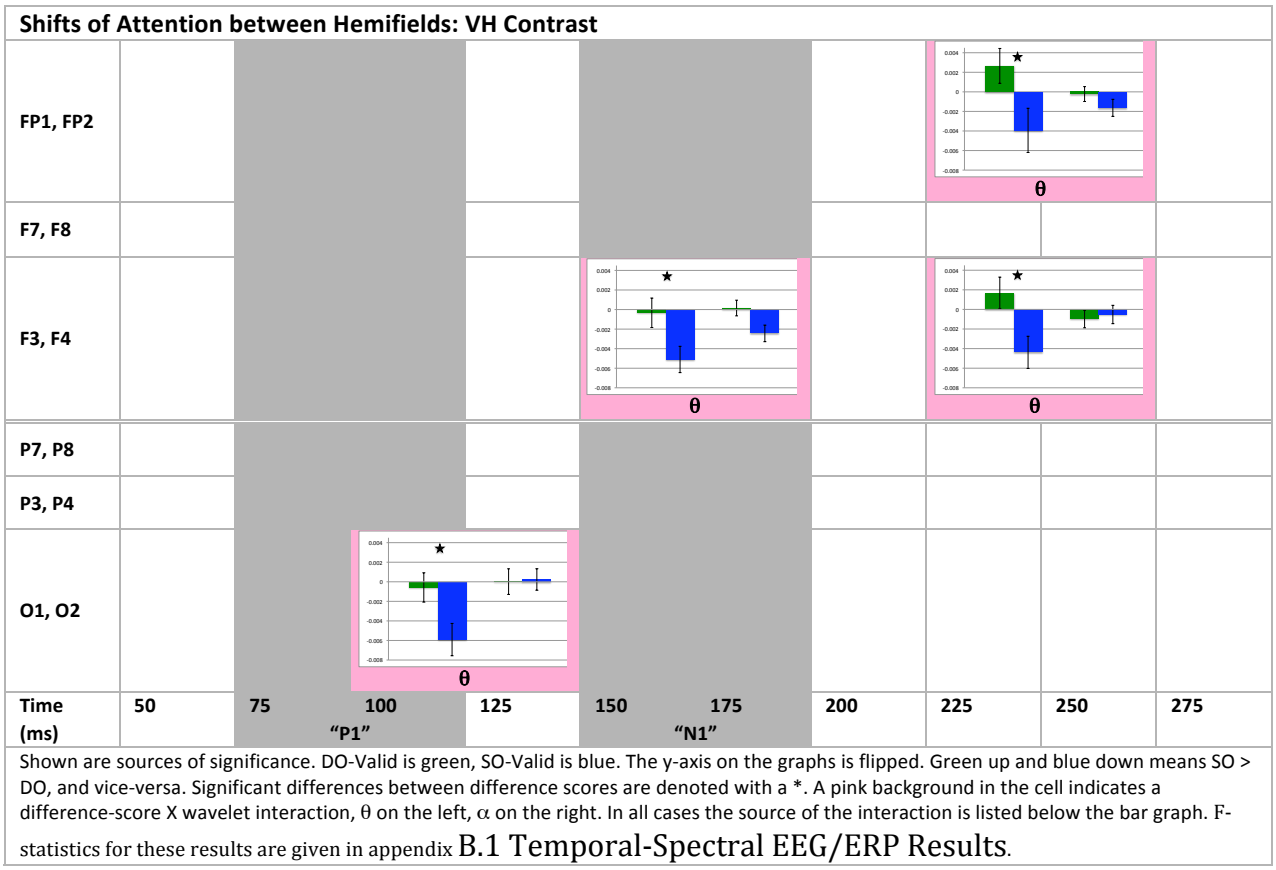

Figure 24

5.1.3 Comparison with behavioral results

A Pearson correlation was conducted between each significant ANOVA result (main effect or interaction) with the concomitant behavioral reaction times. No significant relationship was found in any case.

5.1.4 Discussion of EEG/ERP temporal-spectral analyses

The EEG temporal-spectral analysis assessed OBA by contrasting same object shifts of attention with between object shifts of attention when both sets of shifts are within a hemifield (HV condition-display contrast), or when both sets of shifts are between hemifields (VH condition-display contrast). In the results presented here, clear effects of object-based attention within hemifield (HV) are evident in both the P1 and N1 time

frames, whereas object effects between hemifields (VH), do not fall clearly into these component time frames. This suggests that the P1 and N1 components' attentional modulation is driven primarily by shifts of attention within a hemifield, and that when shifts of attention occur between hemifields, assessing conditions in time frames other than the P1 and N1 components is necessary to understand any differences.

In comparison to the corresponding temporal analysis, the temporal-spectral results here are more robust: significance passes the Holm adjustment to the Bonferroni correction for multiple comparisons; hence conclusions can be drawn between electrode pairs across time even though separate analyses were conducted for each. The present research makes it clear that OBA effects exist across both anterior and posterior electrodes, and the predominant frequency in which significant differences occur is the theta θ band, albeit with a few differences in the alpha α band. First, this suggests that considering different frequencies as levels of a factor in the ANOVA is a reliable way to separate out the specific aspects of the neural signal that truly contribute to significant modulation, and obtain a more robust picture of significance. Second, theta activity interacts with target side in the way predicted by the WhOBAP framework (section 1.3): more theta activity occurs in the SO condition when communication is necessary from anterior electrodes to the posterior right hemisphere, and from left hemisphere electrodes (in processing right targets) to the right hemisphere which is thought to be the seat of attentional control. In the case of the VH condition-display contrast where shifts of attention occur between hemifields, theta SO power is consistently greater than DO power, presumably representing the communication necessary between hemispheres for attentional processing of objects that span the left and right hemifields. In the one occurrence when

alpha activity was significantly different (in the O1, O2 electrode-pair in the HV contrast), SO power is significantly less than DO power. According to the alpha inhibition/gating theory, this suggests that these electrodes represent OBA task relevant signal information which shifts of attention are controlled to be within a hemifield, since alpha inhibition power is relatively low.

Overall, the findings of the EEG temporal-spectral analysis validate those of the EEG temporal analysis: OBA exists when shifts of attention are controlled to be within hemifield in the P1 and N1 component time frames. OBA effects are evident when shifts of attention are controlled to be between hemifields, but do not clearly fall into these component time frames. The key new findings are that results occur in the anterior as well as the posterior electrodes, and that significant differences occur primarily in the theta band (center frequency 5 Hz), with some differences in the alpha band (center frequency 10 Hz), as predicted by the WhOBAP framework introduced in section 1.3.

5.2 MEG/ERMF

Three analyses of the MEG data are presented here. First, a sliding window analysis counterpart to the EEG analysis is done. ANOVAs were conducted per magnetometer-pair, on nine 50 ms windows from 50 ms to 300 ms post-target trigger onset with a 25 ms overlap from one window to the next[26]. The second analysis considers time and magnetometer-pair as factors in the ANOVA, which is done for each of the frontal, temporal, parietal and occipital lobes (referred to as the "Per Lobe ANOVAs"). The third analysis also considers time and magnetometer-pair as factors in an omnibus ANOVA across all lobes (referred to as the "Omnibus ANOVA"). Each analysis builds on and clarifies the previous analysis' results, in order to compose a complete picture of temporal-spectral processing across the entire brain.

5.2.1 Analysis Methods – Sliding windows

Sliding windows: The sliding windows used in the EEG and MEG temporal and EEG temporal-spectral analyses (4.1.3 Analysis Methods – Sliding windows and 4.2.3 Analysis Methods – Sliding windows, 5.1.1 Analysis Methods – Sliding windows) are used in the analysis here. There are nine 50 ms windows from 50 ms to 300 ms post-target trigger onset with a 25 ms overlap from one window to the next.

[26] A second sliding window analysis was conducted per magnetometer-pair on five 50 ms windows from 50 ms to 300 ms post-target onset with no overlap from one window to the next. The purpose of this second analysis was to validate that the results hold with sparser (non-overlapping) coverage of the time-course. These results are included in B.2.3 Results – Sliding windows, non-overlap.

.

Dependent variable: The sliding windows are applied to the wavelet spectrogram transformations of the MEG signal, the values of which represent percent of total power in each specified frequency-band (discussed in section 3.2.4 Wavelets). As in the EEG temporal-spectral analysis (5.1.1 Analysis Methods – Sliding windows), for the signal there are eight wavelets, one wavelet for each frequency band with center frequency: 5, 10, 20, 30, 40, 50, 70, and 80. The dependent variable in a given ANOVA is the mean power of each wavelet of the condition within a given latency window.

Magnetometer pairs: The 12 magnetometer-pairs identified in the MEG temporal analyses (4.2.1 Analysis Methods – Components and 4.2.3 Analysis Methods – Sliding windows) are used here. There are 2 frontal lobe pairs of magnetometers, 4 temporal lobe pairs, 2 parietal lobe pairs, and 4 occipital lobe pairs. The magnetometers chosen are delineated with a red square outline, and their placement is shown in Figure 20 above, and Figure 35 in the Appendix.

ANOVA: As is done in the EEG temporal-spectral analysis (5.1.1 Analysis Methods – Sliding windows), the ANOVA is difference-score (DO-Valid, SO-Valid) X target-side (left, right) X wavelet (5, 10, 20, 30, 40, 50, 70, 80) X magnetometer-side (left, right). ANOVAs are done separately for the HV and VH contrasts, for each sliding window, for each magnetometer pair.

Multiple Comparisons: In using sliding windows in the ANOVA analysis, multiple comparisons are addressed using the Holm adjustment to the Bonferroni correction method.[27]

[27] The p-values included in the correction are those associated with the effects and interactions of interest (all those that contain difference-score as a factor) from all ANOVAs across twelve magnetometer pairs, per condition-display contrast. The Holm adjustment for a given p-value in an increasing sorted sequence is 0.05/(N-n+1), where N is the number of tests and n is the position in the sequence. N in the overlapping sliding windows was calculated as 8 (1 main effect and 7 interactions of interest) X 9 latency windows X 12

5.2.2 Results – Sliding windows

Shifts of attention within hemifield: HV contrast

To assess OBA effects when shifts of attention are **within hemifield** (the "HV" condition-display contrast), DO-Valid in the horizontal displays were contrasted with SO-Valid in the vertical displays in the sliding window analysis. Across the nine latency windows, and twelve magnetometer pairs, there were fifty-seven two- and three-way significant interactions plus two main effects of difference-score. Thirty-five of the interactions were of the predominant, highest order three-way interaction of difference-score X target-side X wavelet. Fifteen of the interactions were of the predominant two-way interaction of difference-score X target-side.

The three-way interaction of difference-score X target-side X wavelet is summarized in Table 1. As with the concomitant EEG analysis (5.1.2 Results – Sliding windows), when frequency is a significant factor, it is so only in the theta θ and alpha α bands. It is a factor in anterior magnetometer pairs only in the theta band, and in posterior magnetometers in both the theta and alpha bands. Left targets start to be processed differentially between condition contrasts earlier than right targets (50 versus 100 ms), and finish earlier at 250 ms, while right targets start differential processing at 100 ms and are still differentially processed at 300 ms. The faster time course for left targets may be reflective of right hemisphere dominance in attentional processing. The frontal magnetometer pair 11, the posterior temporal dorsal-lateral magnetometer pair 23, and the dorsal occipital magnetometer pair 44 were not significantly different anywhere in the timecourse in the

magnetometer pairs = 864. The main effect and 8 interactions of interest are (difference-score, difference-score X target-side, difference-score X wavelet, difference-score X target-side X wavelet, difference-score X magnetometer-side, difference-score X target-side X magnetometer-side, difference-score X wavelet X magnetometer-side, difference-score X target-side X wavelet X magnetometer-side).

HV condition-display contrast. This is not particularly surprising given that the inclusions of magnetometer pairs 11, 23 and 44 were due to the VH condition contrast, but nonetheless it is a testament to the focal nature of signals evident at the MEG sensor level. (See Figure 36 in the appendix). The detailed breakout of all interaction and main effect results are included in Appendix B.2.1 Results – Sliding windows, Figure 37 through Figure 41.

The Tukey post-hoc results are summarized in Table 2. The relative power relationships of SO and DO shifts of attention as a function of frequency and target-side follow a consistent pattern when tabulated across all results. In the theta band, in left targets, SO power is significantly less than DO power (pink cell), whereas in right targets SO power is significantly greater (yellow cell). As hypothesized in section 1.3, theta SO power is greater than DO when long distance communication (between hemispheres or anterior to posterior) is necessary. SO power is less than DO power when long-distance communication is not necessary, as in the case for left targets when visual stream processing, object perception and attention all occur within the posterior right hemisphere. In the alpha band, in left targets, SO power is significantly greater than DO power (green cell), whereas in right targets, it is significantly less (green cell with down diagonal). In considering the alpha inhibition/gating theory discussed in section 1.3, the tabulated analysis thus suggests that the posterior, relatively dorsal-medial adjacent magnetometer pairs 32, 37 and 43 reflect signal information from task irrelevant areas for left targets, since SO power is greater than DO power. In contrast, the results suggest that the posterior, relatively ventral-lateral adjacent magnetometer pairs 20, 21 and 39 are task relevant in processing right targets, since SO power is less than DO power. (See Figure 35

in the appendix for placement of these magnetometer pairs on the MEG sensor helmet). The results do not suggest task relevant magnetometer-pairs for left targets (where SO would be less than DO according to the alpha theory discussed in section 1.3); or task irrelevant magnetometers pairs for right targets (where SO would be greater than DO). This finding is intriguing, and will be revisited in section 5.2.7 Discussion of MEG/ERMF temporal-spectral analyses, together with the results for the per lobe ANOVAs and the omnibus ANOVA.

While there were a greater number of the predominant three-way interactions of difference-score X target-side X wavelet, the predominant two-way interactions of difference-score X target-side all had far stronger F-statistic significance. The F-statistics associated with the 15 two-way interactions have F-values ranging between $F(1,1)=14.42$, $p<0.001$ and $F(1,1)=22.31$, p,0.001 (occipital magnetometer pair 39 at 200ms and at 175ms respectively). In comparison, the 35 three-way interactions have F-values ranging between $F(7,1)=3.33$, $p=0.002$ and $F(7,1)=10.41$, $p<0.001$ (occipital pair 43 at 75 ms and temporal pair 29 at 200 ms respectively). (F-statistics for all significant results are in B.2.1 Results – Sliding windows, Table 12 through Table 16). The pre-dominant two-way interaction of difference-score X target-side (where frequency is not a factor) thus represents a greater proportion of explained vs. unexplained variance per statistic than do other significant results. Tukey post-hoc results of the two-way interaction are summarized in Table 3. In these interactions only right targets in the posterior magnetometer-pairs are ever significant: SO power is always significantly greater than DO power (yellow cell). This finding is also intriguing and will be revisited in section 5.2.7

Discussion of MEG/ERMF temporal-spectral analyses, together with the results for the per lobe ANOVAs and the omnibus ANOVA.

In summary, in the theta band in left targets, SO power is significantly less than DO power, while it is significantly greater in right targets. These results are consistent with the predictions of the WhOBAP framework (section 1.3). SO power is also significantly greater than DO power in right targets when frequency is not a factor. In the alpha band in left targets, SO power is significantly greater than DO power in the posterior, relatively dorsal-medial adjacent magnetometer pairs 32, 37, and 43 suggesting they reflect signal information from task irrelevant areas. The results further suggest that the posterior, relatively ventral-lateral adjacent magnetometer pairs 20, 21 and 39 are task relevant in processing right targets, since alpha-band SO power is significantly less than DO power.

HV contrast: Predominant three-way interaction: difference-score X target-side X wavelet
Summary of Frequency and Target-Side Characteristics Across Sliding Windows

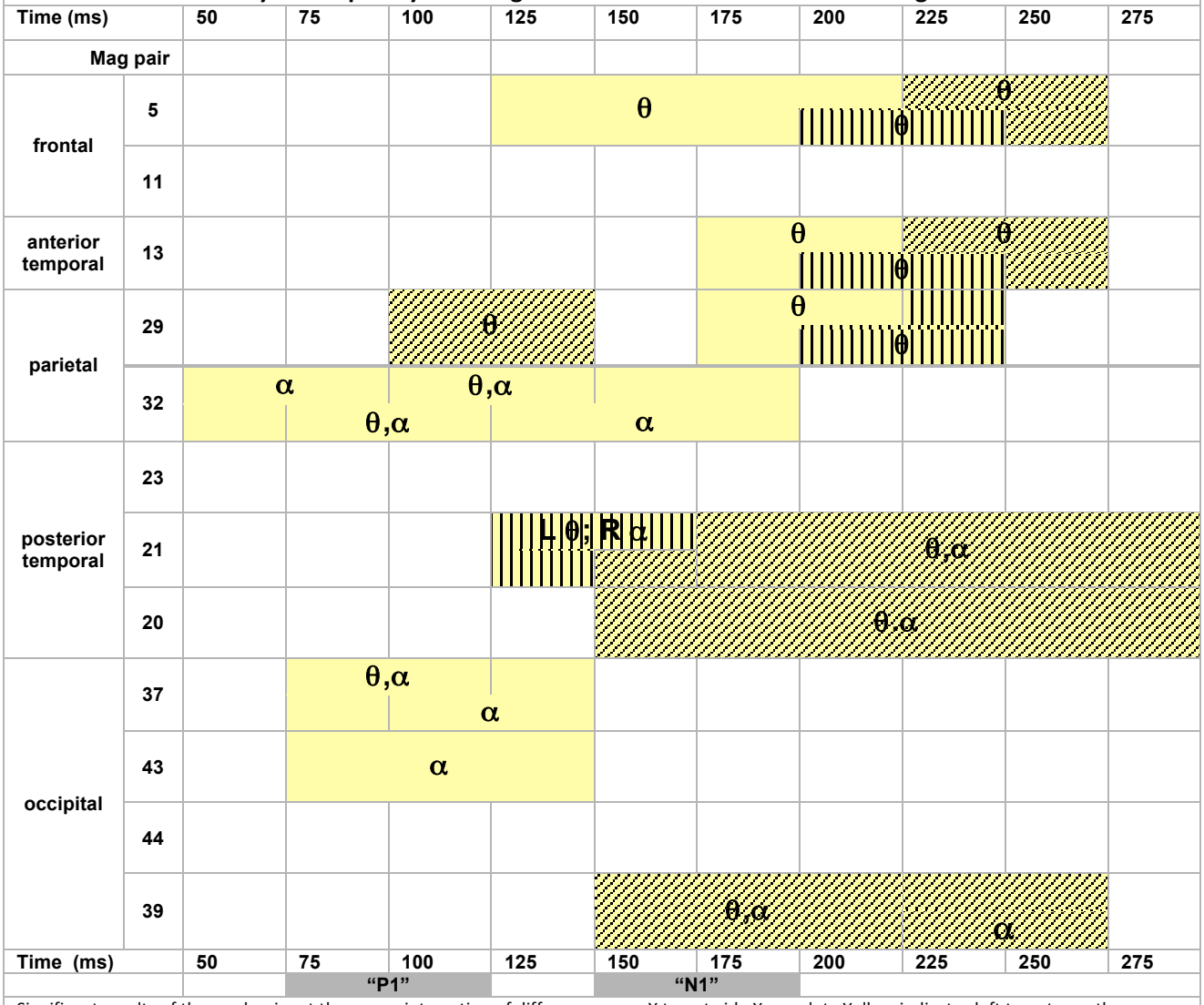

Significant results of the predominant three-way interaction of difference score X target-side X wavelet. Yellow indicates left targets are the source of significance. Up diagonal yellow indicates right targets are the source. Vertical stripe yellow indicates both left and right targets are sources of significance. Left targets start and finish differential processing (50 – 250 ms) before right targets (100 – 300 ms). Significance occurred in the anterior magnetometers only in the theta θ band, and in the posterior magnetometers in both the theta θ and alpha α bands. No significant differences were found in any other wavelet frequency band.

Table 1

HV contrast: Predominant three-way interaction: difference-score X target-side X wavelet Summary of Power Relationships as a Function of Frequency and Target-Side		
frequency band	left targets	right targets
α	SO > DO parietal lobe pair 32 occipital lobe pairs 37 and 43	SO < DO temporal lobe pairs 20 and 21 occipital lobe pair 39
θ	SO < DO	SO > DO
Tabulation of 35 significant three-way interactions: difference-score X target-side X wavelet. in the alpha band in left targets, SO power is greater than DO power in adjacent magnetometer pairs 32, 37 and 43. In the alpha band in right targets, SO power is less than DO power in adjacent magnetometer pairs 20, 21 and 39. See the MEG sensor helmet layout (see Figure 35 in the appendix).		

Table 2

HV contrast: Predominant two-way interaction: difference-score X target-side Summary of Power Relationships as a Function of Target-Side	
left targets	right targets
na	SO > DO, posterior mags
Tabulation of 15 significant two-way interaction: difference-score X target-side	

Table 3

Shifts of attention between hemifields: VH contrast

To assess OBA effects when shifts of attention are **between hemifields** (the "VH" condition-display contrast), DO-Valid in the vertical displays were contrasted with SO-Valid in the horizontal displays. Across the nine latency windows, and twelve magnetometer pairs, there were fifty-one two- and three-way significant interactions. Thirty-two of the interactions were of the predominant, highest order three-way interaction of difference-score X target-side X wavelet. Fourteen of the interactions were of the predominant two-way interaction of difference-score X wavelet.

The three-way interaction is summarized in Table 4. Like the HV display-condition contrast, and the concomitant EEG analysis (5.1.2 Results – Sliding windows), when frequency is a significant factor, it is so only in the theta θ and alpha α bands. It is a factor in anterior magnetometer pairs primarily in the theta band, and in posterior magnetometers

in both the theta and alpha bands. Unlike in the HV condition-display contrast where left targets start and stop significant differential processing sooner than right targets, right targets show significant differences in processing at 50 ms just as left targets do, specifically in the parietal lobe magnetometer pair 29. Throughout the time-course left targets are consistently differentially processed, whereas right targets are only briefly so at the beginning of the time course. The frontal magnetometer pair 5 and the occipital magnetometer pair 39 are not significantly different anywhere in the timecourse in the VH condition-display contrast. This is also not particularly surprising given that the inclusion of magnetometer pairs 5 and 39 were due to the HV display-condition contrast (see Figure 36 in Appendix A.2 MEG Sensor Layout), but again is a testament to the focal nature of the MEG signals as measured from one magnetometer to the next on the scalp surface. The detailed breakout of all interactions is included in B.2.1 Results – Sliding windows, Figure 42 through Figure 45.

Unlike in the HV condition-display contrast, the predominant three-way and two-way interactions for the VH condition-display contrast have F-statistics of the same magnitude, suggesting that the three–way interaction may reflect all the characteristics of interest in that it accounts for as much explained vs. unexplained variance per statistic as the other statistics, and it underscores the contribution of the greatest number of interactions. Specifically, the F-statistics associated with the fifty-one three-way interactions have F-values ranging between $F(7,1) = 2.32$, $p = 0.02$ (occipital pair 43 at 175 ms), and $F(7,1) = 7.51$, $p < 0.001$ (temporal pair 23 at 75 ms), while the F-statistics associated with the fourteen two-way interactions have F-values ranging between $F(7,1) = 3.12$, $p = 0.003$ (occipital pair 43 at 225 ms) and $F(7,1) = 6.16$, $p < 0.001$ (occipital pair 37,

at 150 ms). The F-statistics for all significant results are in B.2.1 Results – Sliding windows, Table 17 through Table 20).

The three-way interaction of difference-score X target-side X wavelet is summarized in Table 5. The relative power relationship of SO and DO shifts of attention as a function of frequency and target-side follows a consistent pattern when tabulated across all results. This pattern is opposite that found in the HV condition-display contrast. In the theta band, in left targets, SO power is significantly greater than DO power, whereas no significant differences exist in right targets. The tabulated two-way interactions of target-side X wavelet (Table 6) however, suggests that SO power is greater than DO power in the theta band in anterior magnetometers, independently of target-side. This possibly suggests that theta power is the mechanism for the spread of attention within an object that crosses hemifields, and that anterior areas in particular have a role in the task. In the three-way interaction in the alpha band: SO power is significantly less than DO power in left targets. In considering the alpha inhibition/gating theory, the finding suggests that magnetometer pairs 23, 32, 37, 43 and 44 (which are clustered together at the junction of the occipital, temporal and parietal lobes) are relevant in task processing of left targets, since SO power is less than DO power. (See Figure 35 in Appendix A.2 MEG Sensor Layout). For right targets, the alpha-band findings in the three-way and two-way interactions together suggest that magnetometer pairs 29 and 23 are task irrelevant, while occipital magnetometer-pairs 37 and 43 are task relevant in OBA processing.

VH contrast: Predominant three-way interaction: difference-score X target-side X wavelet
Summary of Frequency and Target-Side Characteristics Across Sliding Windows

Time (ms)		50	75	100	125	150	175	200	225	250	275
Mag pair											
frontal	5										
	11			θ							
anterior temporal	13								θ		
parietal	29	L θ, R α		θ				θ			
	32	α									
posterior temporal	23	α	α								
	21								θ		
	20								θ		
occipital	37	α				θ, α					
	43	α									
	44	α					α				
	39										
Time (ms)		50	75	100	125	150	175	200	225	250	275
			"P1"			"N1"					

Significant results of the predominant three-way interaction of difference score X target-side X wavelet. Yellow indicates left targets are the source of significance. Up diagonal yellow indicates right targets are the source. Vertical stripe yellow indicates both left and right targets are sources of significance. The wavelet of significance is indicated in Greek letters. With one exception, significance occurred in the anterior magnetometers only in the theta θ band, and in the posterior magnetometers in both the theta θ and alpha α bands. No significant differences were found in any other wavelet frequency band.

Table 4

VH contrast: Predominant three-way interaction: difference-score X target-side X wavelet
Summary of Power Relationships as a Function of Frequency and Target-Side

	Three-way interaction: difference-score X target-side X wavelet	
frequency band	left targets	right targets
α	SO < DO magnetometer pairs 23, 32, 37, 43, 44	SO > DO magnetometer-pairs 29, 23
θ	SO > DO	na

Tabulation of 32 significant three-way interactions: difference-score X target-side X wavelet

Table 5

VH contrast: Predominant two-way interaction: difference-score X wavelet Summary of Power Relationships as a Function of Frequency	
frequency band	
α	SO < DO, occipital magnetometer-pairs 37, 43
θ	SO > DO, anterior magnetometer-pairs SO < DO, occipital magnetometer-pair 44
Tabulation of 14 significant to-way interactions: difference-score X wavelet	

Table 6

In summary, in the theta band in left targets and when target-side is not a factor, SO power is significantly greater than DO power, possibly suggesting that theta activity has a role in OBA processing when perceptual objects cross hemifields. In the alpha-band in left targets, SO power is significantly less than DO power in a group of five magnetometer pairs (23, 32, 37, 43 and 44) clustered at the occipital/temporal/parietal junction suggesting that these areas are task relevant according to the alpha inhibition/gating hypothesis. In the alpha-band in right targets, magnetometer-pairs 29 and 23 are task irrelevant while occipital magnetometers pairs 37 and 43 are task relevant for OBA processing. In contrast to the HV condition-display contrast, left and right targets both start differential processing early in the time course, and left targets continue to be differentially processed throughout.

Discussion – Sliding windows

In both the HV and VH condition-display contrasts, effects exist across both posterior and anterior magnetometers (Table 1 and Table 4). When frequency is a factor in differential processing, it is so in theta θ (center frequency 5 Hz), and alpha α (center frequency 10 Hz) bands. When frequency is a factor in anterior magnetometer pairs, it is primarily in the theta θ band, while it is a factor posteriorly in both the theta θ and alpha α bands. This finding suggests that theta has a differential role in whole brain communication of the attention network in SO versus DO shifts of attention, whereas alpha

has a role posteriorly possibly in the visual stream in both hemispheres. The theta communication hypothesis stemming from the results presented here are consistent with the finding by Green & McDonald (2008) that theta activity is an index of control across the spatial attentional network and is consistent with the WhOBAP framework (section 1.3). The posterior alpha activity can be explained by the alpha inhibition/gating hypothesis of Jensen & Mazaheri (2010), in that in SO vis-à-vis DO processing in different display orientations, different areas are relevant versus irrelevant in the posterior brain.

Different magnetometer pairs emerge between the two condition-display contrasts as not demonstrating significant differences. In the HV contrast, frontal magnetometer pair 11, posterior temporal magnetometer pair 23 and occipital pair 44 are not significantly different in the time-course (Table 1), whereas in the VH contrast, magnetometer frontal pair 5 and occipital pair 39 are not significantly different in the time-course (Table 4). This finding is not surprising given that the inclusions of magnetometer pairs 11, 23 and 44 were due to the VH condition contrast, whereas the inclusions of the magnetometer pairs 5 and 39 were due to the HV condition contrast (See Figure 36 in Appendix A.2 MEG Sensor Layout). Nonetheless, the finding does underscore the focal nature of MEG discussed in 2.1.1 Characteristics of the signals. The magnetometer pairs 23 and 44 for example, which do not show significantly difference processing in the HV contrast, are adjacent to magnetometer-pairs that do: pair 23 is adjacent to pairs 32 and 37, while pair 44 is adjacent to pair 43.

While the highest order significant interaction for both the HV and VH condition-display contrasts was the three-way interaction of difference-score X target-side X wavelet in both, the predominant two-way interaction in the HV condition-display contrast of

difference-score X target-side is particularly relevant in that it, more so than the predominant three-way interaction, accounts for a larger portion of the explained variance relative to the unexplained variance per significant statistic. The finding possibly suggests that target-side modulates OBA more so than does frequency when shifts of attention are controlled to be within hemifield although both are significant factors, while target-side and wavelet contribute relatively equally when shifts of attention are between hemifields.

When shifts of attention are controlled to be within hemifield (HV), left targets start to be processed differentially between condition contrasts earlier than right targets, and finish earlier. Consider the fact that shifts of attention are within hemifield means that shifts occur within a hemisphere's control of the visual stream. Since the right hemisphere has been theorized to have a dominant role in attentional processing in general in addition to its role for processing left targets in the visual stream, early processing of left targets could possibly be reflective of the fact that no inter-hemispheric communication is necessary for visual processing and attention control, while later processing of right targets is possibly a reflection of the fact that inter-hemispheric communication must occur between the left hemisphere visual stream processing and the right hemisphere attentional processing. This communication is theorized be reflected in the slower time-course for right targets observed here.

When shifts of attention are controlled to be between hemifields (VH), right targets show significant processing differences early in the time-course just as left targets do, and left targets continue to be differentially processed throughout the time-course. In the theta band in left targets and when target-side is not a factor, SO power is significantly greater than DO power, possibly suggesting that theta activity has a role in OBA processing when

perceptual objects cross hemifields. The alpha-band results are more complicated, and although can be interpreted in light of the alpha inhibition/gating theory, additional experiments should be conducted to tease out the role of alpha given inter-hemispheric communication to process a perceptual object. At this point, it is difficult to further interpret the meaning of these VH condition results without more analysis specifically designed to do so, as any theorized OBA effects are confounded with effects of inter-hemispheric communication and shifting of visual processing control.

Overall, while the frequencies of significantly different processing (theta and alpha) are the same when shifts of attention are controlled to be within versus between hemifields, the evidence here suggests that the time-space courses of the two are clearly different, with the latter having confounds of object and inter-hemispheric communication effects far more than the former. As discussed earlier, the HV contrast is arguably the cleaner test for object effects, as the cognitive processing associated with communication between hemispheres is not a factor that can differentially impact the timing or signal characteristics of observed object effects, thus creating a confound with actual OBA effects in interpretation. Therefore, the subsequent per lobe and omnibus analyses will focus on the HV condition-display contrast, in which shifts of attention are controlled to be within hemifield.

The key findings in the sliding window analyses for the HV condition-display contrast when shifts of attention are controlled to be within hemifield are thus summarized again here. In the theta band in left targets, SO power is significantly less than DO power, while it is significantly greater in right targets. These results are consistent with the predictions of the WhOBAP framework discussed in section 1.3. SO power is also

significantly greater than DO power in right targets when frequency is not a factor. In the alpha band in left targets, SO power is significantly greater than DO power in the posterior, relatively dorsal-medial adjacent magnetometer pairs 32, 37, and 43 suggesting they reflect signal information from task irrelevant areas. The results further suggest that the posterior, relatively ventral-lateral adjacent magnetometer pairs 20, 21 and 39 are task relevant in processing right targets, since alpha-band SO power is significantly less than DO power.

5.2.3 Analysis Methods – Per Lobe ANOVAs: HV contrast

Time-bins: The time-bins entered in the ANOVAs are the same as the sliding windows (5.2.1 Analysis Methods – Sliding windows). Specifically, there are nine 50 ms time-bins from 50 to 300 ms post-target trigger onset with a 25 ms overlap from one time-bin to the next. The term "time-bin" is adopted as opposed to "sliding window" to underscore the fact that the time-bins are entered as levels of a factor (discussed below), as opposed to previous analyses which conducted the ANOVA separately per sliding window.

Dependent variable: The dependent variable is the mean power of each wavelet (theta θ and alpha α) of the difference-score (DO-Valid and SO-Valid conditions) within a given time-bin. Only theta θ and alpha α wavelets are used in the ANOVA since in previous analyses (5.2.2 Results – Sliding windows), when wavelet is a factor and yields significant findings, the significant results emerge only from power in these two frequency bands.

Magnetometer pairs: A separate ANOVA is done per lobe: occipital, parietal, temporal and frontal. Each ANOVA only includes the magnetometer pairs in a given lobe that exhibit significant differences in difference-score in the HV contrast, in the sliding window analysis (see Table 1). For the frontal lobe only the magnetometer pair 5 is entered

into the ANOVA. For the parietal lobe, pairs 29 and 32 are used. For the temporal lobe, pairs 13, 21 and 20 are entered. Finally for the occipital lobe, magnetometer pairs 37, 39 and 43 are entered into the ANOVA.

MEG Magnetometer Sensor Layout – paired across hemisphere

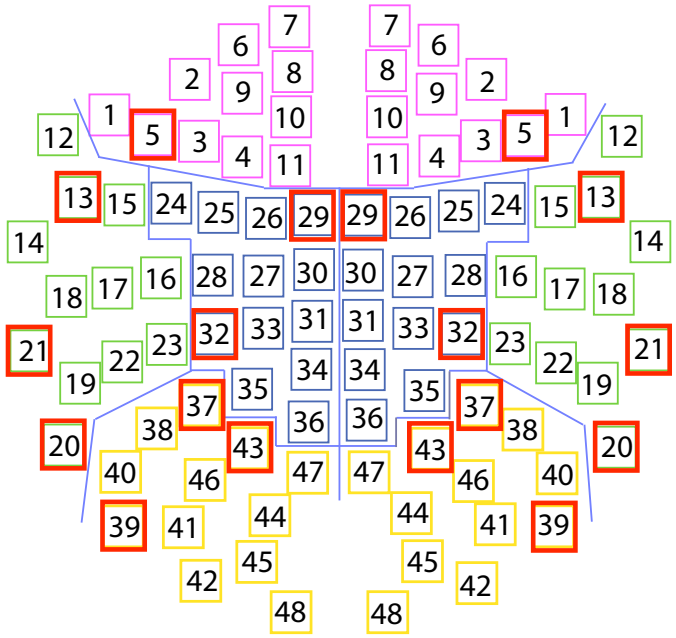

Magnetometers

Frontal pairs (mag left, right)
5 (mag 0341, 1221)

Temporal pairs
13 (mag 0131, 1441)
21 (mag 1541, 2621)
20 (mag 1531, 2631)

Parietal pairs
29 (mag 0631, 1041)
32 (mag 1811, 2221)

Occipital pairs
37 (mag 1631, 2441)
43 (mag 1911, 2311)
39 (mag 1711, 2531)

Pairs delineated with a red square are those used in the magnetometer analysis in all MEG analyses per lobe and omnibus ANOVA analyses.

Figure 25

ANOVA: The ANOVA is based on the previous condition-display contrast analyses ANOVAs (e.g. 5.2.1 Analysis Methods – Sliding windows), with the additional factors of time-bin and magnetometer-pair, and the reduction of levels in wavelet to theta and alpha, as discussed above. The ANOVA for each of the temporal, parietal and occipital lobes is difference-score (DO-Valid, SO-Valid) X time-bin (9 levels) X magnetometer-pair (9 pairs) X target-side (left, right) X wavelet (θ, α) X magnetometer-side (left, right). The ANOVA for the frontal lobe excludes magnetometer-pair as a factor since only one pair (pair 5) is considered.

5.2.4 Results – Per Lobe ANOVAs: HV contrast

Discussion – Per Lobe ANOVAs: HV contrast

The SO vis-à-vis DO power relationships of the per-lobe ANOVA analyses are summarized in Table 7. The detailed breakouts of these ANOVA analyses are included in Appendix B.2.4 Results – Per Lobe ANOVAs.

The pattern of SO vis-à-vis DO power relationships that emerges is generally as predicted by the WhOBAP framework (section 1.3). In left targets in both hemispheres in the theta θ band or when wavelet frequency does not interact, SO power is significantly less than DO power (pink cells). With one exception, in right targets in both hemispheres in the theta band or when wavelet does not interact, SO power is significantly greater than DO power (yellow cells). The exception is two sources in the occipital lobe left hemisphere (yellow cell with down diagonal).

With one exception, in the alpha α band in left targets, SO is greater than DO (green cells, left targets). The exception is one case in the left targets in the right occipital lobe of magnetometer-pair 39 (green cell with down diagonal). In the alpha α band in right targets in the parietal lobe, SO power is significant less than DO power (green cell with down diagonal). In the alpha α band in right targets in the occipital lobe, SO power is significantly greater than DO power (green cells, right targets). Given the WhOBAP framework introduced in section 1.3, these results suggest the right occipital magnetometer of pair 39 provides signal information from task relevant areas for processing left targets (Table 7(d)). ; and the parietal lobe magnetometer-pair 29 provides signal information from task relevant areas for processing right targets (Table 7(b)).

Interestingly, time-bin interacts only in the parietal, and not in the frontal, temporal or occipital lobe ANOVAs. Furthermore, the same pattern of significance exists across time-bins in the parietal lobe ANOVA. The fact that time-bin does not interact in the other lobes suggests that the time-courses of SO versus DO processing may be more similar than different and are thus not visible in this HV condition-display contrast.

In the HV condition-display contrast in the per lobe ANOVAs, the pattern of SO versus DO power as a function of target-side and frequency can be summarized as follows: In the theta band in left targets, SO power is significantly less than DO power, while it is significantly greater in right targets. These same left/right patterns exist when frequency is not a factor. In the alpha band in left targets, SO power is significantly greater than DO power except in one right hemisphere occipital lobe magnetometer 39 in which it is significantly less. In the alpha band in right targets, SO power is significantly greater than DO power in occipital lobe magnetometers while it is significantly less than DO in the parietal lobe magnetometer-pair 29. These findings are consistent with those of the sliding window analysis at the same time they provide a more detailed understanding of alpha-band power as a function of target-side.

The next step is to conduct an omnibus ANOVA across all magnetometers and lobes, to verify that the overall pattern and exceptions are observed with statistical significance accounted for in a single ANOVA. The methods and results of the omnibus ANOVA are in the next two sections respectively.

Summary of Sources of Significance in the Per Lobe ANOVAS

(a) **Frontal lobe – summary of magnetometer pair 5**

	Collapsed across hemisphere	
	Left targets	Right targets
α	na	na
θ	SO < DO (1)	SO > DO (1)

	Left hemisphere			Right hemisphere	
	Left targets	Right targets		Left targets	Right targets
	SO < DO (1)	na		SO < DO (1)	SO > DO (1)

(b) **Parietal lobe – summary across magnetometer pairs 29 (anterior), 32 (posterior)**

	Collapsed across hemisphere	
	Left targets	Right targets
α	SO > DO (5)	SO < DO (7)
θ	SO < DO (10)	SO > DO (3)

Pattern holds in all time-bins in which significance occurs (see Figure 49) and Figure 50.

(c) **Temporal lobe – summary across magnetometer pairs 13 (anterior), 21 & 20 (both posterior)**

	Left hemisphere			Right hemisphere	
	Left targets	Right targets		Left targets	Right targets
	SO < DO (1)	SO > DO (2)		SO < DO (3)	SO > DO (3)

(d) **Occipital lobe – summary across magnetometer pairs 37, 39, 43**

Left hemisphere				Right hemisphere	
	Left targets	Right targets		Left targets	Right targets
α	SO > DO (2)	SO > DO (2)	α	SO > DO (1) SO < DO (1) right mag of pair 39	SO > DO (2)
θ	SO < DO (2)	SO > DO (1) SO < DO (2) left mags of pairs 37, 43	q	SO < DO (2)	SO > DO (3)

The per lobe ANOVA is difference-score X time-bin X magnetometer-pair X target-side X wavelet X magnetometer-side. The frontal lobe ANOVA did not have magnetometer-pair as a factor. Shown is the tabulated summary of the sources of significance. The number of sources are given in parentheses. (a) In the frontal lobe, two three-way interactions are the highest-order significant interactions. The first is difference-score X target-side X wavelet. SO is less than DO in the θ-band in left targets, and greater in the θ-band in right targets. The second is difference-score X target-side X magnetometer-side. SO is les than DO in left targets in the left and right hemispheres, and greater in right targets in the right hemisphere. (b) In the parietal lobe the highest order significant interaction is difference-score X time-bin X magnetometer-pair X target-side X wavelet. SO is significantly greater than DO in left targets in the α-band and in right targets in the θ-band. SO is less than DO in left targets in the θ-band and in right targets in the α-band. (c) In the temporal lobe the highest order interaction is difference-score X magnetometer-pair X target-side X magnetometer-side. SO is less than DO in the left targets in the left and right hemispheres, and greater in right targets in both hemispheres. (d) In the occipital lobe, the highest order significant interaction is difference-score X magnetometer-pair X target-side X wavelet X magnetometer-side. SO is greater than DO the α-band in left and right targets with one exception in the right hemisphere. In the θ-band, SO is greater than DO in right targets in the left hemisphere (in one case) and in the right hemisphere. SO is less than DO in the θ-band in left targets, and (in one case), in right targets in the left hemisphere.

Table 7

5.2.5 Analysis Methods – Omnibus ANOVA: HV contrast

Time-bins: The time-bins are five 50 ms time-bins from 50 to 300 ms post-target trigger onset non-overlapping from one time-bin to the next. Time-bin is entered as a factor with five levels into the omnibus ANOVA. The time-bins are non-overlapping in contrast to the per-lobe ANOVAs (5.2.3 Analysis Methods – Per Lobe ANOVAs: HV contrast) which has nine overlapping time-bins: this in order to reduce the number of levels in the time-bin factor in order to make the ANOVA tractable given the statistical software and hardware available to conduct this analysis.

Dependent variable: As in the per-lobe ANOVA analysis, the dependent variable is the mean power of each wavelet (theta θ and alpha α) of the difference-score (DO-Valid and SO-Valid) within a given time-bin.

Magnetometer pairs: The magnetometer pairs used in the per-lobe analysis are collectively entered as nine levels in a factor. For the frontal lobe only the magnetometer pair 5 was entered into the ANOVA. For the parietal lobe, pairs 29 and 32 were used. For the temporal lobe, pairs 13, 21 and 20 were entered. Finally for the occipital lobe, magnetometer pairs 37, 39 and 43 were entered into the ANOVA. (Figure 25).

ANOVA: The ANOVA is the same as that used in the per lobe analysis with the exception that fewer levels comprised the time-bin factor as discussed above: difference-score (DO-Valid, SO-Valid) X time-bin (5 time-bins) X magnetometer-pair (9 pairs) X target-side (left, right) X wavelet (θ, α) X magnetometer-side (left, right).

5.2.6 Results – Omnibus ANOVA: HV contrast

The highest order interactions are four four-way: difference-score X time-bin X target-side X wavelet (Figure 26), difference-score X magnetometer-pair X target-side X wavelet (Figure 27), difference-score X magnetometer-pair X wavelet X magnetometer-side (Figure 28), and difference-score X magnetometer-pair X target-side X magnetometer-side (Figure 29). A fifth 4-way interaction of difference-score X time-bin X magnetometer-pair X target-side (Figure 30) is significant at p = 0.06. All omnibus ANOVA significant main effects and interactions are shown in Table 8.

Significant interactions for the OMNIBUS ANOVA: HV condition-display contrast
Difference-score X time-bin X magnetometer-pair X target-side X wavelet X magnetometer-side

Source	F	Prob > F	Reference		Source	F	Prob > F	Reference
d*lr	199.26	0			h	6.76	0.0093	
d*lr*w	59	0			b*w	5.93	0.0001	
s	37.22	0			d*b*lr*w	5.53	0.0002	Figure 26
w	30.24	0			m*lr*w	5.1	0	
d*w	21.44	0			d*m*lr*h	3.21	0.0012	Figure 29
d*b*lr	19.25	0			b*lr*w	3.15	0.0133	
d*m*lr	18.61	0			d*m*w	3.09	0.0017	
lr*w	17.69	0			m	2.99	0.0023	
b	12.92	0			m*lr*h	2.84	0.0038	
d*m	12.79	0			d*m*lr*w	2.61	0.0076	Figure 27
m*w	10.11	0			d*b*h	2.59	0.0349	
m*lr	10.07	0			b*lr	2.5	0.0404	
d*m*w*h	8.42	0	Figure 28		b*m*h	1.62	0.0151	
d*lr*h	7.74	0.0054			b*lr*w*h	2.34	0.0529	
d*m*h	7.18	0			d*b*m*lr	1.41	0.063	Figure 30

Legend	
d	difference-score
b	time-bin
m	magnetometer-pair
lr	target-side
w	wavelet
h	magnetometer-side

The omnibus ANOVA is difference-score (DO-Valid vs. SO-Valid) X time-bin (50, 100, 150, 200, 250 ms) X magnetometer-pair (9 pairs) X target-side (left, right) X wavelet (θ, α) X magnetometer-side (left, right).Magnetometer pairs included in the omnibus ANOVA are frontal magnetometer pair 5, parietal lobe pairs 29 and 32, temporal lobe pairs 13, 21 and 20, and occipital pairs 37, 38 and 43. Highest order interactions (4-way) are shaded gray.

Table 8

difference-score X time-bin X target-side X wavelet (Figure 26): These results confirm the pattern that emerges in the sliding window and per-lobe analysis: in left targets in the theta band, SO power is significantly less than DO power (pink cells). In comparison, in right targets in the theta band, SO power is significantly greater than DO power (yellow cells). In both left and right targets in the alpha band, SO power is significantly greater than DO power (green cells). Furthermore, left targets start and finish differential processing sooner than right targets in the alpha (α) band (50 through 100 ms vs. 100 through 250 ms), across magnetometer-pairs and hemispheres In the theta (θ) band right targets continue differential processing later than do left targets across magnetometer-pairs and hemispheres. This finding is consistent with that of the summarized sliding-window ANOVAs, which suggests a time-course in which left targets start and finish differential processing before right targets (see Table 1).

difference-score X magnetometer-pair X target-side X wavelet (Figure 27): These results make it particularly evident that the observed pattern and exceptions discussed above exist consistently across magnetometer pairs. SO power is less than DO in left targets in the theta band (pink cells). SO power is greater than DO power in right targets in the theta band (yellow cells). Across all significant magnetometer pairs in all but the parietal lobe, SO power is greater than DO power in left and right targets in the alpha band (green cells). In the parietal lobe magnetometer pairs, SO is significantly less than DO in right targets in the alpha band (green cells with down diagonal).

difference-score X magnetometer-pair X wavelet X magnetometer-side (Figure 28): The important finding in these results is that it is the left hemisphere magnetometers in the anterior temporal and parietal lobes which exhibit SO power significantly less than

DO power in the alpha band (green cells with down diagonal), which is consistent with the known fact that it is the left hemisphere which processes right hemifield targets in the visual stream, and it is in the right targets in the parietal lobe in which this pattern is evident.

difference-score X magnetometer-pair X target-side X magnetometer-side (Figure 29): This interaction supports the finding in the tabulated results of the per lobe ANOVAs (Table 7), that when frequency does not interact, the relative power relationship between SO and DO is in line with the power relationship in the theta band when frequency is a factor (pink and yellow cells are color coded for the theta band).

difference-score X time-bin X magnetometer-pair X target-side (Figure 30): This interaction also supports the finding that when frequency does not interact, the relative power relationship between SO and DO is in line with the power relationship in the theta band when frequency is a factor. Furthermore it demonstrates that left targets are differentially processed sooner than right targets in the frontal lobe magnetometer pairs, and that in the posterior temporal lobe (pairs 21 and 20) while left targets are differentially processed at start times 150 and 200 ms, right targets are strongly processed from 50 until 300 ms post target trigger onset. This latter pattern is also observed in occipital magnetometer pair 39. Note that these three pairs (temporal lobe pairs 21 and 20, occipital pair 39) are adjacent to each other in the head sensor helmet (See Figure 35 in appendix A.2 MEG Sensor Layout). These results suggest that the difference-score contrasts DO-Valid vs. SO-Valid are differentially processed in the frontal and posterior ventral-lateral temporal and occipital lobes, and similarly processed in the parietal lobe and dorsal-medial magnetometer pairs (pairs 29, 32, 37 and 43).

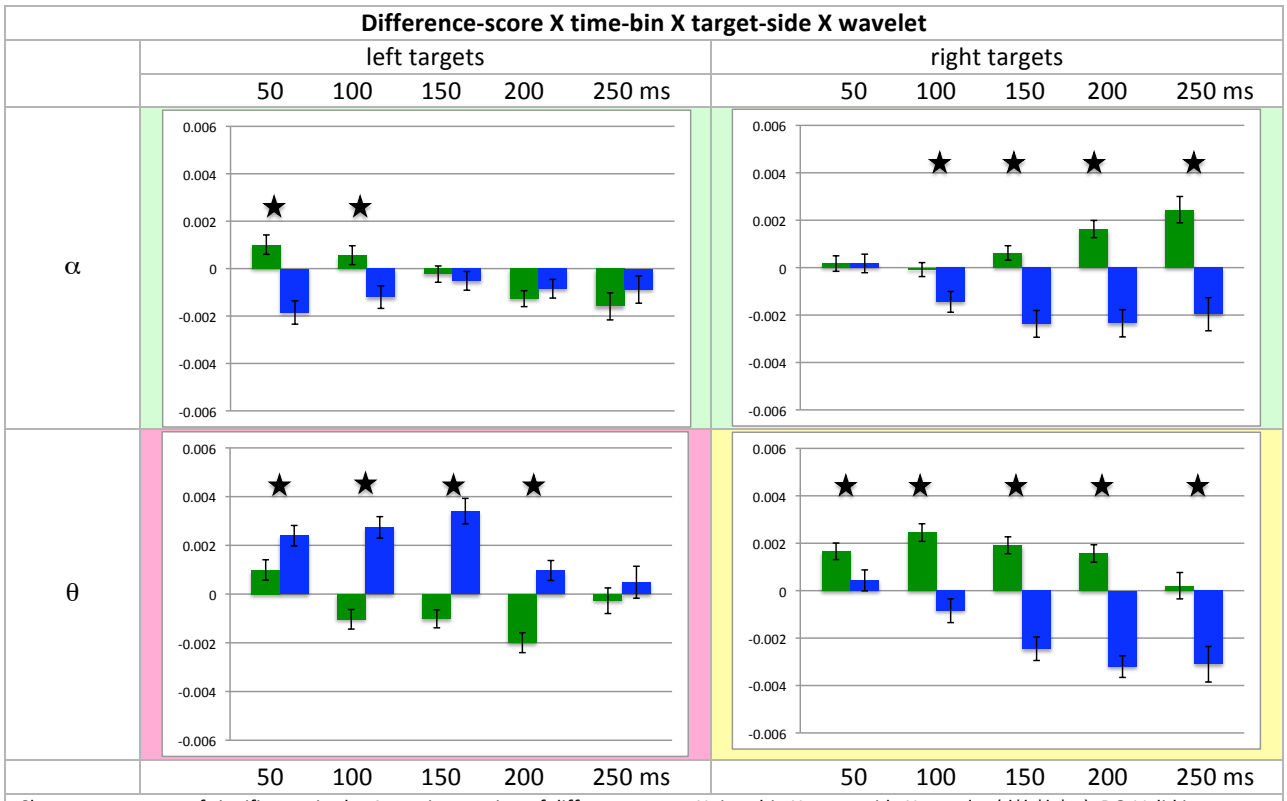

Shown are sources of significance in the 4-way interaction of difference-score X time-bin X target-side X wavelet (d*b*lr*w). DO-Valid is green, SO-Valid is blue. The y-axis on the graphs is flipped. Green up and blue down means SO > DO, and vice-versa. Left targets start and finish differential processing sooner than right targets in the α-band (50 through 100 ms vs. 100 through 250 ms), across magnetometer-pairs and hemispheres. SO power is significantly greater than DO power (DO-Valid < SO-Valid) in the α-band in both left and right targets at all significant time-bins. In the θ-band right targets continue differential processing later than do left targets across magnetometer-pairs and hemispheres. SO power is significantly less than DO power (DO-Valid > SO-Valid) in left targets in the θ-band in bins with start times 50 through 200 ms. SO power is significantly greater than DO power (DO-Valid < SO-Valid) in right targets in the θ-band in time-bins 50 through 250 ms.

Figure 26

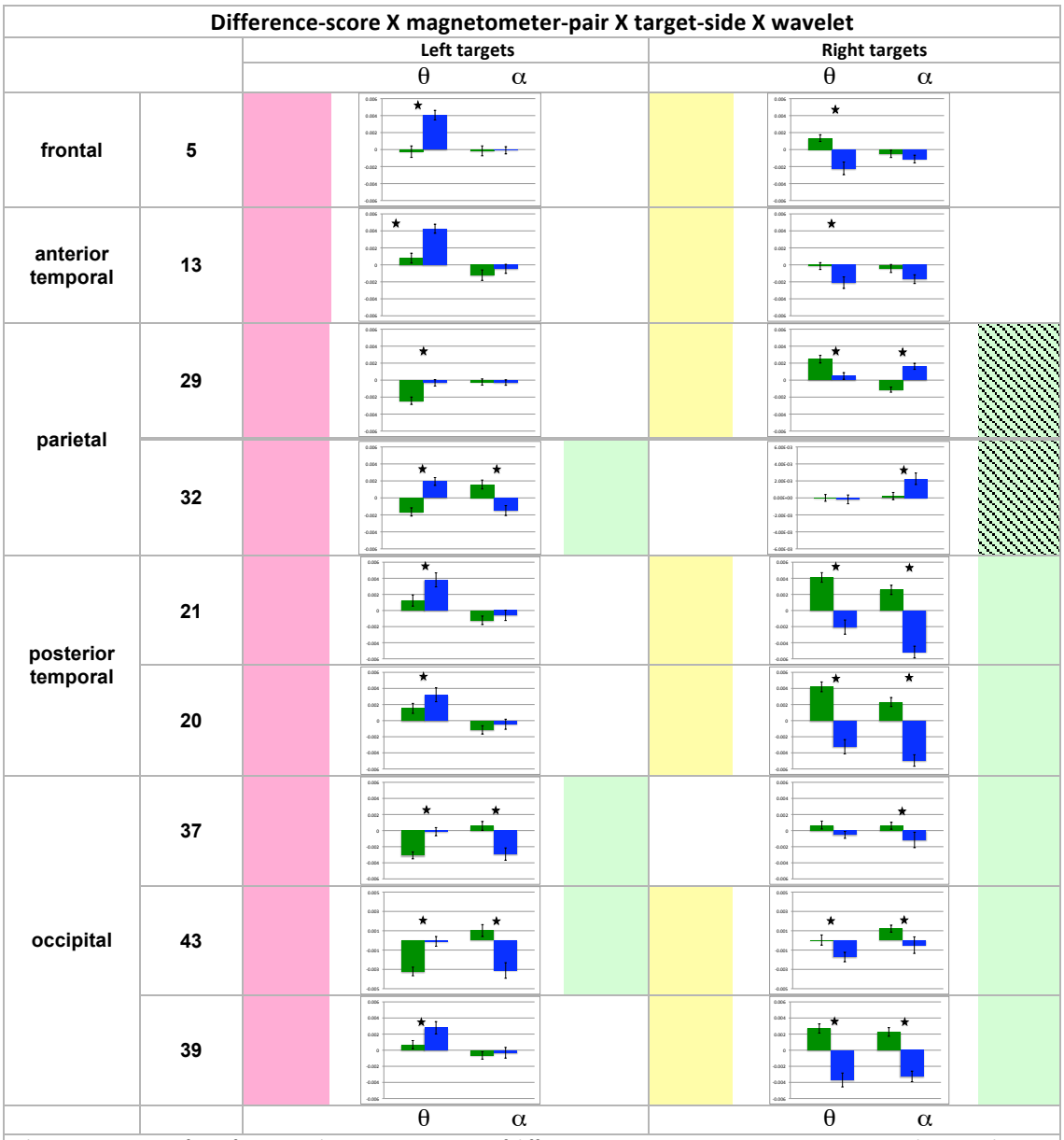

Shown are sources of significance in the 4-way interaction of difference-score X magnetometer-pair X target-side X wavelet (d*m*lr*w). DO-Valid is green, SO-Valid is blue. The y-axis on the graphs is flipped. Green up and blue down means SO > DO, and vice-versa. For left targets in the q-band SO power is less than DO power (DO-Valid > SO-Valid) in all significant magnetometer-pairs (pink cells). For left targets in the a-band, SO power is greater than DO power (DO-Valid < SO-Valid) in all significant magnetometer pairs (left target green cells). In right targets in the a-band in the posterior temporal and occipital magnetometers (similarly to left targets in the a-band), SO power is significantly greater than DO power (DO-Valid < SO-Valid) (right target green cells). For right targets in the a-band in the parietal lobe magnetometers, SO power is less than DO power (DO-Valid > SO-Valid) (right target green cells with down diagonal).

Figure 27

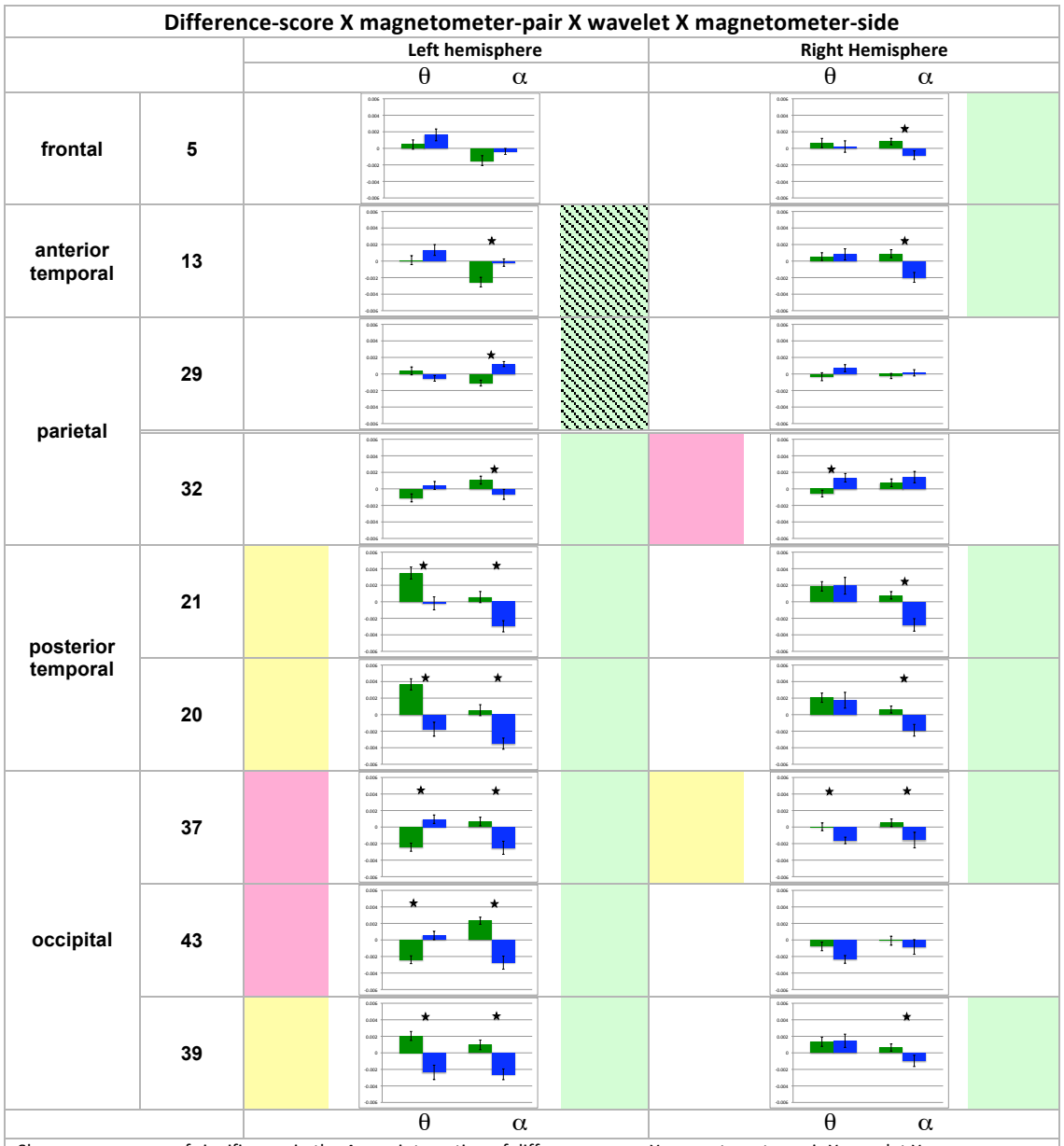

Shown are sources of significance in the 4-way interaction of difference-score X magnetometer-pair X wavelet X magnetometer-side (d*m*w*h). DO-Valid is green, SO-Valid is blue. The y-axis on the graphs is flipped. Green up and blue down means SO > DO, and vice-versa. In the alpha band in significant anterior right-hemisphere magnetometers and posterior left- and right-hemisphere magnetometers (green cells) SO power is greater than DO. Also in the alpha band In significant anterior left-hemisphere magnetometers, SO is less than DO (green cells with down diagonal). In the q-band, SO power is greater than DO power in left posterior ventral-lateral magnetometers 21,20 and 39 (yellow cells); while SO power is less than DO power is left posterior dorsal-medial magnetometer pairs 37 an 43 (pink cells). The right hemisphere has fewer significant sources in the theta band. In the right parietal magnetometer of pair 32 SO power is less than DO (pink cell), while in the right occipital magnetometer of pair 37, SO power is greater than DO power (yellow cell).

Figure 28

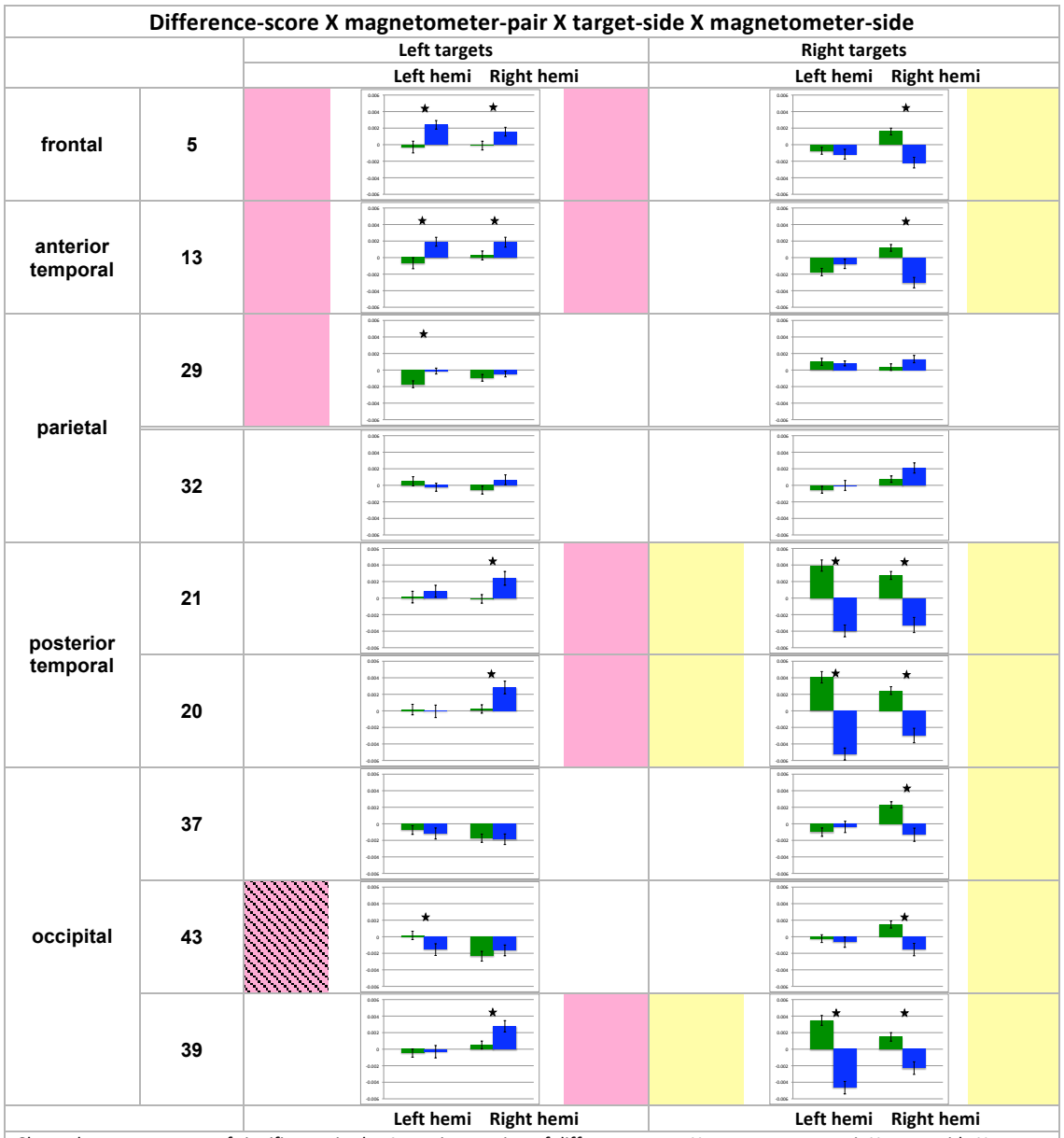

Shown here are sources of significance in the 4-way interaction of difference-score X magnetometer-pair X target-side X magnetometer-side (d*m*lr*h). DO-Valid is green, SO-Valid is blue. The y-axis on the graphs is flipped. Green up and blue down means SO > DO, and vice-versa. SO power is less than DO power (DO-Valid > SO-Valid) in significant left targets in both the left and right hemispheres (pink cells), with an exception in left targets in the left magnetometer of occipital pair 43. In this case SO power is significantly greater than DO power (DO-Valid < SO-Valid) (pink cell with down diagonal). SO power is greater than DO power (DO-Valid < SO-Valid) in significant right targets in both the left and right hemispheres (yellow cells).

Figure 29

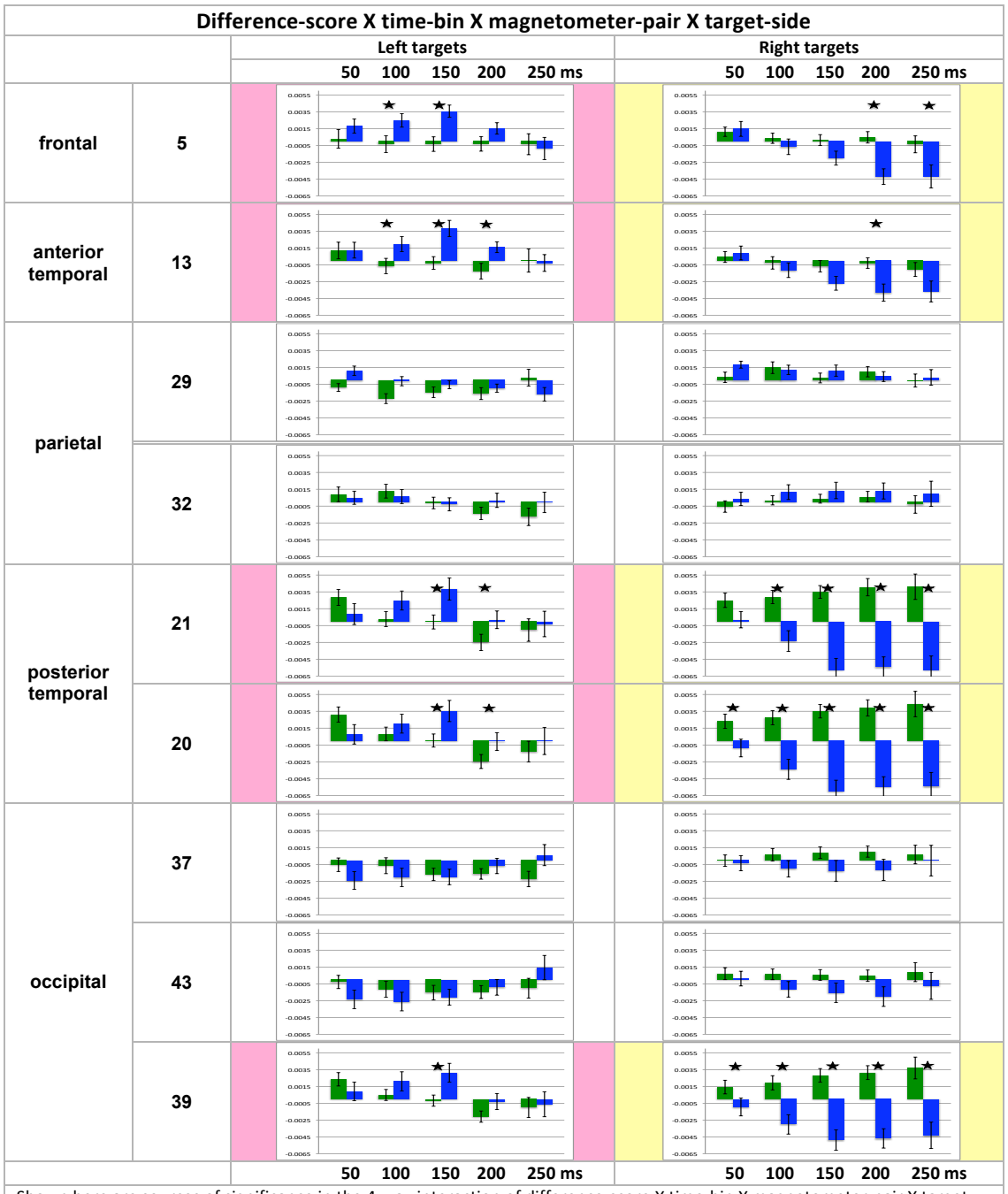

Shown here are sources of significance in the 4-way interaction of difference-score X time-bin X magnetometer-pair X target-side (d*b*m*lr). DO-Valid is green, SO-Valid is blue. The y-axis on the graphs is flipped. Green up and blue down means SO > DO, and vice-versa. In frontal-lobe magnetometer pair 5 left targets start and finish differential processing before right targets. In anterior temporal-lobe magnetometer pair 13, left targets start differential processing before right targets, but finish at the same time. No differential processing of condition contrasts are found in the parietal lobe pairs 29 and 32. In posterior temporal magnetometer pairs 21 and 20, right targets are strongly differentially processed across the time-course compared to left targets. No differential processing of condition contrasts are found in occipital lobe pairs 37 an 43. Occipital pair 39 exhibits the same pattern as posterior temporal lobe pairs 21 and 20. Note that the posterior temporal magnetometer pairs 21 and 20, and occipital lobe pair 39 are all ventral-lateral and adjacent. (See Figure 35 in appendix A.2 MEG Sensor Layout for the relative positions of the magnetometers). Across all magnetometer pairs SO has significantly less power than DO in left targets (pink cells), and significantly more power in right targets (yellow cells).

Figure 30

Discussion – Omnibus ANOVA: HV contrast

Taken together, the results from the five 4-way interactions suggest that there is distinctly different temporal processing of left versus right targets, in the theta θ versus alpha α bands.

First, left targets in the theta band and when frequency is not a factor, are processed with significantly more SO power than DO power, while right targets in the theta band and when frequency is not a factor, are processed with significantly less SO power than DO power. This pattern exists consistently across magnetometer pairs, and follows the prediction set forth in the WhOBAP framework introduced in 1.3.

Second, left and right targets in the alpha band are, for the most part, processed with significantly more SO power than DO power. Again this pattern exists consistently across magnetometer pairs, with the exception that right targets in the parietal lobe magnetometer pairs 29 and 32, are processed with significantly less SO than DO power. Also, the left magnetometers in the anterior temporal pair 13 processes targets with significantly less SO than DO power. According to the WhOBAP framework, we may consider these magnetometers to reflect signals from task relevant areas in OBA processing of right targets.

Third, left targets start and finish differential processing before right targets, particularly in the frontal lobe magnetometer pairs. The exception is in the posterior ventral-lateral temporal lobe and adjacent occipital lobe magnetometer pair. In these magnetometers right targets are strongly significant from 50 until 300 ms, while left targets are significant 150 until 250 ms.

Finally, the results point to an overall spatial pattern of significantly different and similar processing of the DO-Valid vs. SO-Valid difference-score contrast. DO-Valid and SO-Valid are differentially processed in the frontal lobe and posterior ventral-lateral temporal and an adjacent occipital lobe magnetometer pairs. DO-Valid and SO-Valid are similarly processed in the parietal lobe and dorsal medial occipital lobe magnetometer pairs.

5.2.7 Discussion of MEG/ERMF temporal-spectral analyses

OBA exists when shifts of attention are controlled to be within hemifield (HV condition-display contrast), differentially across magnetometers and time, from when shifts of attention are controlled to be between hemifields (VH condition-display contrast). The two contrasts are similar in that OBA effects exist across both posterior and anterior magnetometers. And, when frequency is a factor in processing, it is so in theta θ (center frequency 5 Hz) and alpha α (center frequency 10 Hz) bands.

The sliding window analysis was employed to, among other things, compare results when shifts of attention are controlled to be within a hemifield versus between hemifields. Nevertheless, the former (HV contrast) is arguably the cleaner test for object effects, as the cognitive processing associated with communication between hemispheres is not a factor that can differentially impact the timing or signal characteristics of observed object effects, thus creating a confound with actual OBA effects in interpretation. Therefore, only the HV condition-display contrast was explored in the subsequent per-lobe and omnibus ANOVA analyses. In addition, since differences are found to exist solely in the theta and alpha bands, these two frequencies alone are explored in the subsequent per-lobe and omnibus ANOVA analyses.

The three analyses (sliding window, per-lobe, omnibus) together support the finding that left targets in the theta band and when frequency is not a factor, are processed with significantly less SO power than DO power, while right targets in the theta band and when frequency is not a factor, are processed with significantly more SO than DO power. This pattern exists consistently across magnetometer pairs with only one exception in the occipital lobe in the omnibus ANOVA. The meaning of this exception should be explored in subsequent research. If theta-band power is associated with long-range communication (possibly acting as a carrier wave to enable distant brain regions to phase lock synchronization at higher frequencies, enabling communication), then increased SO power in the theta-band in right targets is possibly a result of the left hemisphere, which processes right hemifield targets in visual processing, communicating with the right hemisphere, which is dominant for attentional processing. Long distance communication via theta band power is not necessary for attentional communication with visual stream processing of left targets, since the both occur in the right hemisphere.

Across the three analyses, left and right targets in the alpha band are, for the most part, processed with significantly more SO than DO power across magnetometer pairs. According to the alpha inhibition/gating theory, these magnetometers render brain signals from task irrelevant areas. Again this pattern exists consistently across magnetometer pairs, with key exceptions. These exceptions are presumed to be in magnetometers that convey signals from OBA task relevant areas. The sliding window analysis suggests that the posterior, relatively ventral-lateral adjacent magnetometer pairs 20, 21 and 39 are task relevant in processing right targets. The per- lobe and omnibus analysis both suggest that parietal magnetometer pair 29 is task relevant in processing right targets. The omnibus

analysis additionally suggests that parietal magnetometer pairs 32 are task relevant in right targets as is the left magnetometer of the anterior temporal pair 13. While there are several candidate magnetometers for task relevant areas for right targets, only one is suggested for task relevant areas for processing left targets: the per lobe analysis suggests that the right occipital magnetometer of pair 39 is task relevant.

In the omnibus ANOVA, left targets start and finish differential processing before right targets across the lobes, but particularly in the frontal lobe magnetometer pairs. It is possible that left targets' temporal benefit here is a result of the right hemisphere dominance in attentional processing. The exception is in the posterior ventral-lateral temporal lobe and an adjacent occipital lobe magnetometer pair. In these magnetometers right targets are strongly processed early on and throughout the time-course. This intriguing finding should be explored in subsequent research in the effort to theorize and understand why this should be the case, as a literature search did not reveal an explanation for why this might be the case.

Finally the omnibus results point to an overall spatial pattern of significantly different and similar processing of the DO-Valid vs. SO-Valid difference-score contrast. The difference-scores are differentially processed in the frontal lobe and posterior ventral-lateral temporal and adjacent occipital lobe magnetometer pairs. In the omnibus ANOVA a clear spatial pattern of significantly different versus similar processing between the DO-Valid vs. SO-Valid difference scores is observed. It is possible that methods specifically tuned for time-series analysis may be better suited to elicit the time-course of object-based attentional processing.

5.3 Temporal-Spectral Analysis Discussion

As in the temporal analyses, to assess OBA while controlling for shifts of attention *within hemifield*, DO-Valid difference signals in the horizontal displays are contrasted with SO-Valid difference signals in the vertical displays (HV condition-display contrast); and to assess OBA while controlling for shifts of attention *between hemifields*, DO-Valid difference signals in the vertical displays are contrasted with SO-Valid difference signals in the horizontal displays (VH condition-display contrast). These contrasts are evaluated using sliding windows (an ANOVA was conducted for each window) for EEG (5.1.2 Results – Sliding windows) and MEG (5.2.2 Results – Sliding windows). Subsequent analyses in MEG were of the HV contrast only, and considered the windows as a factor in per-lobe ANOVAs (5.2.4 Results – Per Lobe ANOVAs: HV contrast), and an omnibus ANOVA (5.2.6 Results – Omnibus ANOVA: HV contrast).

In the EEG temporal-spectral analysis clear effects of object-based attention within hemifield (HV condition-display contrast) were evident in both the P1 and N1 time frames, whereas object effects between hemifields did not cleanly fall into these component time frames. It is possible that OBA shifts of attention within a hemifield are the primary source of the ERP P1 and N1 components, even though the typical analysis of Egly-style paradigms collapses across shifts of attention within and between hemifields. Further research should seek to corroborate this theory. Significance passed the Holm adjustment to the Bonferroni correction for multiple comparisons; hence relational conclusions can be drawn between electrode pairs across time. Such relational conclusions are not typically drawn in classic ERP analysis methods. Additionally, the present results reveal that OBA effects exist across both anterior and posterior electrodes, and the predominant frequencies of significant

differences are the theta (θ) and alpha (α) bands. The fact that significance exists in these two frequency bands is consistent with the WhOBAP framework predictions put forth in section 1.3.

Like the comparable EEG analysis, the MEG temporal-spectral sliding window analysis confirmed that OBA exists when shifts of attention are controlled to be within hemifield (HV condition-display contrast). The effect was apparent across both posterior and anterior magnetometers. When frequency was a factor, it was so in the theta and alpha bands. A tabulated summary of the sliding window ANOVAs suggests the power relationship between DO-Valid vs. SO-Valid (e.g. DO vs. SO) was modulated by target-side (left, right) and frequency band (θ, α) and follows the predictions of the proposed WhOBAP framework. The pattern was then validated and refined for the HV contrast by the subsequent per-lobe ANOVA and omnibus ANOVA analyses.

Subsequent MEG analyses focused on the HV (instead of the VH) condition-display contrast as it is arguably the cleaner test for object effects, as the cognitive processing associated with communication between hemispheres is not a factor that can differentially impact the timing or signal characteristics of observed object effects, thus creating a confound with actual OBA effects in causal interpretation.

In the HV contrast, left targets start and finish differential processing before right targets, particularly in the frontal lobe magnetometer pairs. This temporal advantage possibly reflects right hemisphere dominance in attentional processing. This is consistent with previous research that proposes a frontal lobe role in attentional processing, and further implicates it as having a role in lateralized processing, perhaps in response to the lateralization inherent in visual cognition in more posterior areas. The exception to this

processing order is that right targets are strongly processed early on and throughout the time course in the posterior ventral-lateral temporal lobe and an adjacent occipital lobe magnetometer pair, while left targets are processed starting later for a smaller latency window in these magnetometers. This finding should be explored further in subsequent research, as the pattern was strong and a literature search revealed no specific explanation for this finding.

Left targets in the theta band and when frequency is not a factor, are processed with significantly less SO than DO power, while right targets in the theta band and when frequency is not a factor, are processed with significantly more SO power than DO power. This pattern exists consistently across magnetometer pairs with only one exception in the occipital lobe. The WhOBAP framework predicts this pattern. If theta-band power is associated with long-range communication (possibly acting as a carrier wave to enable distant brain regions to phase lock synchronization at higher information processing frequencies), then increased SO power in the theta-band in right targets is possibly a consequence of the left hemisphere, which processes right hemifield targets in the visual stream, communicating with the right hemisphere, which is dominant for attentional processing.

Left and right targets in the alpha band are, for the most part, processed with significantly more SO power than DO power. Again this pattern exists consistently across magnetometer pairs, with the exception that right targets in the parietal lobe magnetometer pairs are processed with less SO than DO power. Consistent with this finding, left magnetometers in the anterior temporal and parietal lobe process targets with significantly less SO than DO power. The WhOBAP framework also predicts this pattern. If

alpha-band power is associated with gating and inhibition of task irrelevant regions, then when gating/inhibition is reduced for right targets in the left magnetometers in the anterior temporal and parietal lobes, than we may consider these areas to be task relevant for OBA processing of right hemifield targets. A comparable result for left hemifield targets was not found in the omnibus ANOVA. However, the occipital lobe ANOVA found SO power significantly less than DO power in an occipital lobe magnetometer-pair, possibly suggesting that this area is particularly task relevant, given the alpha gating/inhibition hypothesis, in the OBA processing of left hemifield targets.

An important component of the alpha-band gating/inhibition hypothesis is that when such activity is suppressed, the stage is set for information processing in other frequency bands, such as gamma. Gamma-band modulation and synchronization has been associated with attentional processing in extant literature, in some cases phased-locked with the theta frequency for longer distance information processing and communication. This dissertation research has focused in-depth analysis solely on the alpha and theta bands, as these two have the most power in evoked responses, and were the only two frequency bands to exhibit significantly different processing in the ANOVA analysis of the condition contrasts evaluated. As discussed in the context of the WhOBAP framework, the contrasts studied here all involve attention, whereas when gamma-band processing has been found to be significant in the literature, it has been so in attended versus unattended stimuli. Since our analyses involve contrasts between different forms of attended stimuli, it may be the case that while gamma-band information processing is significant, it is not significantly *different* among the contrasts. Using the present data set, a focus on the areas and time frames alpha power is suppressed and an analysis to evaluate gamma-band phase

locking with the theta-band in these areas, will enable further exploration of this hypothesis, as will subsequent experiments.

Finally the results point to an overall spatial pattern of significantly different and similar processing of the DO-Valid vs. SO-Valid difference-score contrast. The difference-scores are differentially processed in the frontal lobe and posterior ventral-lateral temporal and adjacent occipital lobe magnetometer pairs. They are similarly processed in the parietal lobe and dorsal medial occipital lobe magnetometer pairs. It could be that use of a statistical analysis technique specifically designed for evaluating time series may be necessary to fully map out the time-course. This should be explored further in post-dissertation research.

6. Source Localization

6.1 Channel Space vis-à-vis Source Space

In the EEG temporal and temporal-spectral analyses (4.1 EEG/ERP, 5.1 EEG/ERP), significance between conditions was viewed and analyzed at electrode locations on the scalp surface. In the MEG temporal and temporal-spectral analyses (4.2 MEG/ERMF, and 5.2 MEG/ERMF), there is a time-course evolution evident across magnetometers' locations on the scalp surface. These analyses were done in "channel space". The location on the scalp surface was a factor in either 1) the choice of channel to use in the analysis (e.g. in ERP temporal analysis, posterior electrode locations are chosen to view the P1 and N1 attentional components), or 2) in results interpretation (e.g. in the sliding window analysis time-course evolution, the location of the channel is presumed to represent at a coarse level, the location of the underlying signal). In EEG in particular, entire research streams have been built around analyses and results findings in "channel space", independent of attempts to locate the neural source from which the results arise.

With the rapid increase in MEG research over the past decade, there has been an increased interest in determining the neural sources of electromagnetic brain signals, and in conducting analyses considering the neural sources of these signals. That is, there has been an increased interest in analyses in "source space".

Of the three types of channels used in this research: EEG electrodes, MEG magnetometers, and MEG gradiometers, the gradiometers are known to provide the most accurate information on signal source by virtue of their location on the head (Hamalainen

et al., 1993). Given a strong signal in a specific gradiometer over the left occipital cortex, for example, it is likely that the source of that signal lies directly beneath that gradiometer. This is less so the case with magnetometers, and particularly with EEG electrodes. The electrical components of the electromagnetic brain signals are distorted and smeared in passing through the skull and scalp, so electrode location on the head is less informative as to the source of a strong signal seen at that electrode.

Mathematical source localization can use the combination of electrode, magnetometer and gradiometer signal information together with T1-weighted MRI for improved neural source localization accuracy.

As discussed in section 2.1.3 Source Localization, three mathematical models as implemented in the MNE Suite software (Martinos Center for Biomedical Imaging, Harvard University) are employed in the present research for source localization: MNE (minimum norm estimation), dSPM (dynamical statistical map) and sLORETA (low resolution brain electromagnetic tomography).

6.2 Methods

6.2.1 Participants

Two participants from the MEG/EEG/behavioral experiment participated in the MRI/source localization experiment. One participant had viewed the stimuli of the paradigm in horizontal displays; the other had viewed it in the vertical displays (See 3.1.1 The paradigm).

6.2.2 MRI acquisition protocol

The two participants were scanned at the Scientific Imaging and Brain Research

(SIBR) at Carnegie Mellon University with a Siemens Magnetom Verio syngo MR B1. High-resolution anatomical images (1-mm3 resolution) were acquired by using an axial MPRAGE T1-weighted sequence [number of slices_24, slice thickness_0.8, Conc_1, Res_320_320, field of view_256_256 mm2, TR_2300 ms, TI_900 ms, TE_3.65 ms, flip angle_9°]

6.3 Analysis

The raw MRI data for each participant was transferred to a Linux computing cluster at the Center for the Neural Basis of Cognition (CNBC) and co-located with that participants' data from the MEG/EEG/behavioral experiment. The MNE software source localization workflow was then employed (Figure 31) for each of the two participants.

Each participant's raw MRI data were first reconstructed using FreeSurfer (Martinos Center for Biomedical Imaging, Harvard University). Freesurfer creates the surface reconstructions such as the inflated surface, pial surface, and head reconstruction. Talaraich information is added, and various anatomical properties are measured and recorded. The T1 files are then converted into fif format for use with the MNE Suite software (mne_setup_mri). Next, the source space is setup, which includes converting the source space files to fif format, and creating a decimated dipole grid on the white matter surface (mne_setup_source_space). In order to calculate the forward solution the surfaces are parceled into triangular tessellations[28]. A watershed algorithm is employed to create the tessellations (mne_watershed)[29]. When this is complete, separate tessellation representations exist of the outer skull, the inner skull and the outer skin surface. The inner skull surface is used as the boundary for the source space. Next the subject's MEG

[28] A tessellation is a collection of plane figures that fills the plane with no overlaps and no gaps.

[29] In general, a watershed algorithm is an efficient algorithm for edge detection in image processing.

digitization data is aligned with the MRI coordinate transformation. This is done interactively with the help of algorithms and tools for visualization (mne-analyze). The forward solution implemented in MNE Suite uses a boundary-element method (BEM) for setting up a realistic head model based on the constraints of the subject's MRI. Therefore the boundary-element model is setup to assign conductivity values to the different scalp and brain compartments (mne_setup_forward_model). Two of the source localization algorithms in MNE Suite use noise in their source localization calculations (dSPM and sLORETA), so a next step is to create the noise-covariance matrix. This is done from the original epoched data (mne-browse_raw). Finally, the forward solution is computed to determine the magnetic fields and electric potentials at the measurement sensors and electrodes due to dipole sources located on the cortex (mne_setup_forward_solution). Given the forward solution and the noise-covariance matrix the inverse operator is computed (mne_do_inverse_operator). The results include MNE, dSPM and sLORETA solutions, all of which can be interactively viewed and analyzed (mne_analyze).

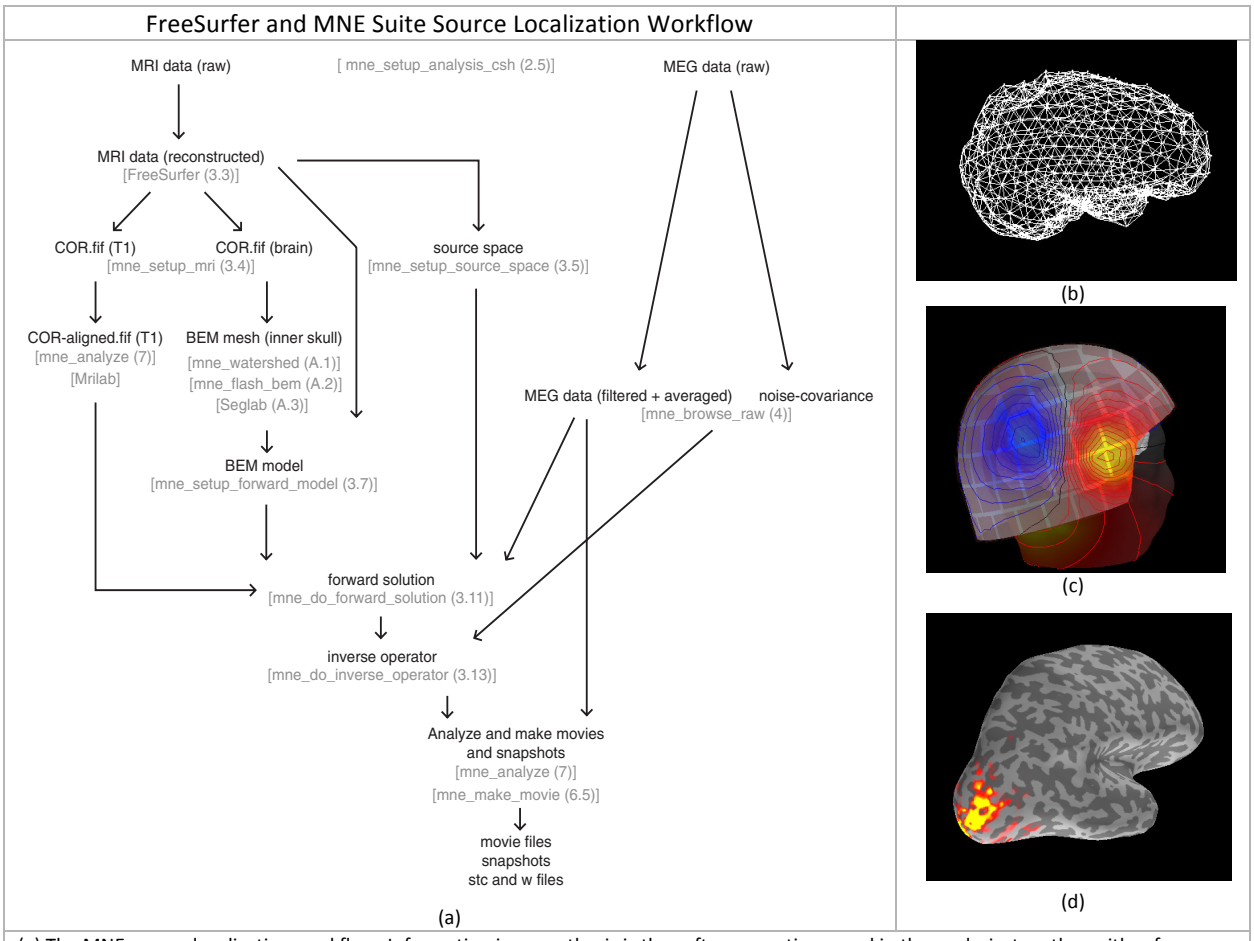

(a) The MNE source localization workflow. Information in parenthesis is the software routines used in the analysis, together with reference guide page numbers. (b) Tessellation of the brain surface resulting from the BEM mesh (inner skull) step. (c) Magnetic field and electric potential maps resulting from calculating the forward solution. (d) Source localization solution resulting from calculating the inverse solution. Figures (a),(c),(d) taken from the MNE software User's Guide, Version 2.7, December 2009. Figure (b) taken from http://www.fmrib.ox.ac.uk/analysis/research/bet/slideshow/s_0100_tessel.htm.

Figure 31

6.4 Results

The dSPM source localization results for the two participants are given in Figure 32. The inflated brain on the left in each image is from the participant who shifted attention vertically in the hemifield between two horizontal rectangle objects (different object or DO condition), while the inflated brain on the right is from the participant who shifted attention vertically in the hemifield within a single vertically oriented rectangle (same object or SO condition). Results shown are for shifts of attention in the left hemifield only. The P1 and N1 component time frames are shaded in gray in the figure.

dSPM Source Localization Results for Horizontal Shifts within the Left Hemifield in 25 ms Steps

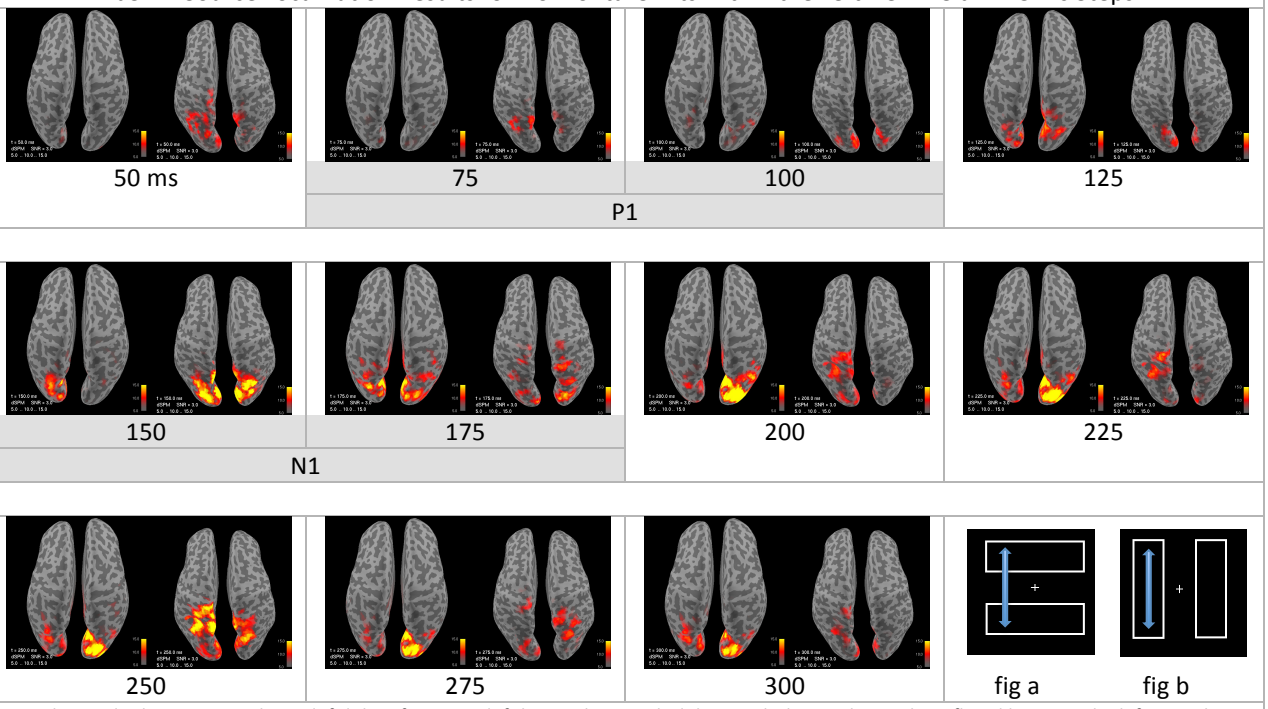

In each singular brain image above, left lobe of image is left hemisphere, right lobe is right hemisphere. The inflated brain on the left in each time frame is from the participant who shifted attention vertically in the hemifield between two horizontal rectangle objects (fig a) in the different object or DO condition; while the inflated brain on the right in each frame is from the participant who shifted attention vertically in the hemifield within a single vertically oriented rectangle (fig b) in the same object or SO condition. Results are for shifts of attention in the left hemifield only.

Figure 32

MNE and sLORETA source localization results can be similarly shown. Furthermore the non-zero signal sources as evident on the boundary surface for all three solutions can

be extracted using the same parameters as for display, for subsequent statistical analysis. The extracted data are a set of signal sources: each signal source is a time series (e.g. from 0 to 300 ms post target trigger onset), with an associated vertex number and set of coordinates (x,y,z). The vertex number and coordinate set refers to one of the triangular tessellations of the brain, as constructed in the FreeSurfer software (Figure 31 (b)).

For the dSPM results shown in Figure 32, there are 2890 non-zero surface signal sources in the left hemisphere for the participant who performed the experiment with the horizontal displays (left inflated brain), and 2959 non-zero sources in the right hemisphere. There are 3831 non-zero signal sources in the left hemisphere for the participant who performed the experiment with the vertical displays (right inflated brain), and 3891 non-zero sources in the right hemisphere. Of particular interest in light of the sensor level results that had both anterior and posterior activity, is that no significance is shown in the anterior part of the brain in the present source space results. Consider that for these pilot results all MNE software defaults, without a priori theoretical consideration of what the values of the various parameters should be, were used in the display parameters. Similarly, these same defaults could be used when extracting the data for statistical analysis in which case analysis would be conducted only on signals in the posterior part of the brain. Post-dissertation research should include an in-depth theoretical consideration of the value of the parameters used in both display and statistical analysis. Changing the threshold of parameters based on theoretical considerations could indeed reveal results of interest in the anterior as well as the posterior part of the brain.

The MNE Suite software also has the capability to fit the equivalent current dipole (ECD) to the signal sources at a single time point. Fitting the ECD is a companion source

localization technique to dSPM, MNE, and sLORETA. The ECD is the hypothetical source of the observed neuromagnetic fields and electric potentials. The model mathematically produces "equivalent" fields to those actually produced by the summed current dipoles of the neurons whose postsynaptic potentials are the true source of the electromagnetic activity (See A.3 Electrophysiological Basis of MEG Signals). Salmelin (2010) discusses in detail how to fit the ECD at the desired time point per condition, per subject, constructing a source model for each. She then forms a combined source model that works for all the conditions for that subject. Based on this common model, cortical areas and time windows that show significant differences between conditions are identified. Then, during group analysis, the individual sources are grouped according to function, location, direction of current flow, and and/or timing, and finally tested for significant effects. Salmelin discusses that when completed, the localization solution should be obvious in the original sensor signals.

Mechanistically, the results of the source localization are sets of time series (signals), each with a coordinate location on the scalp surface. The units of the signal are determined by the specific technique (for example dSPM time series are dimensionless statistical test values). This time series information can be used to display the results, as is done in Figure 32, or can be used in subsequent statistical analysis. To be specific, these results are the first step in a series of steps, including statistical analyses that could lead to a meaningful interpretation of the source localized data. At this step the source localization results suggest only that significant sources are posterior, and that they are appear different between these two individuals. However the latter observation could be due to the display orientation (an interesting difference) and/or due to individual differences of

these two participants (a non-interesting difference). Interpretation beyond these observations would not be sound at this point. Several next steps will be taken as part of post-dissertation plans. A possible series of next steps include the following: Source localize the DO-Valid and SO-Valid difference signal information. Transform the surface data from the source localization results into Talairach coordinates. Choose an algorithm to identify regions of interest (for example the coordinates with the strongest power as the center point for an ROI), and submit the time series associated with each ROI to statistical analyses similar to those done on the magnetometer sensor data discussed in 5.2 MEG/ERMF. It may be useful to conduct an ECD analysis. Note however, that the present results are for two participants. To test for significant differences in conditions in source place, data for more participants needs to be captured. As a reference, the data set used for the ECD source localization discussed in Salmelin (2010), was based on 10 participants in a within-subject experimental paradigm.

7. General Discussion

A key aspect of this dissertation research is that its theoretical basis is broadly derived. One theory of object-based attention (OBA) and space-based attention (SBA) was derived from numerous psychological behavioral and key ERP studies on humans. Ultimately several other research streams contributed substantially to the theoretical basis for this dissertation research, especially streams that presume the role of brain oscillations in dynamic forming networks in cognitive processing. These research streams include single and multi-unit recording studies on monkeys; computational studies; and fMRI, MEG, EEG neuroimaging studies on humans, monkeys and other animals. Within the past ten years, the majority of MEG literature in particular presumes the theory of dynamic forming networks as the mechanism underlying cognitive function. The theoretical basis for the present dissertation research is thus designed to encompass both MEG and EEG research traditions. Furthermore, the methods and analyses are consistent across MEG and EEG, so as to best compare, contrast and build a bridge between the unique contribution each has to make to our understanding of OBA vis-à-vis SBA.

Specifically, this dissertation aims to build a bridge between conventional ERP component analysis, and methods designed to analyze results across time and space in the time-frequency domain, in both EEG and MEG.

7.1 The adapted Egly-style paradigm

In using Egly-style paradigms the presumption is made that between cue onset and target onset attention is spread within the perceptual object in which the cue appears, and

that this spread subsequently contributes to a significantly faster reaction to a target that appears in the same perceptual object as the previous cue, than for a target that appears outside that object. That is, OBA effects are presumed to be exemplified by this faster RT *after* target onset, even though the object effects (spread of attention within the boundaries of the perceptual object) occur *before* target onset (starting with cue onset up to target onset). Importantly, the Egly-paradigm was originally designed as a behavioral paradigm in cognitive psychology. In behavioral paradigms it is well established that typical dependent variables are RT and accuracy, where significantly faster RTs are taken as evidence of significantly faster cognitive processing. With respect to Egly-style paradigms, significant differences in RTs between conditions has been replicated many times, and is taken as robust evidence of OBA. When Martinez and colleagues (2006) adapted the Egly paradigm for use in their ERP study, it is likely that a goal was to create a link between this well-established behavioral finding and its impact on ERP signals. As such they measured the P1 and N1 attentional components resulting *after* target onset. Similarly, when an Egly-style paradigm was adapted in the present research, it was to create a bridge between the ERP time-domain findings of Martinez et al. and EEG/MEG frequency domain findings. In both cases, the analysis of the electromagnetic brain signals was done *after* target onset, extending into the neuroscience domain the presumption that significant effects would be apparent and could be taken as evidence of OBA. Importantly however, the data set of the present research offers potential information not available in behavioral-only paradigms: the ability to link the brain signals occurring between the cue and target (presumably reflecting cognitive processing of the spread of attention within the perceptual object), with the brain signals occurring after target onset (presumably reflecting cognitive

processing of the resulting effects on RT). Therefore a key analysis to conduct post-dissertation (using the present data set), is this potential causal relationship of the brain signals before target onset (after cue onset), and after target onset.

7.2 Results synthesis

In order to build a bridge between conventional ERP component analysis, and methods designed to analyze results across time and space in the time-frequency domain in both EEG and MEG, the first step was to replicate the ERP OBA results of Martinez et al., (2006) using an Egly-style behavioral paradigm: the present research replicated their results in the time domain; then extended them by demonstrating that OBA exists when shifts of attention are controlled to be within hemifield. This latter finding is a new contribution to the OBA literature. Furthermore, this control uncovered OBA effects in the P1 as well as the N1 component time frame: Martinez and colleagues found object effects solely in the N1 component.

MEG results in the time domain analysis were meager. It is possible that more substantial results would be found given a different choice of sensors to analyze. MEG data is far more focal across space than EEG: the EEG signal is smeared by the scalp and skull[30]. Thus MEG signal modulation can vary more dramatically from one magnetometer to the next adjacent magnetometer, than would vary from one EEG electrode to the next. In EEG, a signal modulation of interest is more likely to appear across multiple electrodes, which makes the exact choice of electrode to analyze less critical. Given the focal nature of MEG, the choice of magnetometers to analyze is critical.

[30] The electrical potentials are smeared as they pass through the scalp and skull because of the variations of scalp and skull resistivity. Magnetic fields are not affected by variations in resistivity, and so pass through the scalp and skull unaffected.

The temporal-spectral analyses for both EEG and MEG provided significant results. In EEG, the results for within hemifield shifts of attention occurred within the P1 and N1 component time frames, both confirming that these components are indeed modulated by attention, and further establishing their role when attention is controlled to be within a hemifield. Furthermore, the results revealed that the key frequencies modulated were theta θ (center frequency 5 Hz) and alpha α (center frequency 10 Hz). No significant differences were found in the gamma γ (30 – 80 Hz) range. This is intriguing because extant literature has specifically established the role of gamma processing in attention. The lack of gamma-band significance will be discussed more fully in section 7.5 Gamma γ-band below.

With respect to the theta and alpha frequency bands, when the two attentional object conditions were contrasted, (shifts of attention within an object versus shifts of attention between two objects), significant differences occurred solely within these two frequency bands. The EEG temporal spectral analysis also revealed that anterior electrodes show significant differences. In the conventional ERP literature, OBA is evaluated only at posterior electrodes while significance at anterior electrodes is not investigated.

The MEG temporal-spectral results further revealed the nature and characteristics of OBA processing. In a sliding window analysis, ANOVAs were conducted per MEG magnetometer pair, per sliding window. The MEG analysis first validated the EEG findings that the frequencies of significant processing are the theta and alpha bands. A time course was suggested in which targets presented in the left hemifield start and finish differential processing before targets presented in the right hemifield, lending support to and providing a specific manifestation of previous findings of right hemisphere dominance in

selective attention (Corbetta & Shulman, 2002). When all ANOVA results of the sliding window analysis were tabulated, a specific power relationship pattern between same object (SO) versus different object (DO) processing when shifts of attention are controlled to be within hemifield was suggested. Specifically, in the alpha frequency band, SO power was found to be significantly greater than DO power in left targets, and less in right targets. In the theta frequency band, SO power was found to be significantly less than DO power in left targets, and greater in right targets. This pattern was for the most part validated and refined in the subsequent per-lobe ANOVA and omnibus ANOVA analyses.

Next, an ANOVA was conducted for each of the frontal, temporal, parietal and occipital lobes. In contrast to the sliding window analysis, time was entered as a factor, as was magnetometer pair. When the SO vis-à-vis DO power relationships from the results were tabulated across the four lobes, they both confirmed and refined the pattern suggested by the sliding window analysis. As before, in the alpha band, SO power was found to be significantly greater than DO power in left targets. However there was one exception: in an occipital lobe magnetometer pair, SO was significantly less than DO. Also as before, in the theta band, and when frequency was not a factor, SO power was found to be significantly less than DO power in left targets, and greater in right targets. Unlike the sliding window analysis, in the alpha band in right targets, SO power was significantly less than DO in the parietal lobe but significantly greater than DO in the occipital lobe. The subsequent omnibus ANOVA confirmed the pattern and the exceptions of the SO vis-à-vis DO power relationship.

Finally, a single omnibus ANOVA was conducted across all lobes, and all magnetometer pairs. The results confirmed several of the findings of previous analyses.

First, the time course was confirmed in which targets in the left hemifield are processed before targets in the right hemifield, particularly in the frontal lobe magnetometer pairs. This lends support to the role of the frontal lobe in attentional processing, and furthermore implicates it in lateralized processing, perhaps as directed by the lateralized processing in the visual stream in more posterior areas. This is consistent with the space-based attention finding by Green & McDonald (2008) that theta power is an index of attentional control inherent in the parietal lobe over the frontal and occipital lobes. Second, the omnibus results point to an overall spatial pattern of significantly different and similar processing of SO versus DO processing in the theta-band. They are differentially processed in the frontal lobe and posterior ventral-lateral temporal and adjacent occipital lobe magnetometer pairs. They are similarly processed in the parietal lobe and dorsal medial occipital lobe magnetometer pairs. Third, left and right targets in the alpha band are, for the most part, processed with significantly more SO power than DO power. This pattern exists consistently across magnetometer pairs, with the exception that right targets in the parietal lobe magnetometer pairs are processed with less SO than DO power. Consistent with this finding, left magnetometers in the anterior temporal and parietal lobe process targets with significantly less SO than DO power.

The temporal and temporal-spectral analyses were conducted in "channel space", that is, analysis was done on the signals as measured at the channels (electrodes for EEG, magnetometers for MEG) on the scalp surface. Implicit in this approach is the assumption that the channel location is a coarse proxy for neural source, particularly when drawing conclusions about how attentional processing evolves across the head. The ERP technique (Luck, 2005) involves analysis at electrodes based on their spatial location on the scalp,

and a large body of literature exists using this approach. However, with the rapid increase in MEG research, and the availability of increasingly sophisticated mathematical tools, renewed interest has been placed on determining the neural sources of these sensor signals for subsequent analysis. That is, there is increasing interest is conducting analysis on the signals in "source space".

The last chapter of the dissertation reports the results of localizing the sources of the same object and different object condition signals using three source localization techniques: dSPM, MNE, and sLORETA. Source localization was done for two participants of the original MEG study. Specifically, in order to evaluate same object processing with different object processing when shifts of attention are controlled to be within hemifield, different object trials in the left hemifield for the participant who viewed the horizontal display were localized, as were the same object trials in the left hemifield for the person who viewed the vertical display. Mechanistically, the results of the source localization are sets of time series (signals), each with an associated coordinate location on the scalp surface. The units of the signal are determined by the specific technique (for example dSPM time series are dimensionless statistical test values). This time series information can be used to display the results, and in subsequent statistical analysis. Post dissertation plans include investigating how the surface data can be transformed into Talairach coordinates, and conducting analysis similar to that done on the sensor signals, on the scalp source signals and/or the Talairach transformed signals.

Of particular interest relevant to the present research is to consider the theta θ, alpha α and gamma γ frequency bands independently in source localization. Alpha gating/inhibition activity may have a different neural source pattern than does theta

communication information processing control, which may have a different neural source pattern than does gamma attentional processing. These hypotheses will be explored further in post-dissertation research.

7.3 Theta θ-band

The theory put forward here is that theta activity has a key architectural role in information processing and communications in OBA. The literature discussed in section **1.**1.6 Theta-band frequency and information processing / communication, lends support to this theory, and the "WhOBAP" model introduced in section 1.3 Dual Theoretical Frameworks outlines the framework proposing how it is manifest for OBA. Importantly, the MEG ANOVA analyses results of the present dissertation research are consistent with this framework.

Specifically, SO power was significantly less than DO power for targets presented in the left hemifield, while it was greater for targets presented in the right hemifield. If SO power is an indicator of object processing effects, and if theta oscillations have a role in information processing and communication, then higher SO power in right hemifield targets could be the result of the left hemisphere, which in the visual stream processes right hemifield stimuli, communicating with the right hemisphere, which is thought to be dominant in attentional processing (Corbetta & Shulman, 2002). This both suggests the right hemisphere has a strong role in object-based as well as space-based attentional processing, and is consistent with the finding of Green & McDonald (2008) that theta power is an index of attentional control. Furthermore, consider that theta activity may be the communications vehicle via cross-frequency phase locking with gamma activity (Canolty et al., 2006; Jensen & Colgin, 2007; Palva et al., 2005) for attentional processing

(Bauer et al., 2009). This cross-frequency coupling hypothesis should be explored in post-dissertation research. In summary, theta activity may indeed have a key architectural role in information processing and communication, especially as a carrier of information processed in other frequency bands such as gamma. This is fruitful area for further theory development and investigation.

7.4 Alpha α-band

If alpha-band power is associated with gating and inhibition of task irrelevant regions as suggested in extant literature (Mathewson et al., 2009; Jensen & Mazaheri, 2010), then when gating/inhibition is reduced in a given magnetometer pair, than we may consider the source areas of the signals measured at these magnetometers to be task relevant for OBA processing. The theory is that when alpha-based activity is suppressed, the stage is set for information processing in other frequency bands.

With respect to the specific results of the present research the following subset of analyses revealed SO power significant less that DO power (Table 9). The identified sensors are candidates for further analysis as task relevant for object-based attention processing in other frequency bands such as gamma. The pattern than emerges is that anteriorly, the left temporal magnetometer of pair 13, and the left parietal magnetometer of pair 29 exhibit significantly lower SO than DO power independent of target side. SO power is significantly less than DO power in the parietal lobe (anterior and posterior) for right targets. SO power is significantly less than DO power in the occipital lobe for left targets. Post dissertation research should consider these sensor locations as representing candidate areas which host selective attention processing of left and right targets.

Sources of alpha α-band power in which SO is significantly less then DO (SO < DO)						
MEG/EEG	**Figure/Table**	**Analysis**	**Sensor(s)**	**Lobe**	**Target side**	**Time frame (ms)**
MEG	Figure 37	sliding window	left mag of pair 13	left temporal		175-225
MEG	Figure 28	omnibus	left mag of pair 13	left temporal		
MEG	Figure 28	omnibus	left mag of pair 29	left parietal		
MEG	Figure 38	sliding window	mag pair 29	parietal		50-100
MEG	Table 7 (b)	per lobe	mag pair 29	parietal	right	50-100, 150-250
MEG	Figure 27	omnibus	mag pair 29	parietal	right	
MEG	Table 7 (b)	per lobe	mag pair 32	parietal	right	50-150
MEG	Figure 27	omnibus	mag pair 32	parietal	right	
MEG	Table 7 (d)	per lobe	right mag of pair 39	right occipital	left	
EEG	Figure 23	sliding window	electrode pair O1,O2	occipital	left	150-200

Results are summarized Tukey-post hoc analyses for which SO power was significantly less than DO power. Source figures or tables for each analysis is given. Analysis types were: (1) sliding window: ANOVAs were conducted per sensor-pair, on nine 50 ms windows from 50 ms to 300 ms post-target trigger onset with a 25 ms overlap from one window to the next; (2) per lobe: time and sensor-pair were factors in the ANOVA, which was done for each of the frontal, temporal, parietal and occipital lobes; (3) omnibus: time and magnetometer-pair were factors in an omnibus ANOVA across all lobes. Table layout approximates anterior to posterior, top to bottom. Entries above the double line are for sensors on the anterior part of the brain, those below are for sensors on the posterior part of the brain. Left temporal mag of pair 13, and left parietal mag of pair 29 exhibit significantly lower SO power independent of target side. SO power is significantly less than DO power in the parietal lobe for right targets. SO power is significantly less than DO power in the occipital lobe for left targets.

Table 9

7.5 Gamma γ-band

There is good reason, based on extant literature, to expect gamma-band significance during focused attention (Muller et al., 1996; Fries et al., 2001; Tallon-Baudry et al., 2005). However, no gamma-band significance was observed in the present experiment. There are several possible reasons. First, when gamma-band processing has been found to be significant in the literature, it has been so in attended versus unattended conditions. In Muller et al. (1996), the attended condition consisted of a single moving attended bar, while the unattended condition consisted of two bars moving incoherently in opposite

directions so that attention would not be focused on one or the other; In Fries et al. (2001), monkeys attended to relevant stimulus, while ignoring an irrelevant one in the visual field (attention was never focused on the irrelevant stimulus over the course of a trial): populations of neurons driven by the attended stimulus exhibited increased spiking synchrony in the gamma range compared to neurons driven by the unattended stimulus. In Tallon-Baudry et al., (2005), in the unattended condition the shape on the screen was never attended to during the trial because it was irrelevant to the task of specifying the color change in the fixation cross. This dissertation research, in contrast, studied three conditions in which the target was ultimately attended in order for the participant to specify whether it was a T or L. Since our analyses involve contrasts between different attended conditions, it may be the case that gamma-band information processing was indeed significant, just not significantly *different*. To test for gamma-band significance in the present study, analysis should be done comparing the signals post target-trigger onset with brain signals that occurred when no focused attention was deployed, such as was the case when subjects eyes were closed in pre-study calibration recording. Second, electromagnetic data is noisy, and while the power in the lower frequency bands (theta and alpha) is large enough so as not to be dominated by the noise, it is possible that the power is gamma-band is not powerful enough, especially when there are not enough trials to increase the signal to noise ratio via averaging. In the present data set, the least number of trials averaged for a given participant for a given condition was 18, while the most was 72 (these are two examples of the number of trials that remained after incorrect, outlier, and trials with eye-movement/blink artifacts were removed)[31]. It is highly likely that too few

[31] Consider these numbers in the context of what Dr. Steve Luck recommended for ERP processing at the 2009 ERP Bootcamp: assuming

trials were available to increase the signal to noise ratio enough so that gamma significance would be made evident. Finally, much existing evidence suggests gamma band significance is strongly dependent on alpha power (Moore et al., 2008; Mathewson et al., 2009; Jensen & Mazaheri, 2010) and theta-band phase (Fries, 2005; Palva et al., 2005; Canolty, 2006; Demiralp, 2007; Jensen & Colgen, 2007; Womelsdorf & Fries, 2007). Specifically, gamma band power has been shown to be high when alpha power is low, and low when alpha power is high; and gamma band power has likewise been shown to be high when the phase of theta is positive, and low when the phase of theta is negative. The present analysis did not specifically account for these relationships between the different frequency bands in analyzing gamma-band: rather gamma-band was analyzed without specific consideration of to its relationship to alpha power or theta phase. As such, statistical averages included much data is which gamma power has been shown to be low and insignificant in similar conditions. This compounded with the fact that electromagnetic data is noisy, is enough to swamp out any gamma significance that may exist. Post dissertation research should include using alpha-band power as a spatial filter (that is, identify the magnetometers in which alpha power is low), and using theta-phase as a temporal filter (methods on how to accomplish this need to be investigated), to investigate whether gamma-band significance is uncovered.

7.6 Conclusion

In the extensive literature on visual attention, perhaps the topics most investigated are those which concern the underlying representations upon which this attentional

differences of conditions exist in the P1 and N1 components, a minimum of 300 trials per condition is recommended to guarantee that the differences will be evident.

selection operates and how the attentional selection processes are manifested: What are the set of processes that allow and determine how some subset of the visual input is selected for further cognitive processing? How are these attentional processes manifest in the time-space course of cognitive processing? How do these attentional processes differ when the underlying representations of attentional selection differ? How are they the same? While these topics remain active areas of research, the goal of this dissertation research was to make advances in answering these questions. The results presented here suggest a set of processes, some of which are consistent with what is known from or suggested in extant literature, and some of which are new and to be further investigated. Specifically the findings here suggest a set of oscillatory processes, which determine how some subset of visual input is selected for further cognitive processing: the alpha gating/inhibition process, the theta communication control process, and the gamma attention process. The results suggest a time-course of faster cognitive processing for targets presented in the left hemifield versus targets presented in the right hemifield, lending support to and providing a specific manifestation of previous findings of right hemisphere dominance in selective attention. Previous literature found a role for theta activity in attentional control in space-based attention. The present research likewise found that theta activity has a key role in object-based attention, a role that is consistent with theta serving as a communication control process.

In summary, this dissertation research has both made advances in answering key research questions concerning object-based attention, and raised new questions for further investigation: If a set of oscillatory processes are theorized to allow and determine how some subset of the visual input is selected for further cognitive processing, what is the

exact nature of these processes over space and over time? What are their neural sources? These topics are ripe for further investigation in order to increase our understanding of the cognitive process of object based vis-à-vis space-based attention.

References

Abrahms, R. A. and M. B. Law (2000). "Object-based visual attention with endogenous orienting." Perception & Psychophysics **62**(4): 818-833.

Anderson, K. L., R. Rajagovindan, et al. (2010). "Theta oscillations mediate interaction between prefrontal cortex and medial temporal lobe in human memory." Cerebral Cortex **20**(7): 1604-1612.

Avci, E. (2007). "Performance comparison of wavelet families for analog modulation classification using expert discrete wavelet neural network system." Expert Systems with Applications **33**: 23-35.

Avrahami, J. (1999). "Objects of attention, objects of perception." Perception & Psychophysics **61**(8): 1604-1612.

Bauer, F., S. W. Cheadle, et al. (2009). "Gamma flicker triggers attentional selection without awareness." Proceedings of the National Academy of Sciences **106**(5): 1666-1671.

Bertrand, O. and C. Tallon-Baudry (2000). "Oscillatory gamma activity in humans: a possible role for object representation." International Journal of Psychophysiology **38**: 211-223.

Behrmann, M., R. S. Zemel, et al. (1998). "Object-based attention and occlusion: Evidence from normal participants and a computational model." Journal of Experimental Psychology: Human Perception and Performance **24**(4): 1011-1036.

Behrmann, M., R. S. Zemel, et al. (2000). "Occlusion, Symmetry, and Object-Based Attention: Replay to Saiki (2000)." Journal of Experimental Psychology: Human Perception and Performance **26**(4): 1497-1505.

Besserve, M., M. Philippe, et al. (2007). "Prediction of performance level during a cognitive task from ongoing EEG oscillatory activities." Clinical Neurophysiology **119**(4): 897-908.

Borisyuk, R., Y. Kazanovich, et al. (2009). "A neural model of selective attention and object segmentation in the visual scene: An approach based on partial synchronization and star-like architecture of connections." Neural Networks **22**: 707-719.

Cacioppo, J., L. G. Tassinary, et al., Eds. (2007). The handbook of psychophysiology, Cambridge University Press.

Canolty, R. T., E. Edwards, et al. (2006). "High Gamma Power is Phase-Locked to Theta Oscillations in Human Neocortex." Science **313**: 1626-1628.

Cavanagh, J. F., M. X. Cohen, et al. (2009). "Prelude to and resolution of an error: EEG phase synchrony reveals cognitive control dynamics during action monitoring." The Journal of Neuroscience **29**(1): 98-105.

Chalk, M., J. L. Herrero, et al. (2010). "Attention Reduces Stimulus-Driven Gamma Frequency Oscillations and Spike Field Coherence in V1." Neuron **66**: 114-125.

Chen, Z. and K. Cave (2006). "Reinstating object-based attention under positional certainty: The importance of subjective parsing." Perception & Psychophysics **68**(6): 992-1003.

Chen, Y., A. K. Seth, et al. (2003). "The power of human brain magnetoencephalographic signals can be modulated up or down by changes in an attentive visual task." Proceedings of the National Academy of Sciences **100**(6): 3501-3506.

Cohen, D. (1972). "Magnetoencephalography: Detection of the Brain's Electrical Activity with a Superconducting Magnetometer." Science **175**(4022): 664-666.

Cole, G., A. Gellatly, et al. (2001). "Effect of Object Onset on the Distribution of Visual Attention." Journal of Experimental Psychology: Human Perception and Performance **27**(6): 1356-1368.

Corbetta, M. and G. L. Shulman (2002). "Control of goal-directed and stimulus-driven attention in the brain." Nature Reviews Neuroscience **3**: 201-215.

Demiralp, T., Z. Bayraktaroglu, et al. (2007). "Gamma amplitudes are coupled to theta phase in human EEG during visual perception." International Journal of Psychophysiology **64**: 24-30.

Diba, K. and G. Buzsáki (2008). "Hippocampal network dynamics constrain the time lag between pyramidal cells across modified encironments." The Journal of Neuroscience **28**(50): 13448-13456.

Duncan, J. (1984). "Selective attention and the organization of visual information." Journal of Experimental Psychology: General **113**: 501-517.

Duzel, E., R. Habib, et al. (2003). "A multivariable, spatiotemporal analyss of electromagnetic time-frequency data of recognition memory." NeuroImage **18**: 185-197.

Efron, B. and R. J. Tibshirani (1994). An Introduction to the Bootstrap, Chapman and Hall/CRC.

Egly, R., J. Driver, et al. (1994). "Shifting Visual Attention Between Obejcts and Locations: Evidence From Nornal and Parietal Lesion Subject." Journal of Experimental Psychology: General **123**(2): 161-177.

Engel, A. K., P. Fries, et al. (2001). "Dynamic predictions: Oscillations and synchrony in top-down processing." Nature Reviews Neuroscience **2**: 704-716.

Fagaly, R. L. (2006). "Superconducting quantum interference device instruments and applications." Review of Scientific Instruments **77**(101101): 1-45.

Fries, P. (2005). "A mechanism for cognitive dynamics: neuronal communication through neuronal coherence." Trends in Cognitive Neurosciences **9**(10): 474-480.

Fries, P., D. Nikolic, et al. (2007). "The gamma cycle." Trends in Neurosciences **30**(7): 309-316.

Fries, P., J. J. Reynolds, et al. (2001). "Modulation of Oscillatory Neuronal Synchronization by Selective Visual Attention." Science **291**: 1560-1563.

Garolera, M., R. Coppola, et al. (2007). "Amygdala activation in a¡ective priming: a magnetoencephalogram study." NeuroReport **18**(14): 1449-1453.

Goldsmith, M. and M. Yeari (2003). "Modulation of Object-Based Attention by Spatial Focus Under Endogenous and Exogenous Orienting." Journal of Experimental Psychology: Human Perception and Performance **29**(5): 897-918.

Green, J. J. and J. J. McDonald (2008). "Electrical Neuroimaging Reveals Timing of Attentional Control Activity in Human Brain." PLOS Biology **6**(4): 730-738.

Gross, J., F. Schmitz, et al. (2004). "Modulation of long-range neural synchrony reflects temporal limitations of visual attention in humans." Proceedings of the National Academy of Sciences **101**(35): 13050-13055.

Haddad, R. A. and A. N. Akansu (1993). "Time-frequency localization in transforms, subbands, and wavelets: a critical review." Optical Engineering **32**(7): 1411-1428.

Hamalainen, M., R. Hari, et al. (1993). "Magnetoencephalography-theory, instrumentation, and applications to noninvasive studies of the working human brain." Reviews of Modern Physics **65**(2): 413-497.

Hamalainen, M. S. and R. J. Iimoniemi (1994). "Interpreting magnetic fields of the brain: minimum norm estimates." Medical and Biological Enginering and Computing **32**: 35-42.

Handy, T. C., Ed. (2005). Event-Related Potentials: A Methods Handbook. Cambridge, The MIT Press.(Hamalainen and Iimoniemi 1994)

Hansen, P. C., M. L. Kringelbach, et al., Eds. (2010). MEG: An Introduction to Methods, Oxford University Press.

He, X., S. Fan, et al. (2004). "Cue Validity and Object-Based Attention." Journal of Cognitive Neuroscience **16**(6): 1085-1097.

Herrington, T. M. and J. A. Assad (2010). "Temporal Sequence of Attentional Modualtion in the Lateral Intraparietal Area and Middle Temporal Area during Rapid Covert Shifts of Attention." The Journal of Neuroscience **30**(9): 3287-3296.

Ho, M.-C. and P. Atchley (2009). "Perceptual Load Modulates Object-Based Attention." Journal of Experimental Psychology: Human Perception and Performance **35**(6): 1661-1669.

Ho, M.-C. and S.-L. Yeh (2009). "Effects of instantaneous object input and past experience on object-based attention." Acta Psychologica **132**: 31-39.

Hopf, J.-M., M. A. Schoenfeld, et al. (2005). "The temporal flexibility of attentional selection in the visual cortex." Current Opinion in Neurobiology **15**: 183-187.

Jensen, O. (2005). "Reading the hippocampal code by theta phase-locking." Trends in Cognitive Neurosciences **9**(12): 551-553.

Jensen, O. and L. L. Colgin (2007). "Cross-frequency coupling between neuronal oscillations." Trends in Cognitive Sciences **11**(7): 267-269.

Jensen, O. and A. Mazaheri (2010). "Shaping functional architecture by oscillatory alpha activity: gating by inhibition." Frontiers in Human Neuroscience **4**: 1-8.

Jin, Y., J. P. O'Halloran, et al. (2006). "Alpha EEG predicts visual reaction time." International Journal of Neuroscience **116**(9): 1035-1044.

Jongen, E. M. M., F. T. Y. Smulders, et al. (2006). "Varieties of attention in neutral trials: Linking RT to ERPs and EEG frequencies." Psychophysiology **43**(1): 113-125.

Kahana, M. J., D. Seelig, et al. (2001). "Theta returns." Current Opinion in Neurobiology **11**: 739-744.

Karashima, A., N. Katayama, et al. (2010). "Enhancement of synchronization between hippocampal and amygdata theta waves associated with pontine wave density." Journal of Neurophysiology **103**(5): 2318-3225.

Kastner, S. and L. G. Ungerleider (2000). "Mechanisms of Visual Attention in the Human Cortex." Annual Review of Neuroscience **23**: 315-341.

Lamy, D. and H. Egeth (2002). "Object-based selection: The role of attentional shifts." Perception & Psychophysics **64**(1): 52-66.

Lindsen, J. P., R. Jones, et al. (2010). "Neural components underlying subjective preferential decision making." NeuroImage **50**: 1626-1632.

Linnell, K. J., G. W. Humphreys, et al. (2005). "Action modulates object-based selection." Vision Research **45**: 2268-2286.

List, A. and L. C. Robertson (2007). "Inhibition of Return and Object-Based Attentional Selection." Journal of Experimental Psychology: Human Perception and Performance **33**(6): 1322-1334.

Lopes da Sliva, F. H. (2010). Electrophysiological Basis of MEG Signals. MEG: An

Introduction to Methods. P. C. Hansen, M. L. Kringelbach and R. Salmelin. New York, Oxford University Press.

Lu, Z.-L. and L. Kaufman, Eds. (2003). Magnetic Source Imaging of the Human Brain. Mahwah, NJ, Lawrence Erlbaum Associates.

Luck, S. J. (2005). An Introduction to the Event-Related Potential Technique The MIT Press; 1st edition.

Mangun, G. R. and L. A. Buck (1998). "Sustained visual-spatial attention produces costs and benefits in response time and evoked neural activity." Neuropsychologia **36**(3): 189-200.

Marino, A. C. and B. J. Scholl (2005). "The role of closure in defining the "objects" of object-based attention." Perception & Psychophysics **67**(7): 1140-1149.

Martınez, A., W. Teder-Salejarvi, et al. (2006). "Objects Are Highlighted by Spatial Attention." Journal of Cognitive Neuroscience **18**(2): 298-310.

Martinez, A. g., D. S. Ramanathan, et al. (2007). "The Role of Spatial Attention in the Selection of Real and Illusory Objects." The Journal of Neuroscience **27**(30): 7963-7973.

Martinovic, J., T. Gruber, et al. (2007). "Induced gamma band responses predict recognition delays during object identification." Journal of Cognitive Neuroscience **19**(6): 921-934.

Mathewson, K. E., G. Gratton, et al. (2009). "To See or Not to See: Prestimulus alpha Phase Predicts Visual Awareness." Journal of Neuroscience **29**(9): 2725-2732.

Matsukura, M. and S. P. Vecera (2006). "The return of object-based attention: Selection of multiple-region objects." Perception & Psychophysics **68**(7): 1163-1175.

Medin, D. L., B. H. Ross, et al. (2005). Cognitive Psychology, Fourth Edition, John Wiley & Sons.

Moore, C. M. and C. Fulton (2005). "The spread of attention to hidden portions of occluded surfaces." Psychonomic Bulletin & Review **12**(2): 301-306.

Moore, C. M., S. Yantis, et al. (1998). "Object-Based Visual Selection: Evidence From Perceptual Completion." Psychological Science **9**(2): 104-110.

Moore, R. A., A. Gale, et al. (2006). "Theta phase locking across the neocortex reflects cortico-hippocampal recursive communication during goal conflict resolution." International Journal of Psychophysiology **60**(3): 260-273.

Moore, R. A., A. Gale, et al. (2008). "Alpha power and coherence primarily reflect neural activity related to stages of motor response during a continues monitoring task." International Journal of Psychophysiology **69**(2): 79-89.

Muller, M. M., J. Bosch, et al. (1996). "Visually induced gamma-band responses in human elecroencephalographic activity." Experimental Brain Research **112**: 96-102.

Nunez, P. L. and R. Srinivasan (2005). Electric Fields of the Brain: The Neurophysics of EEG, Oxford University Press.

Olson, C. R. (2001). "Object-based vision and attention in primates." Current Opinion in Neurobiology **11**: 171-179.

Otten, L. J. and M. D. Rugg (2005). Interpreting Event-Related Brain Potentials. Event-Related Potentials: A Methods Handbook. T. C. Handy. Cambridge, MIT Press.

Palva, J. M., S. Palva, et al. (2005). "Phase Synchrony among Neuronal Oscillations in the Human Cortex." Journal of Neuroscience **25**(15): 3962-3972.

Pavlova, M., N. Birbaumer, et al. (2006). "Attentional Modulation of Cortical Neuromagnetic

Gamma Response to Biological Movement." Cerebral Cortex **16**: 321-327.

Roelfsema, P. R. (2006). "Cortical Algorithms for Perceptual Grouping." Annual Review of Neuroscience **29**: 203-227.

Roelfsema, P. R., V. A. F. Lamme, et al. (1998). "Object-based attention in the primary visual cortex of the macaque monkey." Nature (Letters) **395**: 376-381.

Roelfsema, P. R., M. Tolboom, et al. (2007). "Different Processing Phases for Features, Figures, and Selective Attention in the Primary Visual Cortex." Neuron **56**: 785-792.

Saalmann, Y. B., I. N. Pigarev, et al. (2007). "Neural Mechanisms of Visual Attention: How Top-Down Feedback Highlights Relevant Locations." Science **316**.

Salmelin, R. (2010). Muti-Dipole Modeling in MEG. MEG: An introduction to methods. P. C. Hansen, M. L. Kringelbach and R. Salmelin. New York CIty, Oxford University Press.

Sato, N. and Y. Yamaguchi (2007). "Theta synchronization networks emerge during human object-place memory encoding." NeuroReport **18**(5): 419-424.

Schaul, N. (1998). "The fundamental neural mechanisms of electroencelphalography." Electroencephalography and clinical Neurophysiology **106**: 101-107.

Schoenfeld, M. A., C. Tempelmann, et al. (2003). "Dynamics of feature binding during object-selective attention." Proceedings of the National Academy of Sciences **100**(20): 11806-11811.

Scholl, B. J. (2001). "Object and attention: the state of the art." Cognition **80**: 1-46.

Shomstein, S. and M. Behrmann (2006). "Cortical systems mediating visual attention to both objects and spatial locations." Proceedings of the National Academy of Sciences **103**(30): 11387–11392.

Seidenbecher, T., T. R. Laxmi, et al. (2003). "Amygdalar and hippocampal theta rhythm

syncrhonization during fear memory retrieval." Science **301**(5634): 846-850.

Simon-Tov, T., A. Mendelsohn, et al. (2007). "Bihemispheric Leftward Bias in a Visuospatial Attention-Related Network." The Journal of Neuroscience **27**(42): 11271-11278.

Smigasiewicz, K., S. Shalgi, et al. (2010). "Left visual-field advantage in the dual-stream RSVP task and reading-direction: A study in three nations." Neuropsychologia **48**: 2852-2860.

Stark, H., T. Rothe, et al. (2007). "Theta activity attenuation correlates with avoidance learning progress in gerbils." Rapid Communication of Neuroscience Research **18**(6): 549-552.

Swartz, B. E. and E. S. Goldensohn (1998). "Timeline of the history of EEG and associated fields." Electroencephalography and clinical Neurophysiology **106**: 173-176.

Tallon-Baudry, C., O. Bertrand, et al. (2005). "Attention modulates gamma-band oscillations differently in the human lateral occipital cortex and fusiform gyrus." Cerebral Cortex **15**: 654-662.

Torrence, C. and G. P. Compo (1998). "A Practical Guide to Wavelet Analysis." Bulletin of the America Meteorlogial Society **79**(1): 61-78.

Taulu, S. and J. Simola (2006). "Spatiotemporal signal space separation method for rejecting nearby interference in MEG measurements." Physics in Medicine and Biology **51**: 1759-1768.

Tomarken, A. J. and R. C. Serlin (1986). "Comparison of ANOVA Alternatives Under Variance Heterogeneity and Specfic Noncertrality Structures." Psychological Bulletin **99**(1): 90-99.

Turatto, M., V. Mazza, et al. (2005). "Crossmodal object-based attention: Auditory objects affect visual processing." Cognition **96**: B55-B64.

van Wingerden, M., M. Vinck, et al. (2010). "Theta-band phase locking of orbitofrontal neurons during reward expectancy." The Journal of Neuroscience **30**(20): 7078-7087.

Varela, F., J.-P. Lachaux, et al. (2001). "The Brainweb: Phase Synchronization and Large-scale Integration." Nature Reviews Neuroscience **2**: 229-239.

Vecera, S. P. (1994). "Grouped Locations and Object-Based Attention: Comment on Egly, Driver, and Rafal (1994)." Journal of Experimental Psychology: General **123**(3): 316-320.

Vetterli, M. (1992). "Wavelets and Filter Banks: Theory and Design." IEEE Transaction on Signal Processing **40**(9): 2207-2232.

Volberg, G., K. Kliegl, et al. (2009). "EEG alpha oscillations in the preparation for global and local processing predict behaivoral performance." Human Brain Mapping **30**(7): 2173-2183.

von Stein, A., C. Chiang, et al. (2000a). "Top-down processing mediated by interareal synchronization." Proceedings of the National Academy of Sciences **97**(26): 14748-14753.

von Stein, A. and J. Sarnthein (2000b). "Different frequencies for different scales of cortical integration: from local gamma to long range alpha/theta synchronization." International Journal of Psychophysiology **38**: 301-313.

Watson, S. E. and A. F. Kramer (1999). "Object-based visual selective attention and perceptual organization." Perception & Psychophysics **61**(1): 31-49.

Willingham, D. T. (2004). Cognition the Thinking Animal, Second Edition. Upper Saddle River, NJ, Pearson Prentice Hall.

Womelsdorf, T., P. Fries, et al. (2006). "Gamma-band synchronization in visual cortex

predicts speed of change detection." Nature Letters **439**(9): 733-736.

Womelsdorf, T. and P. Fries (2007). "The role of neuronal synchronization in selective attention." Current Opinion in Neurobiology **17**: 154-160.

Womelsdorf, T., J.-M. Schoffelen, et al. (2007). "Modulation of Neuronal Interactions Through Neuronal Synchronization." Science **316**: 1609-1612.

Yamagishi, N., D. E. Callan, et al. (2003). "Attentional modulation of oscillatory activity in human visual cortex." NeuroImage **20**: 98-113.

Yaniv, D. and G. Richter-Levin (2000). "LTP in the rat basal amygdala induced by perirhinal cortex stimulation in vivo." NeuroReport **11**(3): 525-530.

Yantis, S. and J. T. Serences (2003). "Cortical mechanisms of space-based and object-based attentional control." Current Opinion in Neurobiology **13**: 187-193.

Appendix A

A.1 EEG Electrode Layout

EEG Electrode Layout

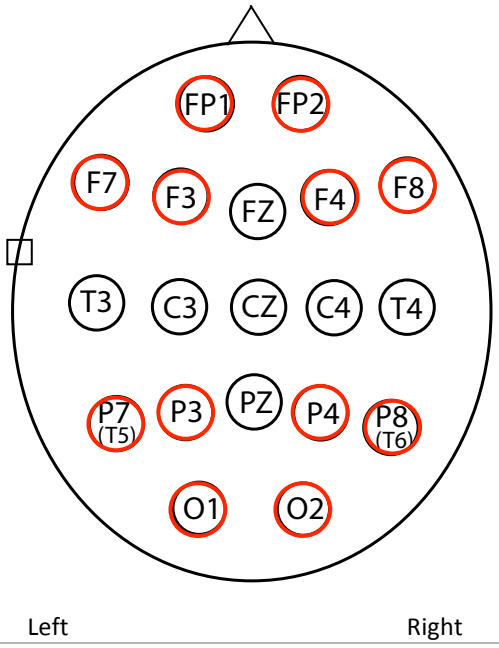

EEG Electrode Layout (10-20 electrode layout system) with 19 electrodes and left mastoid reference (small square) Electrodes circled in red are used in the analyses

Figure 33

A.2 MEG Sensor Layout

MEG Sensor Layout

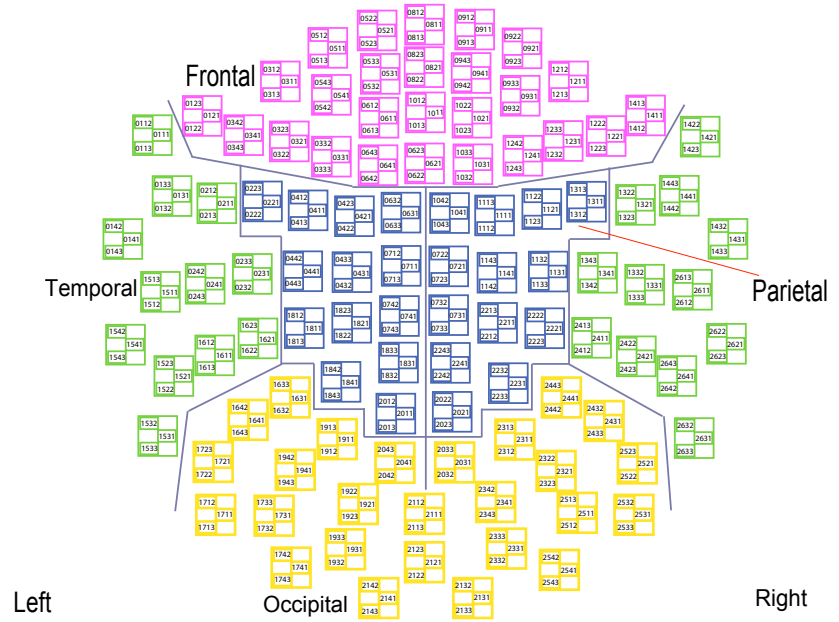

Each sensor consists of one magnetometer, and two planar gradiometers. The magnetometers measure the strength of the magnetic field (in units of Tesla) over time, The Gradiometers measure the strength of the change in the magnetic field over space, over time. Gradiometer units are Tesla/meter.

Figure 34

MEG Magnetometer Pairs Used in the ANALYSES

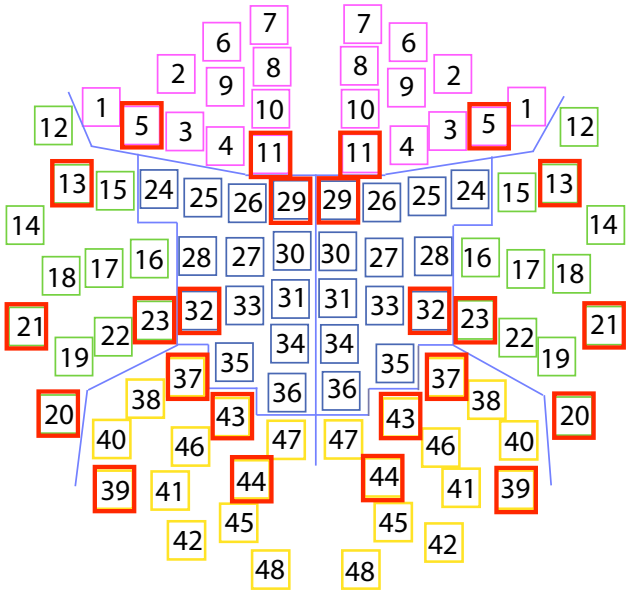

Magnetometers

Frontal pairs (mag left, right)
5 (mag 0341, 1221)
11 (mag 0641, 1032)

Temporal pairs
13 (mag 0131, 1441)
23 (mag 1621, 2411)
21 (mag 1541, 2621)
20 (mag 1531, 2631)

Parietal pairs
29 (mag 0631, 1041)
32 (mag 1811, 2221)

Occipital pairs
37 (mag 1631, 2441)
43 (mag 1911, 2311)
44 (mag 1921, 2341)
39 (mag 1711, 2531)

Pairs delineated with a red square are those used in the magnetometer analysis in all MEG analyses in this dissertation research.

Figure 35

12 magnetometer pairs with highest power in HV display-condition contrast	12 magnetometer pairs with highest power in VH display-condition contrast
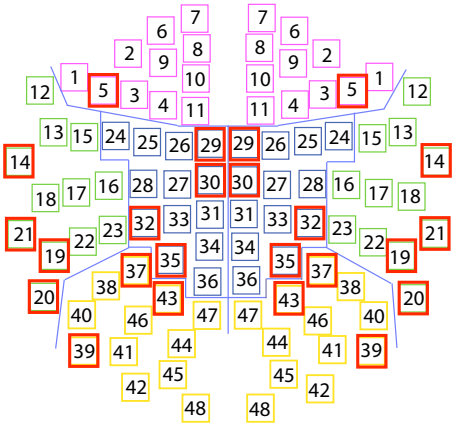	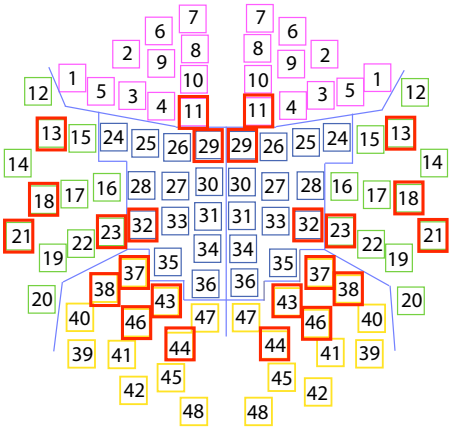

A spectral wavelet analysis was done on all magnetometers in the 48 pairs for each of the two condition-display contrasts: "HV" where DO-Valid in the horizontal displays is contrast with SO-Valid in the vertical displays, and "VH" where DO-Valid in the vertical displays is contrast with SO-Valid in the horizontal displays. The spectral wavelet analysis resulted in eight wavelets for the signal in each magnetometer, one for each frequency band with center frequency: 5, 10, 20, 30, 40, 50, 70, and 80. (Often a notch filter is used to remove 60 Hz power line noise in electromagnetic signals. In the present research the 60 Hz wavelet is not included in the analysis as the way to eliminate the 60 Hz power line noise). In each contrast (HV, VH), for each magnetometer, each of the eight wavelets were scanned across time starting in the N1 time frame (150 ms post target trigger onset), and the time point containing the largest power was noted, along with the time point and the sensor. Then for each contrast, across all magnetometers, and all wavelets, the power values were ordered in descending value. In each contrast, the magnetometer with the highest power value was selected as well as its hemisphere counterpart. Then the magnetometer with the next highest power value was selected as well as its hemisphere counterpart (if the hemisphere counterpart was not already selected in the previous step). Magnetometers were selected using this algorithm in each contrast until 6 pairs of 12 magnetometers were selected. A single merged list of 12 pairs was selected as follows: the five magnetometer pairs in common between the two contrasts were selected (Temporal lobe 21, Parietal lobe 29 & 32, Occipital Lobe 37 & 43). Since no magnetometers were common in the frontal lobe and one pair was identified in each contrast, they were both added to the list (5 from the HV contrast, and 11 from the VH contrast). Since the occipital lobe is key in visual perception, one pair from each contrast was added to the list (39 from the HV contrast, and 44 from the HV contrast). To insure broad coverage of the head, the next most anterior magnetometer was added to the list: Temporal pair 13 from the VH contrast. To counter, the most posterior temporal pair 20 in the HV contrast was added. Finally, from visual inspection of the two graphs, it was clear that the parietal-temporal-occipital junction was key. Also, visual inspection of the source signals revealed that the largest signal modulations were in the temporal lobe. Therefore the temporal lobe pair 23 that abuts this junction, from the VH contrast list was added.

Figure 36

A.3 Electrophysiological Basis of MEG Signals

MEG is the technique of measuring the magnetic fields generated by brain activity, just as EEG is the technique of measuring the electric potentials generated by the same brain activity. Both provide large-scale millisecond resolution measures of modulations of the synaptic potential fields around their background levels. The neurons that are the main sources of MEG and EEG measured activity are pyramidal neurons, since they are typically

arranged in palisades with the apical dendrites aligned allowing individual neuronal currents to sum into measurable currents and associated magnetic fields on the scalp surface. The minimum number of synchronously active neurons necessary to record a magnetic signal using MEG is estimated to be approximately 50,000, but can be far more, into the millions or billions. There are two forms of neuronal activation: the action potential and the more protracted postsynaptic potentials. The two main kinds of postsynaptic potentials are the excitatory postsynaptic potential (EPSP) and the inhibitory postsynaptic potential (IPSP). The EPSP results in a magnetic field sink while the IPSP results in the magnetic field source. Summed over tens of thousands of neurons, it is the postsynaptic potentials that give rise to a measurable MEG and EEG signals. The more synchronously active neurons, the stronger the signal (Lopes de Silva, 2010).

A.4 ERP "Components"

Although there is no universally accepted definition of what constitutes an ERP "component" (Handy, 2005), Cacioppo et al. (2007), provide the following discussion of the alternative explanation of what can constitute an ERP component.

The most common meaning is to assume that its existence is a reflection of neurophysiologic activity that corresponds to some psychological process. Mechanistically, components can be defined in three (but not necessarily mutually exclusive) ways. First, components can be defined in terms of the positive and negative peaks that are observed in the ERP waveform. Second, components can be defined as aspects of the ERP waveform that covary across subjects, conditions, and/or location on the scalp in response to experimental manipulations. Third, components can be defined in terms of those neural structures that generate them. The adoption of one or other of these definitions will have

important consequences for the interpretation of the component structure of the ERP waveform. Different analyses procedures will be required depending on which component definition is adopted (Cacioppo et al., 2007).

In the present research the presumption of the P1 and N1 ERP components as reflecting neurophysiologic activity of attention within target time-frames is adopted in the ERP temporal analysis in section 4.1 EEG/ERP. OBA and SBA are shown to modulate these components consistent with previous findings in extant ERP literature. For the remaining analyses (MEG temporal, ERP temporal-spectral and MEG temporal-spectral), this presumption is not made. Rather than identifying the component time windows within which to look for significant differences a priori, an assumption free approach to analysis is adopted. Sliding latency windows starting at 50 ms and finishing 300 ms post target are all evaluated for differences between conditions. However, the results are discussed in reference to the P1 and N1 time frame component windows as well as across all latency windows in the time-course.

Appendix B

B.1 Temporal-Spectral EEG/ERP Results

Shifts of Attention within Hemifield: HV Contrast - F-statistics for Figure 23.									
FP1, FP2		F(7,1) = 4.47, p < 0.001			F(7,1) = 3.45, p = 0.001				
F7, F8					F(7,1) = 5.10, p < 0.001				
						F(7,1) = 4.53, p < 0.001			
F3, F4		F(7,1) = 3.54, p = 0.001							
P7, P8		F(7,1) = 7.70, p < 0.001			F(7,1) = 3.58, p = 0.001				
P3, P4		F(7,1) = 5.29, p < 0.001							
O1, O2		F(7,1) = 6.84, p < 0.001			F(7,1) = 4.45, p < 0.001				
			F(7,1) = 3.84, p < 0.001						
Time (ms)	50	75	100 "P1"	125	150	175 "N1"	200	225	250	275

F-statstics for significant sliding window ANOVAs. A a yellow background indicates a difference-score X target side X wavelet interaction; a pink background indicates a difference-score X wavelet interaction.

Table 10

Shifts of Attention between Hemifields: VH Contrast – F-statistics for Figure 24.									
FP1, FP2							F(7,1) = 3.60, p = 0.001		
F7, F8									
F3, F4					F(7,1) = 4.03, p < 0.001		F(7,1) = 4.78, p < 0.001		
P7, P8									
P3, P4									
O1, O2			F(7,1) = 3.61, p = 0.001						
Time (ms)	50	75	100 "P1"	125	150	175 "N1"	200	225	250	275

F-statstics for significant sliding window ANOVAs. A pink background indicates a difference-score X wavelet interaction.

Table 11

B.2 Temporal-Spectral MEG/ERMF Results

B.2.1 Results – Sliding windows

Detailed Breakout: HV Contrast

Bar graphs

In order to ascertain the positive or negative direction of differences and to examine all-order interactions, Table 1 is expanded to include bar graphs of the ANOVA results for all significant interactions. These are plotted for the frontal, and anterior temporal lobe magnetometer pairs (Figure 37)[32], the parietal lobe pairs (Figure 38)[32], the posterior temporal lobe pairs (Figure 39 and Figure 40)[32], and the occipital lobe pairs (Figure 41)[32].

[32] Only θ and α bands are graphed, as significant only ever occurred in these frequency bands. All bar graphs are graphed to the same scale, in order to facilitate visual comparison across graphs. The y-axis is reversed (due to implementation details): increasing power is down and decreasing power is up.

Shifts of Attention within Hemifield: HV Contrast										
Time (ms)	**50**	**75**	**100**	**125**	**150**	**175**	**200**	**225**	**250**	**275**
Frontal lobe Magnetometer pairs										
5				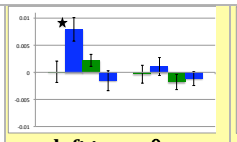 **left targs, θ**		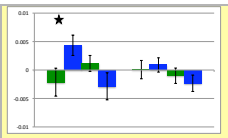 **left targs, θ**		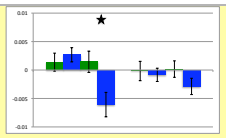 **right targs, θ**		
					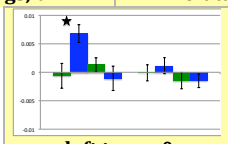 **left targs, θ**		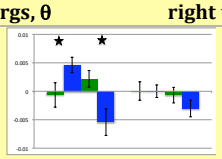 **left & right targs, θ**			
11										
Anterior Temporal lobe Magnetometer pairs										
13						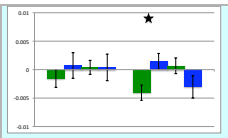 **mag 0131 (L), α**				
						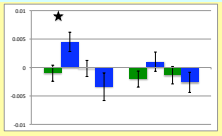 **left targs, θ**		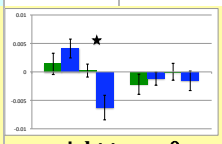 **right targs, θ**		
							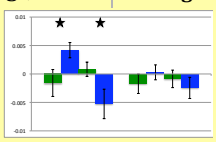 **left & right targs, θ**			
Time (ms)	**50**	**75**	**100**	**125**	**150**	**175**	**200**	**225**	**250**	**275**

Shown are sources of significance. DO-Valid is green, SO-Valid is blue. The y-axis on the graphs is flipped. Green up and blue down means SO > DO, and vice-versa. Significant differences between difference scores are denoted with a *. A blue background indicates a difference-score X magnetometer side X wavelet interaction, θ on the left, α on the right, and within each frequency the left magnetometer on the left, the right magnetometer on the right; a yellow background indicates a difference-score X target side X wavelet interaction, θ on the left, α on the right, and within each frequency left targets on the left, right targets on the right. The source(s) of the interaction are labeled. The y-axis is reversed: increasing power is down, decreasing power is up. F-statistics for these results are given in Table 12.

Figure 37

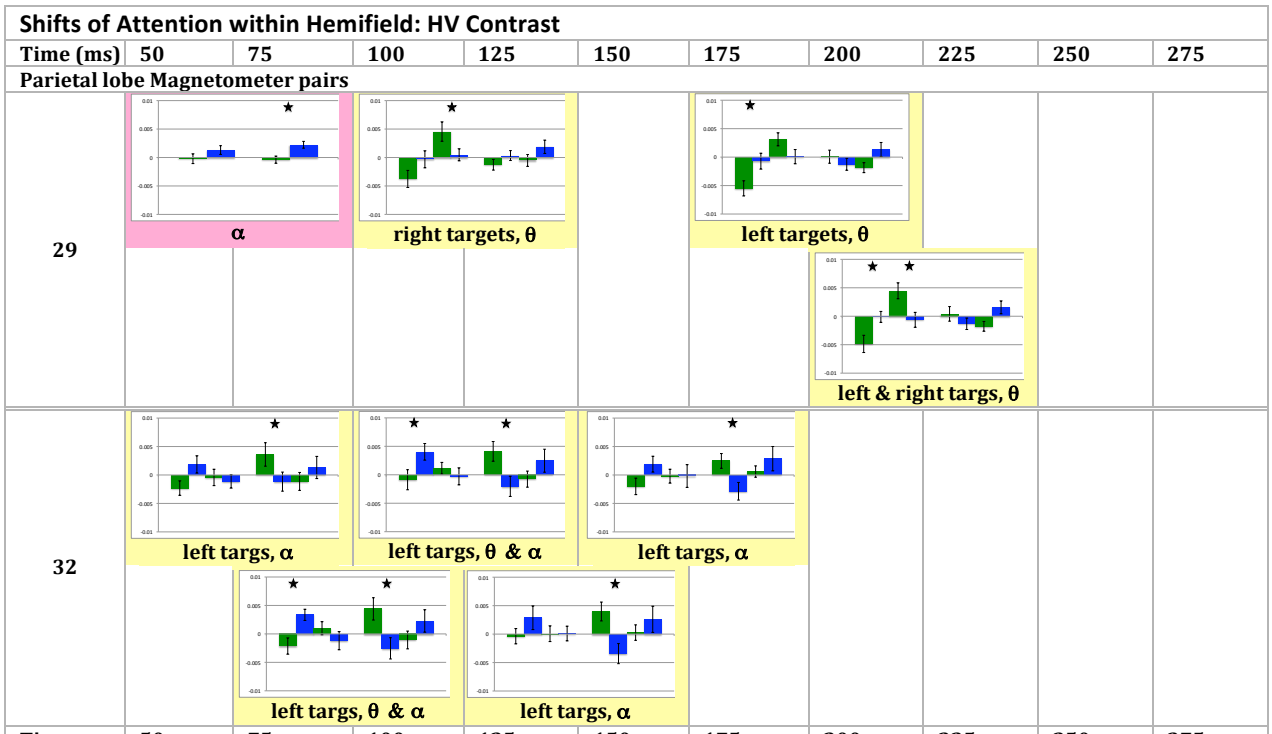

Shown are sources of significance. DO-Valid is green, SO-Valid is blue. The y-axis on the graphs is flipped. Green up and blue down means SO > DO, and vice-versa. Significant differences between difference scores are denoted with a *. A pink background in the cell indicates a difference-score X wavelet interaction, θ on the left, α on the right; a yellow background indicates a difference-score X target side X wavelet interaction, θ on the left, α on the right, and within each frequency left targets on the left, right targets on the right. The source(s) of the interaction are labeled. The y-axis is reversed: increasing power is down, decreasing power is up. F-statistics for these esults are given in Table 13.

Figure 38

Shifts of Attention within Hemifield: HV Contrast

Time (ms)	50	75	100	125	150	175	200	225	250	275
Posterior Temporal lobe Magnetometer pairs 23 and 21										
23										
21						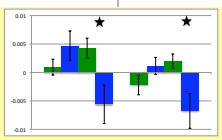 right targs, θ & α		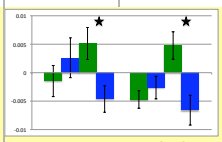 right targs, θ & α		
				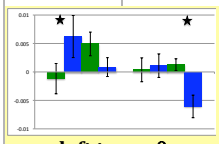 left targs, θ right targs, α		 right targs		 right targs		
					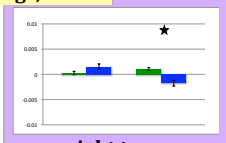 right targs		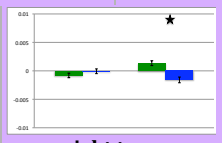 right targs		 main effect diffscore	
					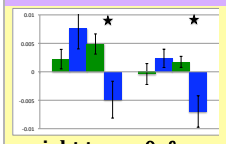 right targs, θ & α		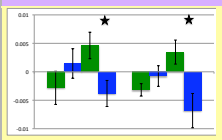 right targs, θ & α		 right targs	
									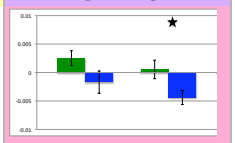 α	
									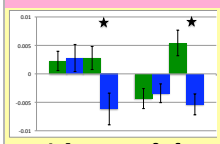 right targs, θ & α	
Time (ms)	**50**	**75**	**100**	**125**	**150**	**175**	**200**	**225**	**250**	**275**

Shown are sources of significance. DO-Valid is green, SO-Valid is blue. The y-axis on the graphs is flipped. Green up and blue down means SO > DO, and vice-versa. Significant differences between difference scores are denoted with a *. A pink background in the cell indicates a difference-score X wavelet interaction, θ on the left, α on the right; a purple background indicates a difference-score X target side interaction, left targets on the left, right targets on the right; a yellow background indicates a difference-score X target side X wavelet interaction, θ on the left, α on the right, and within each frequency left targets on the left, right targets on the right. A green background indicates a main effect of difference-score. The source(s) of the interaction are labeled. The y-axis is reversed: increasing power is down, decreasing power is up. F-statistics for these esults are given in Table 14.

Figure 39

Shifts of Attention within Hemifield: HV Contrast										
Time (ms)	**50**	**75**		**125**	**150**	**175**	**200**	**225**	**250**	**275**
Posterior Temporal lobe Magnetometer pair 20										
20									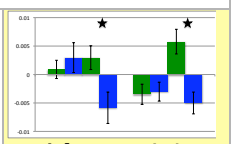 **right targs, θ & α**	
									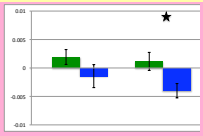 **α**	
					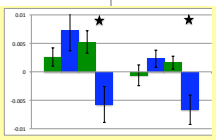 **right targs, θ & α**		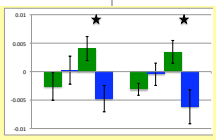 **right targs, θ & α**		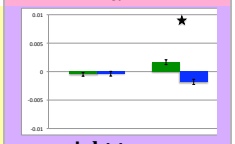 **right targs**	
					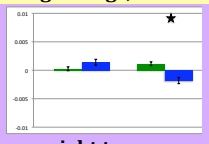 **right targs**		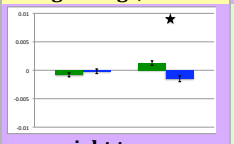 **right targs**		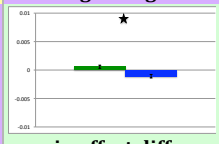 **main effect diffscore**	
						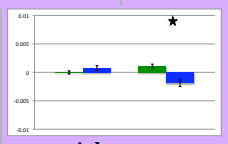 **right targs**		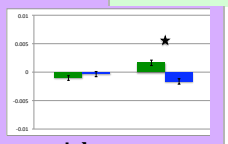 **right targs**		
						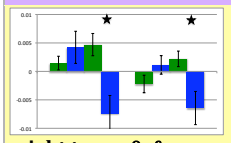 **right targs, θ & α**		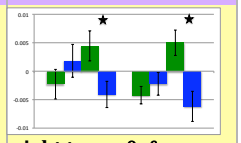 **right targs, θ & α**		
Time (ms)	**50**	**75**	**100**	**125**	**150**	**175**	**200**	**225**	**250**	**275**

Shown are sources of significance. DO-Valid is green, SO-Valid is blue. The y-axis on the graphs is flipped. Green up and blue down means SO > DO, and vice-versa. Significant differences between difference scores are denoted with a *. A pink background in the cell indicates a difference-score X wavelet interaction, θ on the left, α on the right; a purple background indicates a difference-score X target side interaction, left targets on the left, right targets on the right; a yellow background indicates a difference-score X target side X wavelet interaction, θ on the left, α on the right, and within each frequency left targets on the left, right targets on the right. A green background indicates a main effect of difference-score. The source(s) of the interaction are labeled. The y-axis is reversed: increasing power is down, decreasing power is up. F-statistics for these esults are given in Table 15.

Figure 40

Shifts of Attention within Hemifield: HV Contrast										
Time (ms)	**50**	**75**	**100**	**125**	**150**	**175**	**200**	**225**	**250**	**275**
Occipital lobe Magnetometer pairs										
37		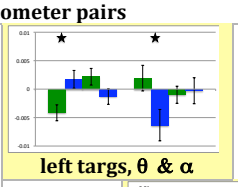 left targs, θ & α	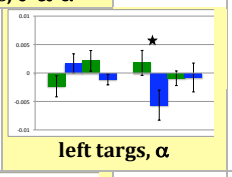 left targs, α							
43		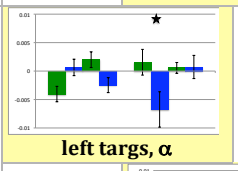 left targs, α	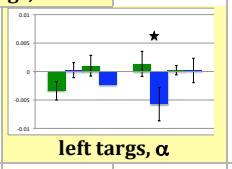 left targs, α				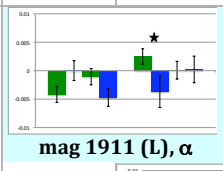 mag 1911 (L), α	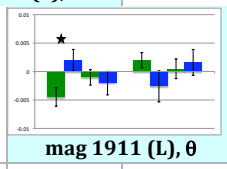 mag 1911 (L), θ		
44										
39					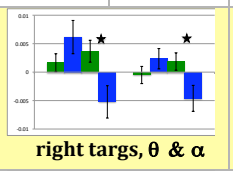 right targs, θ & α		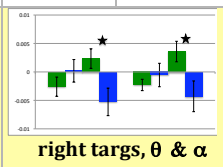 right targs, θ & α	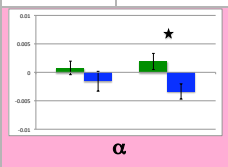 α		
					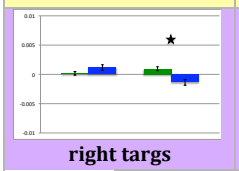 right targs		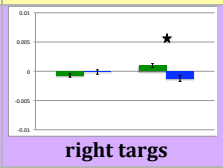 right targs	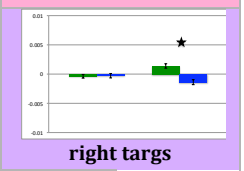 right targs		
						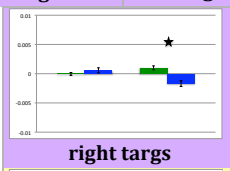 right targs		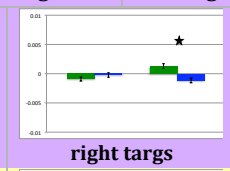 right targs		
						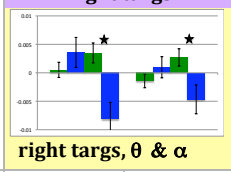 right targs, θ & α		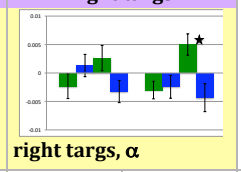 right targs, α		
Time	**50**	**75**	**100**	**125**	**150**	**175**	**200**	**225**	**250**	**275**

Shown are sources of significance. DO-Valid is green, SO-Valid is blue. The y-axis on the graphs is flipped. Green up and blue down means SO > DO, and vice-versa. Significant differences between difference scores are denoted with a *. A pink background in the cell indicates a difference-score X wavelet interaction, θ on the left, α on the right; a purple background indicates a difference-score X target side interaction, left targets on the left, right targets on the right; a blue background indicates a difference-score X magnetometer side X wavelet interaction, θ on the left, α on the right, and within each frequency the left magnetometer on the left, the right magnetometer on the right; a yellow background indicates a difference-score X target side X wavelet interaction, θ on the left, α on the right, and within each frequency left targets on the left, right targets on the right. The source(s) of the interaction are labeled. The y-axis is reversed: increasing power is down, decreasing power is up. F-statistics for these esults are given in Table 16.

Figure 41

F-statistics

The F-statistics for the HV condition-contrast bar graphs in the previous section are given here for the frontal, and anterior temporal lobe magnetometer pairs (Table 12), the parietal lobe pairs (Table 13), the posterior temporal lobe pairs (Table 14 and Table 15), and the occipital lobe pairs (Table 16).

Shifts of Attention within Hemifield: HV Contrast – F-statistics for Figure 37										
Time (ms)	**50**	**75**	**100**	**125**	**150**	**175**	**200**	**225**	**250**	**275**
Frontal lobe Magnetometer pairs										
5				**F(7,1) = 5.58, p < 0.001**		**F(7,1) = 4.27, p < 0.001**		**F(7,1) = 3.62, p < 0.001**		
					F(7,1) = 4.41, p < 0.001		**F(7,1) = 7.20, p < 0.001**			
11										
Anterior Temporal lobe Magnetometer pairs										
13						**F(7,1) = 3.70, p = 0.001**				
						F(7,1) = 3.48, p = 0.001		**F(7,1) = 3.52, p = 0.001**		
							F(7,1) = 5.01, p < 0.001			
Time (ms)	**50**	**75**	**100**	**125**	**150**	**175**	**200**	**225**	**250**	**275**
F-statstics for significant sliding window ANOVAs. A yellow background indicates a difference-score X target side X wavelet interaction; a blue background indicates a difference-score X magnetometer side X wavelet interaction.										

Table 12

Shifts of Attention within Hemifield: HV Contrast – F-statistics for Figure 38										
Time (ms)	**50**	**75**	**100**	**125**	**150**	**175**	**200**	**225**	**250**	**275**
Parietal lobe Magnetometer pairs										
29	**F(7,1) = 3.73, p = 0.001**		**F(7,1) = 4.44, p < 0.001**			**F(7,1) = 7.05, p < 0.001**				
							F(7,1) = 10.41, p < 0.001			
32	**F(7,1) = 4.04, p < 0.001**		**F(7,1) = 6.43, p < 0.001**		**F(7,1) = 3.78, p = 0.001**					
		F(7,1) = 8.79, p < 0.001		**F(7,1) = 4.61, p < 0.001**						
Time (ms)	**50**	**75**	**100**	**125**	**150**	**175**	**200**	**225**	**250**	**275**
F-statstics for significant sliding window ANOVAs. A yellow background indicates a difference-score X target side X wavelet interaction; a pink background indicates a difference-score X wavelet interaction.										

Table 13

Shifts of Attention within Hemifield: HV Contrast – F-statistics for Figure 39										
Time (ms)	**50**	**75**	**100**	**125**	**150**	**175**	**200**	**225**	**250**	**275**
Posterior Temporal lobe Magnetometer pairs 23 and 21										
23										
21						F(7,1) = 6.40, p < 0.001		F(7,1) = 4.92, p < 0.001		
				F(7,1) = 3.55, p = 0.001		F(1,1) = 19.99, p < 0.001		F(1,1) = 19.22, p < 0.001		
					F(1,1) = 20.61, p < 0.001		F(1,1) = 17.40, P < 0.001		F(1,1) = 22.32, p < 0.001	
					F(7,1) = 6.01, p < 0.001		F(7,1) = 5.29, p < 0.001		F(1,1) = 20.14, p < 0.001	
									F(7,1) = 3.39, p = 0.002	
									F(7,1) = 4.35, p < 0.001	
Time (ms)	**50**	**75**	**100**	**125**	**150**	**175**	**200**	**225**	**250**	**275**
F-statstics for significant sliding window ANOVAs. A yellow background indicates a difference-score X target side X wavelet interaction; a purple background indicates a difference-score X target-side interaction; a pink background indicates a difference-score X wavelet interaction.										

Table 14

Shifts of Attention within Hemifield: HV Contrast – F-statistics for Figure 40										
Time (ms)	**50**	**75**		**125**	**150**	**175**	**200**	**225**	**250**	**275**
Posterior Temporal lobe Magnetometer pair 20										
20									F(7,1) = 4.47, p < 0.001	
									F(7,1) = 3.01, p = 0.004	
					F(7,1) = 7.18, p < 0.001		F(7,1) = 5.25, p < 0.001		F(1,1) = 20.13, p < 0.001	
					F(1,1) = 21.37, p < 0.001		F(1,1) = 16.53, p < 0.001		F(1,1) = 17.89, p < 0.001	
						F(1,1) = 21.37, p < 0.001		F(1,1) = 19.27, p < 0.001		
						F(7,1) = 7.18, p < 0.001		F(7,1) = 5.01, p < 0.001		
Time (ms)	**50**	**75**	**100**	**125**	**150**	**175**	**200**	**225**	**250**	**275**
F-statstics for significant sliding window ANOVAs. A yellow background indicates a difference-score X target side X wavelet interaction; a purple background indicates a difference-score X target-side interaction; a pink background indicates a difference-score X wavelet interaction.										

Table 15

Shifts of Attention within Hemifield: HV Contrast – F-statistics for Figure 41										
Time (ms)	**50**	**75**	**100**	**125**	**150**	**175**	**200**	**225**	**250**	**275**
Occipital lobe Magnetometer pairs										
37		**F(7,1) = 3.67, p = 0.001**								
			F(7,1) = 3.82, p < 0.001							
43		**F(7,1) = 3.33, p = 0.002**					**F(7,1) = 3.99, p < 0.001**			
			F(7,1) = 3.78, p = 0.001					**F(7,1) = 3.18, p = 0.003**		
44										
39					**F(7,1) = 5.63, p < 0.001**		**F(7,1) = 4.72, p < 0.001**		**F(7,1) = 3.23, p = 0.002**	
					F(1,1) = 17.61, p < 0.001		**F(1,1) = 14.42, p < 0.001**		**F(1,1) = 15.28, p < 0.001**	
						F(1,1) = 22.31, p < 0.001		**F(1,1) = 16.44, p < 0.001**		
						F(7,1) = 6.70, p < 0.001		**F(7,1) = 3.81, p < 0.001**		
Time (ms)	**50**	**75**	**100**	**125**	**150**	**175**	**200**	**225**	**250**	**275**
F-statstics for significant sliding window ANOVAs. A yellow background indicates a difference-score X target side X wavelet interaction; a blue background indicates a difference-score X magnetometer side X wavelet interaction; a purple background indicates a difference-score X target-side interaction; a pink background indicates a difference-score X wavelet interaction.										

Table 16

Detailed Breakout: VH Contrast

Bar graphs

In order to ascertain the positive or negative direction of differences, Table 4 is expanded to include bar graphs of the ANOVA results. These are plotted for the frontal and anterior temporal lobe magnetometer pairs (Figure 42)[33], the parietal lobe pairs (Figure 43)[33], the posterior temporal lobe pairs (Figure 44)[33] and the occipital lobe magnetometer pairs (Figure 45)[33].

[33] Only θ and α bands are graphed, as significant only ever occurred in these frequency bands. All bar graphs are graphed to the same scale, in order to facilitate visual comparison across graphs. The y-axis is reversed (due to implementation details): increasing power is down and decreasing power is up.

Shifts of Attention between Hemifields: VH Contrast										
Time (ms)	**50**	**75**	**100**	**125**	**150**	**175**	**200**	**225**	**250**	**275**
Frontal lobe Magnetometers										
5										
11		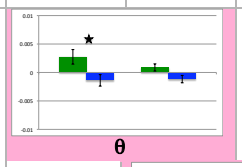 θ	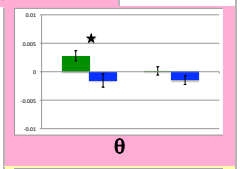 θ	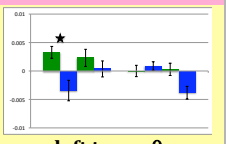 left targs, θ						
Anterior Temporal lobe Magnetometers										
13								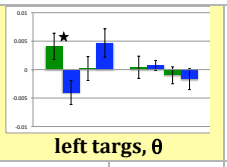 left targs, θ		
Time (ms)	**50**	**75**	**100**	**125**	**150**	**175**	**200**	**225**	**250**	**275**

Shown are sources of significance. DO-Valid is green, SO-Valid is blue. The y-axis on the graphs is flipped. Green up and blue down means SO > DO, and vice-versa. Significant differences between difference scores are denoted with a *. A pink background in the cell indicates a difference-score X wavelet interaction θ on the left, α on the right; a yellow background indicates a difference-score X target side X wavelet interaction, θ on the left α on the right, and within each frequency left targets on the left, right targets on the right. The source(s) of the interaction are labeled. The y-axis is reversed: increasing power is down, decreasing power is up. F-statistics for these esults are given in Table 17.

Figure 42

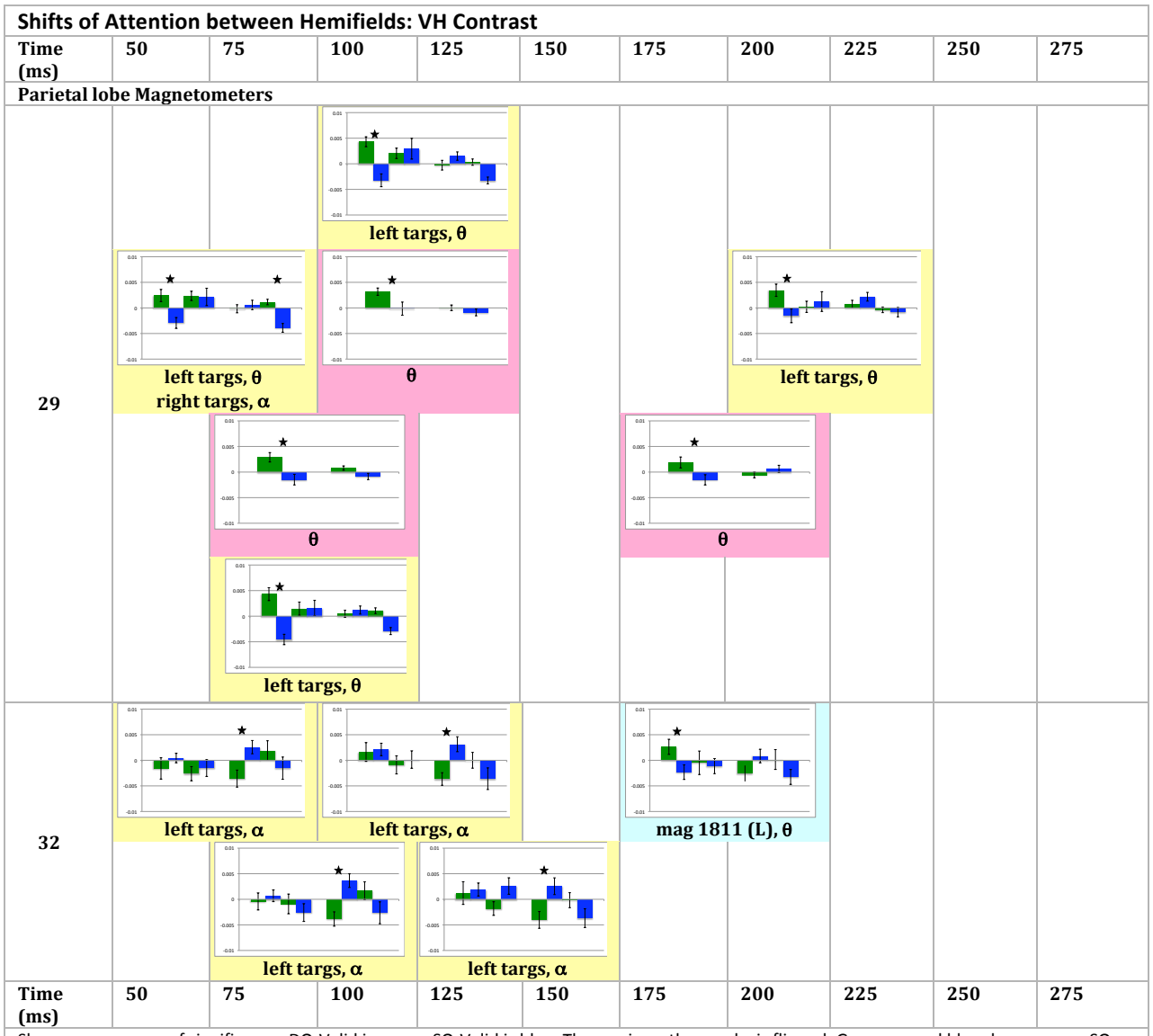

Shown are sources of significance. DO-Valid is green, SO-Valid is blue. The y-axis on the graphs is flipped. Green up and blue down means SO > DO, and vice-versa. Significant differences between difference scores are denoted with a *. A pink background in the cell indicates a difference-score X wavelet interaction, θ on the left, α on the right; a blue background indicates a difference-score X magnetometer side X wavelet interaction, θ on the left, α on the right, and within each frequency the left magnetometer on the left, the right magnetometer on the right; a yellow background indicates a difference-score X target side X wavelet interaction, θ on the left, α on the right, and within each frequency left targets on the left, right targets on the right. The source(s) of the interaction are labeled. The y-axis is reversed: increasing power is down, decreasing power is up. F-statistics for these esults are given in Table 18.

Figure 43

Shifts of Attention between Hemifields: VH Contrast										
Time (ms)	**50**	**75**	**100**	**125**	**150**	**175**	**200**	**225**	**250**	**275**
Posterior Temporal lobe Magnetometers										
23	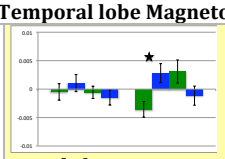 **left targs, α**		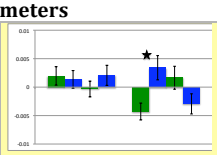 **left targs, α**							
		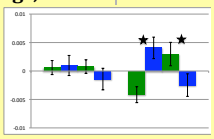 **left targs, α right targs, α**		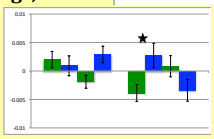 **left targs, α**						
21								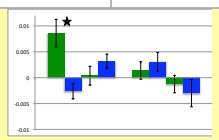 **left targs, θ**		
									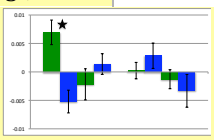 **left targs, θ**	
20								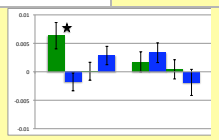 **left targs, θ**		
									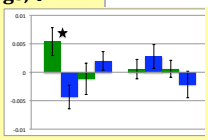 **left targs, θ**	
Time (ms)	**50**	**75**	**100**	**125**	**150**	**175**	**200**	**225**	**250**	**275**

Shown are sources of significance. DO-Valid is green, SO-Valid is blue. The y-axis on the graphs is flipped. Green up and blue down means SO > DO, and vice-versa. Significant differences between difference scores are denoted with a *. A yellow background indicates a difference-score X target side X wavelet interaction, θ on the left, α on the right, and within each frequency, left targets on the left, right targets on the right. The source(s) of the interaction are labeled. The y-axis is reversed: increasing power is down, decreasing power is up. F-statistics for these esults are given in Table 19.

Figure 44

Shifts of Attention between Hemifields: VH Contrast										
Time (ms)	**50**	**75**	**100**	**125**	**150**	**175**	**200**	**225**	**250**	**275**
Occipital lobe Magnetometers										
37					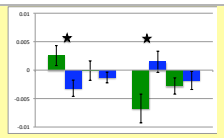 left targs, θ & α					
	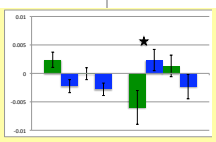 left targs, α		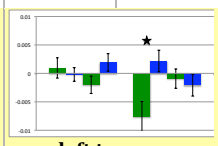 left targs, α		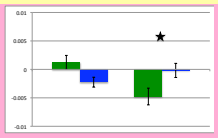 α		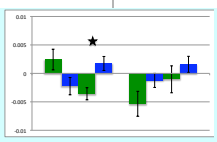 mag 2441 (R), θ			
		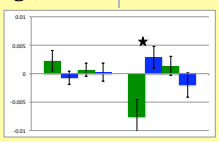 left targs, α		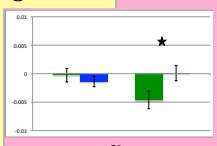 α		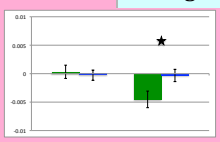 α				
				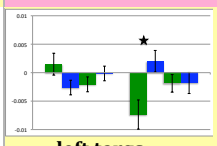 left targs, α						
				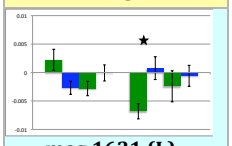 mag 1631 (L), α						
43					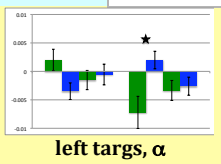 left targs, α		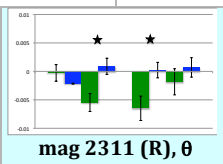 mag 2311 (R), θ mag 1911 (L), α			
	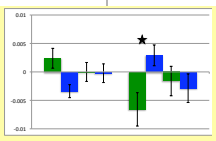 left targs, α		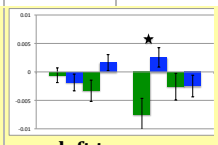 left targs, α		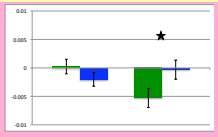 α		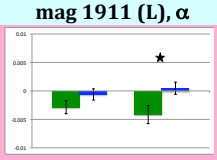 α			
		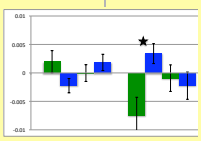 left targs, α		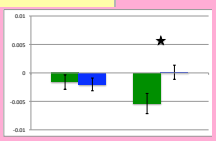 α		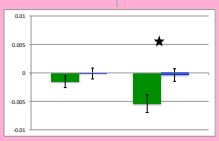 α		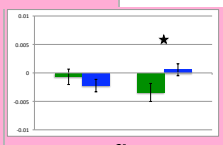 α		
				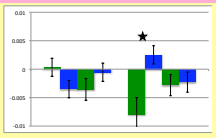 left targs, α		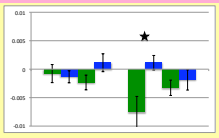 left targs, α		 mag 1911 (L), α		

Shifts of Attention between Hemifields: VH Contrast										
44	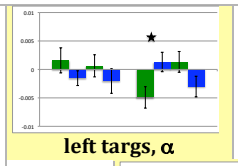		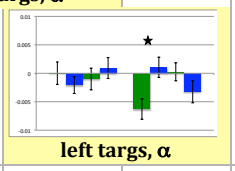			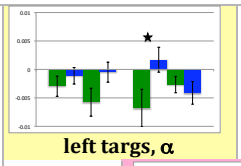	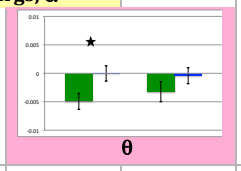			
39										
Time (ms)	50	75	100	125	150	175	200	225	250	275

Shown are sources of significance. DO-Valid is green, SO-Valid is blue. The y-axis on the graphs is flipped. Green up and blue down means SO > DO, and vice-versa. Significant differences between difference scores are denoted with a *. A pink background in the cell indicates a difference-score X wavelet interaction, θ on the left, α on the right; a blue background indicates a difference-score X magnetometer side X wavelet interaction, θ on the left, α on the right, and within each frequency the left magnetometer on the left, the right magnetometer on the right; a yellow background indicates a difference-score X target side X wavelet interaction, θ on the left, α on the right, and within each frequency left targets on the left, right targets on the right. The source(s) of the interaction are labeled. The y-axis is reversed: increasing power is down, decreasing power is up. F-statistics for these esults are given in Table 20.

Figure 45

F-statistics

The F-statistics for the VH condition-contrast bar graphs in the previous section are given here for the frontal and anterior temporal lobe magnetometer pairs (Table 17), the parietal lobe pairs (Table 18), the posterior temporal lobe pairs (Table 19) and the occipital lobe magnetometer pairs (Table 20).

Shifts of Attention between Hemifields: VH Contrast – F-statistics for Figure 42										
Time (ms)	50	75	100	125	150	175	200	225	250	275
Frontal lobe Magnetometers										
5										
11		F(7,1) = 4.05, p < 0.001	F(7,1) = 5.24, p < 0.001	F(7,1) = 2.93, p = 0.005						
Anterior Temporal lobe Magnetometers										
13								F(7,1) = 5.27, p < 0.001		
Time (ms)	50	75	100	125	150	175	200	225	250	275

F-statstics for significant sliding window ANOVAs. A yellow background indicates a difference-score X target side X wavelet interaction; a pink background indicates a difference-score X wavelet interaction.

Table 17

Shifts of Attention between Hemifields: VH Contrast – F-statistics for Figure 43										
Time (ms)	**50**	**75**	**100**	**125**	**150**	**175**	**200**	**225**	**250**	**275**
Parietal lobe Magnetometers										
29			F(7,1) = 6.58, p < 0.001							
	F(7,1) = 4.88, p < 0.001		F(7,1) = 3.41, p = 0.001				F(7,1) = 3.53, p = 0.001			
		F(7,1) = 4.74, p < 0.001				F(7,1) = 4.40, p < 0.001				
		F(7,1) = 5.66, p < 0.001								
32	F(7,1) = 3.67, p = 0.001		F(7,1) = 4.80, p < 0.001			F(7,1) = 2.67, p = 0.01				
		F(7,1) = 5.48, p < 0.001		F(7,1) = 5.79, p < 0.001						
Time (ms)	**50**	**75**	**100**	**125**	**150**	**175**	**200**	**225**	**250**	**275**
F-statstics for significant sliding window ANOVAs. A yellow background indicates a difference-score X target side X wavelet interaction; a blue background indicates a difference-score X magnetometer side X wavelet interaction; a pink background indicates a difference-score X wavelet interaction.										

Table 18

Shifts of Attention between Hemifields: VH Contrast – F-statistics for Figure 44										
Time (ms)	**50**	**75**	**100**	**125**	**150**	**175**	**200**	**225**	**250**	**275**
Posterior Temporal lobe Magnetometers										
23	F(7,1) = 5.45, p < 0.001		F(7,1) = 6.61, p < 0.001							
		F(7,1) = 7.51, p < 0.001		F(7,1) = 6.83, p < 0.001						
21								F(7,1) = 6.34, p < 0.001		
									F(7,1) = 6.78, p < 0.001	
20								F(7,1) = 4.57, p < 0.001		
									F(7,1) = 5.06, p < 0.001	
Time (ms)	**50**	**75**	**100**	**125**	**150**	**175**	**200**	**225**	**250**	**275**
F-statstics for significant sliding window ANOVAs. A yellow background indicates a difference-score X target side X wavelet interaction.										

Table 19

Shifts of Attention between Hemifields: VH Contrast – F-statistics for Figure 45										
Time (ms)	50	75	100	125	150	175	200	225	250	275
Occipital lobe Magnetometers										
37	F(7,1) = 5.58, p < 0.001	F(7,1) = 6.82, p < 0.001	F(7,1) = 5.79, p < 0.001	F(7,1) = 3.90, p < 0.001 F(7,1) = 5.56, p < 0.001 F(7,1) = 4.14, p < 0.001	F(7,1) = 3.50, p = 0.001 F(7,1) = 6.16, p < 0.001	F(7,1) = 3.18, p = 0.003	F(7,1) = 4.59, p < 0.001			
43	F(7,1) = 4.43, p < 0.001	F(7,1) = 5.64, p < 0.001	F(7,1) = 4.87, p < 0.001	F(7,1) = 4.14, p < 0.001 F(7,1) = 5.49 p < 0.001	F(7,1) = 4.46, p < 0.001 F(7,1) = 4.50, p < 0.001	F(7,1) = 4.07, p < 0.001 F(7,1) = 2.32, p = 0.02	F(7,1) = 3.96, p < 0.001 F(7,1) = 3.37, p = 0.002	F(7,1) = 3.12, p = 0.003 F(7,1) = 4.84, p < 0.001		
44	F(7,1) = 3.85, p < 0.001	F(7,1) = 5.19, p < 0.001				F(7,1) = 3.45, p = 0.001	F(7,1) = 3.39, p = 0.002			
39										
Time (ms)	50	75	100	125	150	175	200	225	250	275

F-statstics for significant sliding window ANOVAs. A yellow background indicates a difference-score X target side X wavelet interaction; a blue background indicates a difference-score X magnetometer side X wavelet interaction; a pink background indicates a difference-score X wavelet interaction.

Table 20

Comparison of HV vs. VH contrast – Sliding windows

Time-space course of HV vs. VH: Figure 46 visually contrasts the time-space course of HV (OBA for shifts of attention within hemifield) vis-à-vis VH (OBA for shifts of attention between hemifields) starting from target trigger onset until 300 ms for the overlapping 50 ms latency windows. In order to focus solely on contrasting time-space course patterns between these two conditions, the specific effect/interaction information discussed above are not reiterated in the figure. Each pair of blue-colored squares represents a significant difference via some interaction in the condition contrast DO-Valid vs. SO-Valid (HV or VH) in that magnetometer pair.

First, is it clear that the time-space course of significant differences between the Valid-DO vs. Valid-SO conditions are different for shifts within a hemifield (HV) versus

shifts between hemifields (VH). When shifts of attention are within a hemifield, significance starts in the parietal lobe magnetometers, feeds back to the occipital lobe, and then feeds forward and ventral laterally to the frontal and temporal magnetometer pairs respectively by 125 ms post target trigger onset. Then between 150 and 250 ms there is significantly different activity throughout the whole brain. At 275 ms the activity is seen only in the posterior, ventral-lateral temporal lobe magnetometer pairs. In contrast to HV where there is a clear feedback/feedforward/feed lateral time course by 125 ms post target trigger onset, in the VH condition when shifts of attention are between hemifields, a core set of dorsal magnetometer pairs, particularly in the occipital lobe, show significant difference from target trigger onset persistently until 250 ms post target trigger onset. Like the HV contrast, significant differences toward the end of the time course are seen posterior-ventral-laterally in the temporal lobe magnetometers, but unlike the HV contrast, in which such activity starts at 125 ms, it starts 100 ms later at 225 ms in the VH contrast.

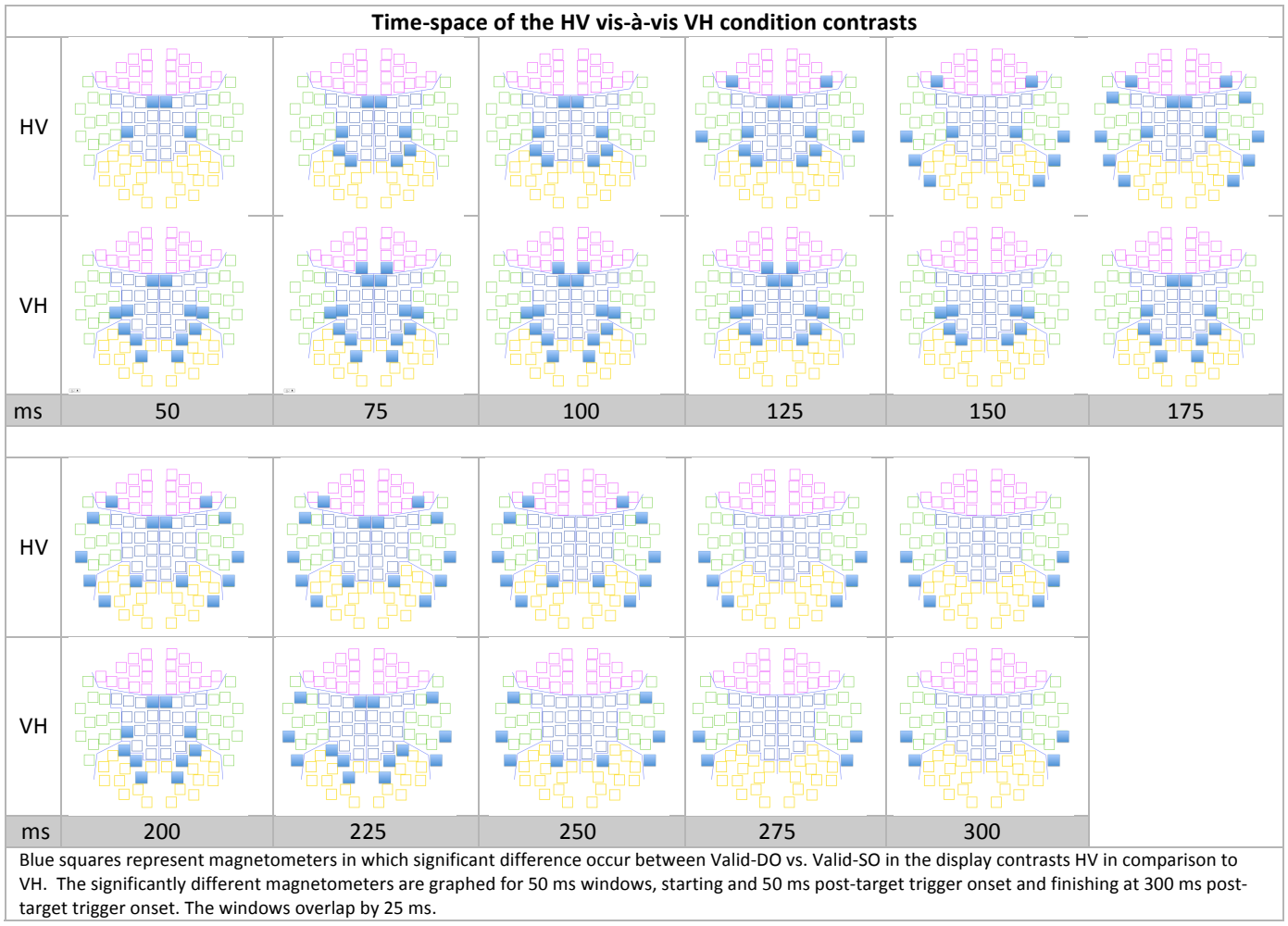

Blue squares represent magnetometers in which significant difference occur between Valid-DO vs. Valid-SO in the display contrasts HV in comparison to VH. The significantly different magnetometers are graphed for 50 ms windows, starting and 50 ms post-target trigger onset and finishing at 300 ms post-target trigger onset. The windows overlap by 25 ms.

Figure 46

Time-space-frequency course of HV vs. VH: Although not evident in Figure 46, it is evident from Table 1 and Table 4 that when significance differences are due to interactions with wavelet, they occur in the theta (θ - center frequency 5 Hz) and alpha (α - center frequency 10 Hz) bands. Furthermore, significant differences in the anterior magnetometer pairs occur, for the most part, in the theta range for both the HV and VH contrasts. The interesting exception is that in the anterior parietal magnetometer pair 29 in the early part of the time course there is alpha activity from 50 to 100 ms in both contrasts. In comparison, significant differences in the posterior magnetometer pairs occur in both the theta and alpha bands in the HV contrast, and, for the most part, in the alpha band in the VH

contrast. The interesting exception in the VH contrast is that in the posterior ventral-lateral temporal lobe pairs 20 and 21 toward the end of the time course (225 ms), significance occurs in the theta range in the VH contrast, as is the case with the HV contrast. Like the counterpart EEG analysis, significant differences occur within both the HV and VH condition contrasts, and the pattern is different between the two. The MEG results, however, additionally suggest a full time-course from 50 to 300 ms post target trigger onset of frequency and spatial information in both condition-display contrasts that is not evident in the EEG results.

Predominant interactions in HV vs. VH: Also evident in Table 1 vis-à-vis Table 4, and summarized in Table 21, is that in the HV condition-display contrast the predominant two-way interaction is difference-score X target-side (cells with purple backgrounds), whereas in the VH condition-display contrast the predominant two-way interaction is difference-score X wavelet (cells with pink backgrounds). This suggests that when shifts of attention are within hemifield, target-side modulates processing more so than does frequency. In contrast, when shifts of attention are between hemifields, frequency modulates processing more so than does target-side. In both contrasts however, these two-way interactions are mostly qualified with three-way interactions of difference-score X target-side X wavelet (Table 22).

Evident in Table 21 and Table 22 is an emerging pattern of SO vis-à-vis DO power that interacts with target-side and frequency-band. Since Table 21 and Table 22 are tabulated (vs. statistical) summaries of the individual sliding window ANOVAs, the next step is to verify that such patterns exist given statistical corroboration by entering time as a

factor into the ANOVA. The cell colors in Table 22 are a forward reference for comparison purposes, and will be discussed in concert with these subsequent analyses.

Predominant two-way interactions in HV vs. VH contrast – sliding window analysis				
	(a) Shifts within hemifield (HV)		(b) Shifts between hemifields (VH)	
	Two-way interaction: difference-score X target-side		Two-way interaction: difference score X wavelet	
frequency band	left targets	right targets	left targets	right targets
α	na	SO > DO, posterior mags (valid – DO > valid – SO)	SO < DO, occipital mags 37, 43 (valid – DO < valid – SO)	
θ			SO > DO, anterior mags (valid – DO > valid – SO) SO < DO, occipital mag 44 (valid – DO < valid – SO)	

Tabular summary of the predominant two-way ANOVAs in the HV condition-display contrast (Figure 37 through Figure 41) and in the VH condition-display contrast (Figure 42 through Figure 45 respectively). (a) In the HV contrast, the predominant two-way interaction is difference-score (Valid-DO, Valid-SO) X target-side (left, right). In right targets SO power is significantly greater than DO power. No significant results exist for left targets. (b) In the VH contrast, the predominant two-way interaction is difference-score X wavelet (q,a). In the alpha band, SO power is always less than DO power. In the theta band, SO power is greater than DO power in the anterior magnetometers, and less than DO power in the occipital magnetometer pair 44. In comparison, these summaries suggest that when shifts of attention are within hemifield, target-side modulates differential object-based attention cognitive processing more so than does frequency. When shifts of attention are between hemifields, frequency modulates object-based attention cognitive processing more so than does target-side.

Table 21

Predominant three-way interactions in HV vs. VH contrast – sliding window analysis				
	(a) Shifts within hemifield (HV)		(b) Shifts between hemifields (VH)	
	Three-way interaction: difference-score X target-side X wavelet			
frequency band	left targets	right targets	left targets	right targets
α	SO > DO (valid – DO > valid – SO)	SO < DO (valid – DO < valid – SO)	SO < DO (valid – DO < valid – SO)	SO > DO (valid – DO > valid – SO)
θ	SO < DO (valid – DO < valid – SO)	SO > DO (valid – DO > valid – SO)	SO > DO (valid – DO > valid – SO)	na

Tabular summary of the predominant three-way interaction in both the HV and VH condition-display contrast (Figure 37 through Figure 41 and Figure 42 through Figure 45). The predominant three-way interaction is difference-score (DO-Valid, SO-Valid) X target-side (left, right) X wavelet (q,a). (a) in the HV contrast in the alpha range SO power is always greater than DO power in left targets, and always less than DO power in right targets. In the theta range, the opposite is the case: SO power is always less than DO power in left targets, and greater in right targets. The cell colors are a forward reference for comparison with the per lobe ANOVAs and omnibus ANOVA results. (b) summaries in the VH contrast are opposite those in the HV contrast. In the alpha range, SO power is always less than DO power in left targets, and greater in right targets. In the theta range, SO power is greater than DO power in left targets. There are no significant results in right targets.

Table 22

B.2.2 Analysis Methods – Sliding windows, non-overlap

Sliding windows: There are five 50 ms windows from 50 ms to 300 ms post-target trigger onset with no overlap from one window to the next.

Dependent variable: The dependent variable in a given ANOVA is the mean power of each wavelet of the condition within a given latency window, just as in 5.2.1 Analysis Methods – Sliding windows. There are eight wavelets, one wavelet for each frequency band with center frequency: 5, 10, 20, 30, 40, 50, 70, and 80.

Magnetometer pairs: The 12 magnetometer-pairs are those used in 5.2.1 Analysis Methods – Sliding windows, and identified in the MEG temporal analyses (4.2.1 Analysis Methods – Components and 4.2.3 Analysis Methods – Sliding windows). There are 2 frontal lobe pairs of magnetometers, 4 temporal lobe pairs, 2 parietal lobe pairs, and 4 occipital lobe pairs. The magnetometers chosen are delineated with a red square outline, and their placement is shown in Figure 20 above, and Figure 35 in the Appendix.

ANOVA: Just as in 5.2.1 Analysis Methods – Sliding windows, the ANOVA is difference-score (DO-Valid, SO-Valid) X target-side (left, right) X wavelet (5, 10, 20, 30, 40, 50, 70, 80) X magnetometer-side (left, right). ANOVAs are done separately for the HV and VH contrasts, for each sliding window, for each magnetometer pair.

Multiple Comparisons: In using sliding windows in the ANOVA analysis, multiple comparisons are addressed using the Holm adjustment to the Bonferroni correction method. The correction is less stringent for the non-overlapping versus the overlapping

sliding windows (5.2.1 Analysis Methods – Sliding windows) because there are few windows in the latter case.[34]

B.2.3 Results – Sliding windows, non-overlap

Shifts of attention within hemifield: HV contrast

A summary of the significant differences due to all interactions for the HV contrast, with non-overlapping latency windows is given in Table 23. Notably, no additional significant differences appeared in the non-overlapping window analysis over and above those found in the overlapping analysis, even though fewer windows enabled a less restrictive Holm adjustment to the Bonferroni correction to be adopted.

With one exception, when frequency is a factor in anterior magnetometer pairs, it is so in the θ band, while when it is a factor posteriorly; it is so in both the θ and α bands. When target presentation side is a factor, left targets start to be processed differentially between condition contrasts earlier than right targets, and finish earlier, while right targets are still differentially processed at 300 ms. The predominant two-way interaction of difference-score X target-side occurs in right targets in posterior magnetometers (purple with down diagonal). In conclusion, the results confirm that the findings of the overlapping sliding window analysis of the HV condition-display contrast hold with sparser coverage (non-overlapping latency windows) of the time course.

---

[34] The p-values included in the correction are those associated with the effects and interactions of interest (all those that contain difference-score as a factor) from all ANOVAs across twelve magnetometer pairs, per condition-display contrast. The Holm adjustment for a given p-value in an increasing sorted sequence is 0.05/(N-n+1), where N is the number of tests and n is the position in the sequence. N in the overlapping sliding windows was calculated as 8 (1 main effect and 7 interactions of interest) X 5 latency windows X 12 magnetometer pairs = 480. The main effect and 8 interactions of interest are (difference-score, difference-score X target-side, difference-score X wavelet, difference-score X target-side X wavelet, difference-score X magnetometer-side, difference-score X target-side X magnetometer-side, difference-score X wavelet X magnetometer-side, difference-score X target-side X wavelet X magnetometer-side).

HV contrast: All Significant Interactions and Main Effects
Summary of Frequency and Target-Side Characteristics Across Non-overlapping Sliding Windows

Time (ms)		50	100	150	200	250
Mag pair						
frontal	5			θ	θ	
	11					
anterior temporal	13				θ	
parietal	29	α	θ		θ	
	32	α	θ, α	α		
posterior temporal	23					
	21			θ, α	θ, α	θ, α α
	20			θ, α	θ, α	θ, α α
occipital	37		α			
	43		α		mag 1911 (L) α	
	44					
	39			θ, α	θ, α	α
Time (ms)		50	100	150	200	250
		"P1"		"N1"		

A main effect of difference score has a green background. A purple background indicates a difference-score X target-side interaction. A pink background in the cell indicates a difference-score X wavelet interaction; a blue background indicates a difference-score X magnetometer side X wavelet interaction; a yellow background indicates a difference-score X target side X wavelet interaction. A green background indicates a main effect of difference-score. When target-side is a factor (yellow and purple backgrounds), a solid color indicates that left targets are the source of significance; up right diagonal lines indicate that right targets are the source of significance; vertical lines indicate that both left and right targets are sources of significance. When wavelet is a factor (yellow, pink, blue backgrounds), the wavelet frequency source of significance is labeled (theta θ and/or alpha α).

Table 23

Shifts of attention between hemifields: VH contrast

A summary of the significant differences due to all interactions for the VH contrast, with non-overlapping latency windows is given in Table 24. Unlike in the HV contrast where the relaxed multiple correction (because of fewer windows) did not result in additional significant interactions, three additional significant differences appeared here when windows did not overlap. A two-way interaction of difference-score X wavelet was significant in the θ range in anterior parietal magnetometer pair 29 at 50 ms. In occipital magnetometer pair 37, there was an additional source of θ significance in the difference-score X wavelet interaction at 150 ms (α was already significant in the more restrictive case). Similarly, in occipital magnetometer pair 43 an additional source of θ significance in the difference-score X target-side X wavelet interaction at 150 ms (α was significant in the more restrictive case).

When frequency is a significant factor, it is so only in the theta θ and alpha α bands. It is a factor in anterior magnetometer pairs primarily in the theta band, and in posterior magnetometers in both the theta and alpha bands. Right targets show significant differences in processing at 50 ms just as left targets do, specifically in the parietal lobe magnetometer pair 29. Throughout the time-course left targets are consistently differentially processed, whereas right targets were only briefly so at the beginning of the time course. In conclusion, the results confirm that the findings of the overlapping sliding window analysis of the VH condition-display contrast hold with sparser coverage (non-overlapping latency windows) of the time course.

VH contrast: All Significant Interactions and Main Effects Summary of Frequency and Target-Side Characteristics Across Non-Overlapping Sliding Windows						
Time (ms)		50	100	150	200	250
Mag pair						
frontal	5					
	11		θ θ			
anterior temporal	13					
parietal	29	L, θ; R, α θ	θ θ		θ	
	32	α	α			
posterior temporal	23	α	α			
	21					θ
	20					θ
occipital	37	α	α	θ & α θ, α	mag 2441 (R), θ	
	43	α	α	θ & α α	mag 2311 (R), θ mag 1911 (L), α α	
	44	α			θ	
	39					
Time (ms)		50	100	150	200	250

A main effect of difference score has a white background with a label. A pink background in the cell indicates a difference-score X wavelet interaction; a blue background indicates a difference-score X magnetometer side X wavelet interaction; a yellow background indicates a difference-score X target side X wavelet interaction. The source(s) of the interaction are labeled. Significance sources not also significant in the non-overlapping window analysis are underlined here.

Table 24

B.2.4 Results – Per Lobe ANOVAs

Frontal lobe

The highest order interactions in the frontal lobe ANOVA are two three-way interactions: the first is difference-score X target-side X wavelet $F(1,17) = 37.42$, $p < 0.001$. The sources of significance for this interaction are graphed in Figure 47. The second three-way interaction is difference-score X target-side X magnetometer-side $F(1,17) = 5.91$, $p = 0.02$. The sources of significance for this interaction are shown in Figure 48.

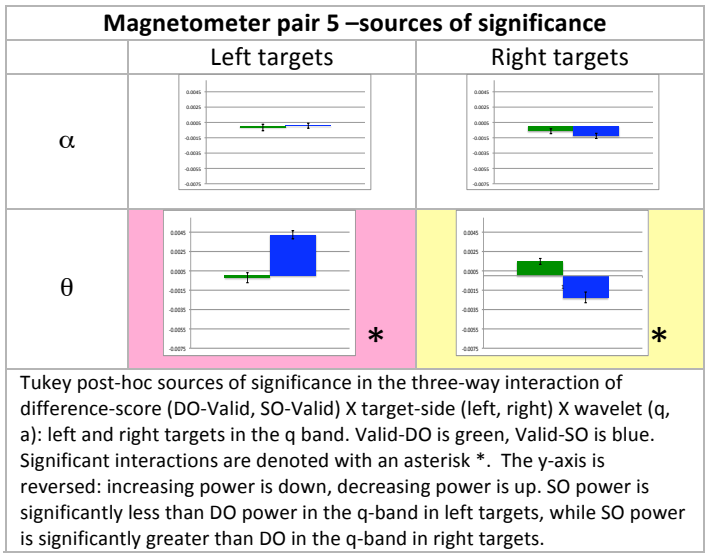

Tukey post-hoc sources of significance in the three-way interaction of difference-score (DO-Valid, SO-Valid) X target-side (left, right) X wavelet (q, a): left and right targets in the q band. Valid-DO is green, Valid-SO is blue. Significant interactions are denoted with an asterisk *. The y-axis is reversed: increasing power is down, decreasing power is up. SO power is significantly less than DO power in the q-band in left targets, while SO power is significantly greater than DO in the q-band in right targets.

Figure 47

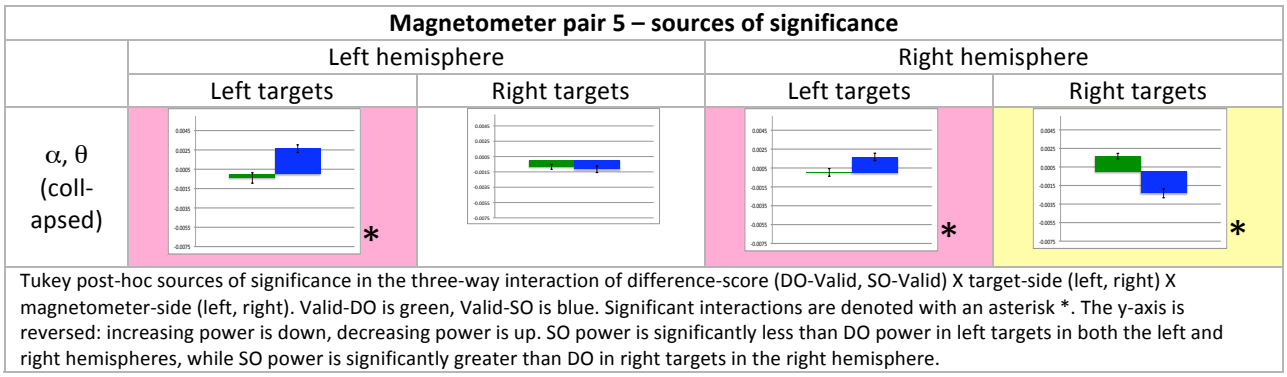

Tukey post-hoc sources of significance in the three-way interaction of difference-score (DO-Valid, SO-Valid) X target-side (left, right) X magnetometer-side (left, right). Valid-DO is green, Valid-SO is blue. Significant interactions are denoted with an asterisk *. The y-axis is reversed: increasing power is down, decreasing power is up. SO power is significantly less than DO power in left targets in both the left and right hemispheres, while SO power is significantly greater than DO in right targets in the right hemisphere.

Figure 48

Parietal lobe

The highest order significant interaction in the parietal lobe ANOVA is difference-score X time-bin X magnetometer-pair X target-side X wavelet $F(8,17) = 3.49$, $p < 0.001$. The tukey post-hoc sources of significance are given in Figure 49 for magnetometer pair 29, and Figure 50 for magnetometer pair 32.

Magnetometer pair 29 (anterior) – sources of significance

(a) **α-band**

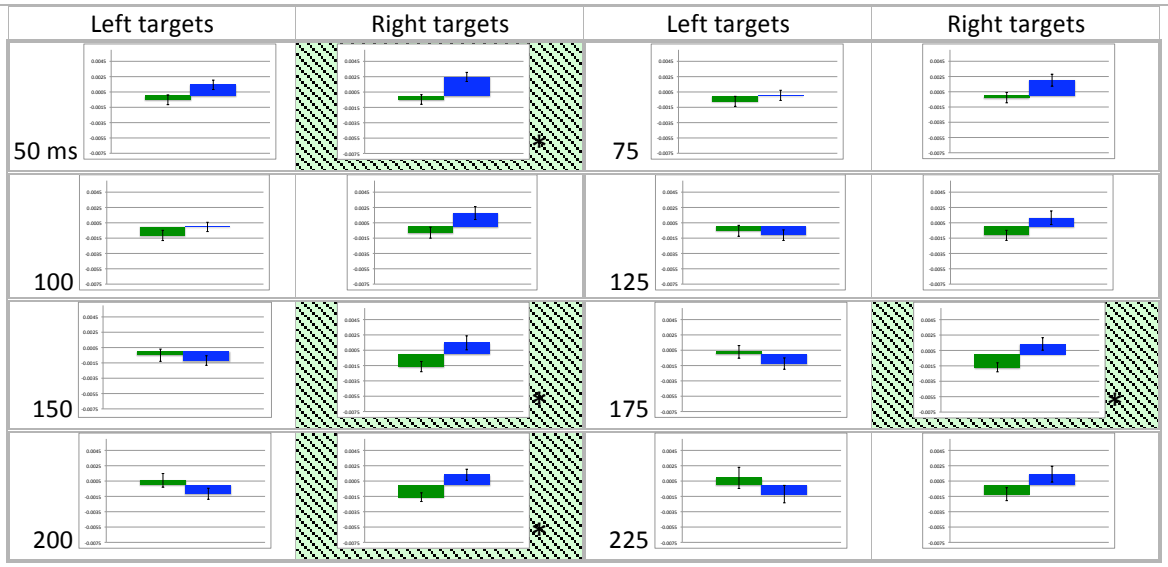

(b) **θ-band**

Tukey post-hoc sources of significance in the five-way interaction of difference-score (DO-Valid, SO-Valid) X time-bin (9) X magnetometer-pair (29, 32) X target-side (left, right) X wavelet (q, a). This figure shows the results for magnetometer pair 29. The nine time bins are 50, 75, 100, 125, 150, 175, 200, 225, and 250 ms. Within each time bin left targets are shown on the left, right targets on the right. Significant interactions are denoted with an asterisk *. The y-axis is reversed: increasing power is down, decreasing power is up. Sources of significance in the a-band are in right targets at time-bin start time of 50, 150, 175 and 200 ms: SO power is less than DO power in all cases. Sources of significance in the q-band are both left and right targets at time-bin start times 100, 175 and 200 ms. In left targets SO power is less than DO power, while in right targets SO power is greater than DO.

Figure 49

Magnetometer pair 32 (posterior)– sources of significance

(a) **α-band**

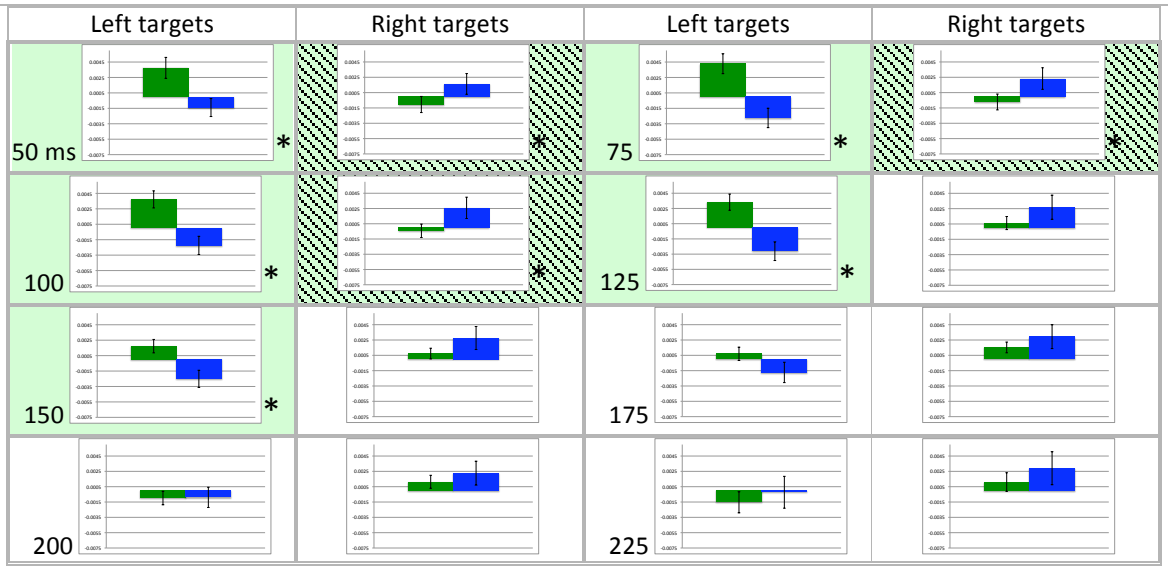

(b) **θ-band**

Tukey post-hoc sources of significance in the five-way interaction of difference-score (DO-Valid, SO-Valid) X time-bin (9) X magnetometer-pair (29, 32) X target-side (left, right) X wavelet (q, a). This figure shows the results only for magnetometer pair 32. The nine time bins are 50, 75, 100, 125, 150, 175, 200, 225, and 250 ms. Within each time bin left targets are shown on the left, right targets on the right. Significant interactions are denoted with an asterisk *. The y-axis is reversed: increasing power is down, decreasing power is up. Sources of significance in the a-band are in the left and right targets in time-bins with start times 50, 75 and 100 ms; and in left targets only in time-bins with start time 125 and 150 ms. In the a-band, when significance is due to left targets, SO is significantly greater than DO power, whereas when significance is due to right targets SO power is less than DO. Sources of significance in the q-band are in the left targets in time-bins starting at 50, 75, 100, 125, 150, 175 and 200 ms: SO is less than DO in these cases.

Figure 50

Temporal lobe

The highest order significant interaction in the temporal lobe ANOVA is difference-score X magnetometer-pair X target-side X magnetometer-side $F(2,17) = 4.75$, $p = 0.01$. The tukey post-hoc sources of significance are given in Figure 51.

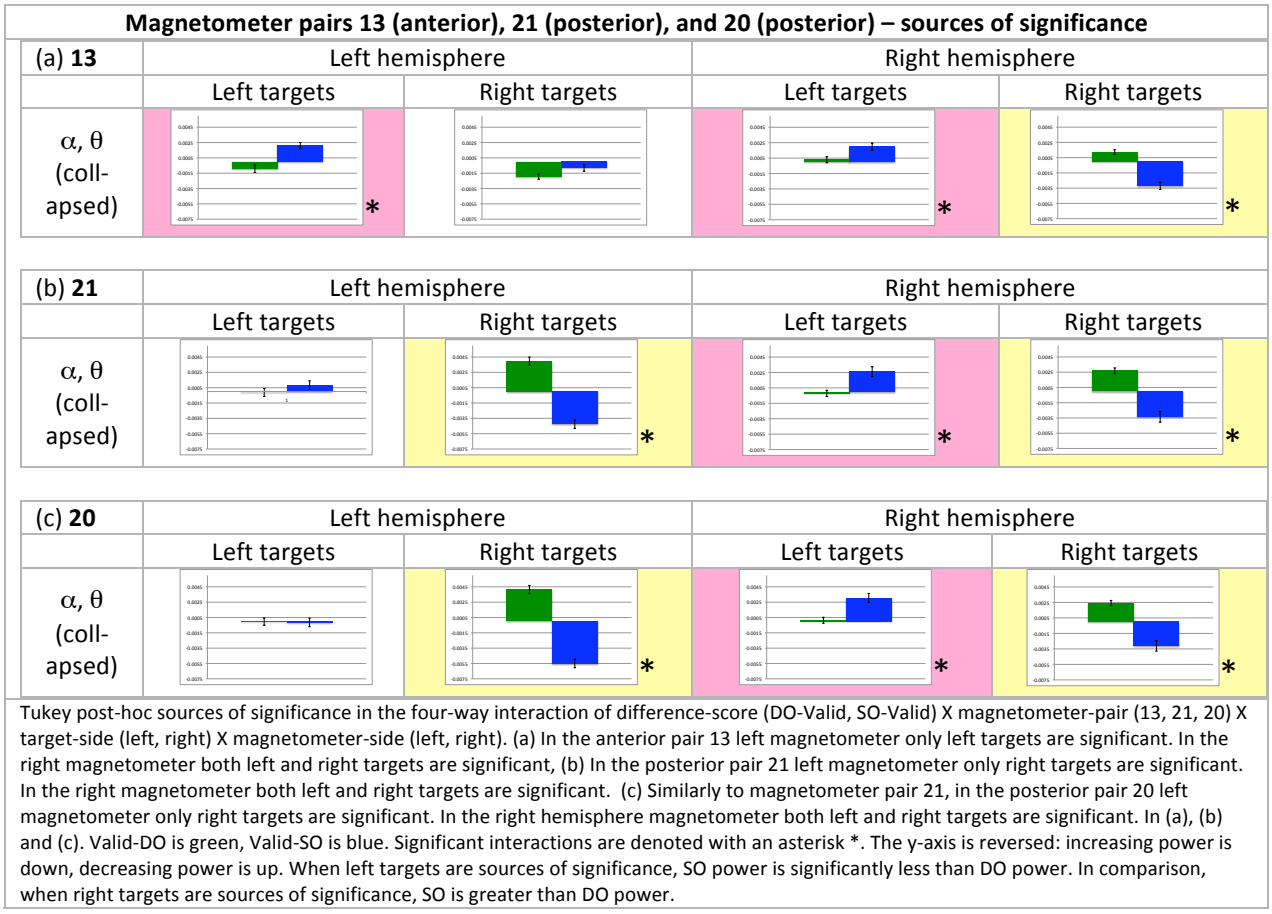

Tukey post-hoc sources of significance in the four-way interaction of difference-score (DO-Valid, SO-Valid) X magnetometer-pair (13, 21, 20) X target-side (left, right) X magnetometer-side (left, right). (a) In the anterior pair 13 left magnetometer only left targets are significant. In the right magnetometer both left and right targets are significant, (b) In the posterior pair 21 left magnetometer only right targets are significant. In the right magnetometer both left and right targets are significant. (c) Similarly to magnetometer pair 21, in the posterior pair 20 left magnetometer only right targets are significant. In the right hemisphere magnetometer both left and right targets are significant. In (a), (b) and (c). Valid-DO is green, Valid-SO is blue. Significant interactions are denoted with an asterisk *. The y-axis is reversed: increasing power is down, decreasing power is up. When left targets are sources of significance, SO power is significantly less than DO power. In comparison, when right targets are sources of significance, SO is greater than DO power.

Figure 51

Occipital lobe

The highest order significant interaction in the occipital lobe ANOVA is difference-score X magnetometer-pair X target-side X wavelet X magnetometer-side $F(2,17) = 3.27$, $p = 0.04$. Tukey post-hoc sources of the significance are shown in Figure 52.

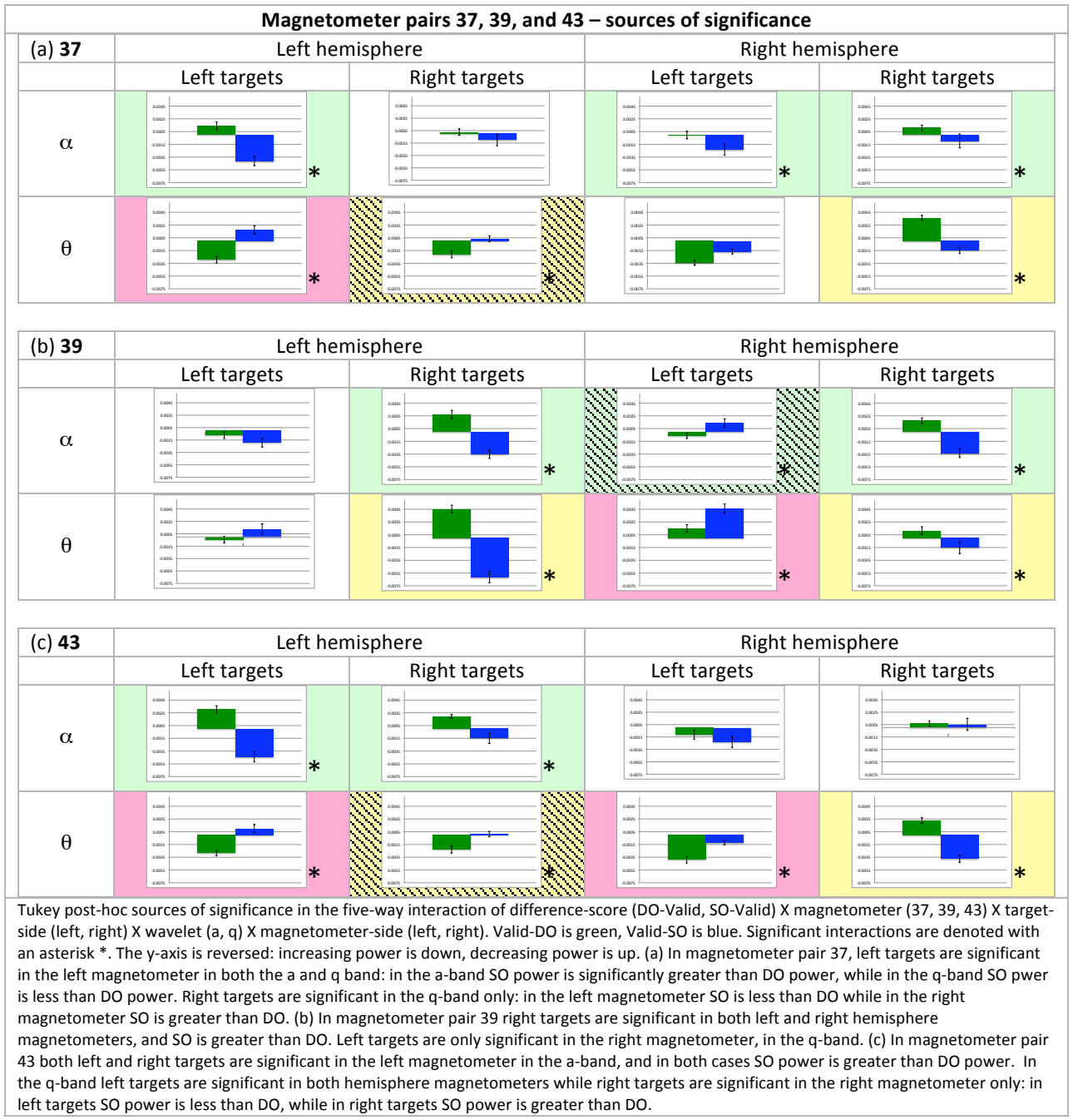

Tukey post-hoc sources of significance in the five-way interaction of difference-score (DO-Valid, SO-Valid) X magnetometer (37, 39, 43) X target-side (left, right) X wavelet (a, q) X magnetometer-side (left, right). Valid-DO is green, Valid-SO is blue. Significant interactions are denoted with an asterisk *. The y-axis is reversed: increasing power is down, decreasing power is up. (a) In magnetometer pair 37, left targets are significant in the left magnetometer in both the a and q band: in the a-band SO power is significantly greater than DO power, while in the q-band SO pwer is less than DO power. Right targets are significant in the q-band only: in the left magnetometer SO is less than DO while in the right magnetometer SO is greater than DO. (b) In magnetometer pair 39 right targets are significant in both left and right hemisphere magnetometers, and SO is greater than DO. Left targets are only significant in the right magnetometer, in the q-band. (c) In magnetometer pair 43 both left and right targets are significant in the left magnetometer in the a-band, and in both cases SO power is greater than DO power. In the q-band left targets are significant in both hemisphere magnetometers while right targets are significant in the right magnetometer only: in left targets SO power is less than DO, while in right targets SO power is greater than DO.

Figure 52